Master's thesis

NTNU
Norwegian University of Science and Technology
Faculty of Economics and Management
Dept. of Industrial Economics and Technology Management

Ivar Refsdal
Tobias Spinnangr Sindre

Impact of Production Technology Flexibility in a Multi-horizon Stochastic Hydrogen Facility Location Problem

Master's thesis in Applied Economics and Operations Research
Supervisor: Peter Schütz
June 2023

NTNU
Norwegian University of
Science and Technology

Ivar Refsdal
Tobias Spinnangr Sindre

Impact of Production Technology Flexibility in a Multi-horizon Stochastic Hydrogen Facility Location Problem

Master's thesis in Applied Economics and Operations Research
Supervisor: Peter Schütz
June 2023

Norwegian University of Science and Technology
Faculty of Economics and Management
Dept. of Industrial Economics and Technology Management

NTNU
Norwegian University of
Science and Technology

NTNU
Kunnskap for en bedre verden

Department of Industrial Economics

TIØ4905 - Master Thesis in Applied Economics and Operations Research

Impact of Production Technology Flexibility in a Multi-horizon Stochastic Hydrogen Facility Location Problem

Author:
Ivar Refsdal, Tobias Spinnangr Sindre

Supervisor:
Peter Schütz

June, 2023

Preface

This report was composed during the spring semester of 2023 as a part of the Master's Thesis in Applied Economics and Optimization at NTNU, TIØ4905, and is a continouation of our work with the immsersion project in Applied Economics and Optimization at NTNU, TIØ4500 (Refsdal & Sindre, 2022).

We want to express our profound gratitude to our academic supervisor Peter Schütz, whose invaluable guidance, feedback, and time invested in assisting us with this project were critical. His deep expertise and unwavering support were key in determining the trajectory and substance of our research, for which we remain profoundly grateful.

Additionally, we wish to extend our acknowledgment to Nord Pool and the Ocean Hyway Cluster. Their provision of essential data and insights was instrumental in our analysis. Their collaboration and support significantly contributed to the fruition of our research.

Trondheim, 9th of June, 2023

Ivar Refsdal & Tobias Spinnangr Sindre

Abstract

Hydrogen presents an exciting opportunity as a zero-emission fuel, particularly for heavy-duty and long-haul vehicles. This potential makes it a key player in reducing Norway's greenhouse gas emissions. Over recent years, the Norwegian Government has put an extensive focus towards initiating a large-scale clean hydrogen supply chain in Norway, giving substantial subsidies towards relevant research and private industry projects. Consequently, many decision-makers are now planning hydrogen production operations, facing crucial choices about the location, timing, and approach for establishing production facilities. Their objective is to meet future demand at the lowest possible cost. Notably, electricity expenses make up 70-88% of the total cost of producing emission-free hydrogen. As such, leveraging the flexibility of different production technologies could help optimize these costs.

This thesis explores the influence of the flexibility offered by hydrogen production technologies on investment decisions for hydrogen facilities in Norway, considering the uncertainties of electricity prices and future hydrogen demand in the transportation sector.

We introduce a multi-stage, multi-horizon stochastic model for facility location to encapsulate uncertainty and variations in electricity prices at an operational level and long-term uncertainties in demand at a strategic level. This model seeks to minimize total anticipated investment, production, and transportation costs. It encompasses strategic decisions related to plant investments, including location, capacity, and technology choices. The model allows for stepwise improvements in production efficiency and technology-related investment costs. Capacity installed in earlier stages is employable to meet demand in later stages. When electricity prices become known, the model accordingly optimizes production during the operational stage. By integrating multiple time periods at this stage, our model captures hourly electricity price fluctuations, thus assessing the impact of operational flexibility, granted by technology, on strategic investment decisions. To the best of our knowledge, this is the first instance of a multi-horizon facility location problem being presented in the literature.

We developed a Lagrange relaxation to improve solution times and handle larger problems. However, the commercial solver Gurobi outperformed this approach for problems solvable within our 48-hour (172,800 seconds) maximum timeframe.

Our findings suggest production flexibility has minimal impact on investment decisions in the Norwegian context due to low hourly volatility in electricity prices. The primary determinants are rather found to be production efficiency and investment costs. Alkaline technology, being more cost-effective, therefore dominates Norway's hydrogen supply chain in 2023 and 2028, while the more flexible PEM technology becomes preferred by 2033 as the cost disparity narrows. Cost distribution aligns with previous studies: 60-70% production, 5-10% investment, 20-30% transportation. A distributed supply chain with an average hydrogen transport distance of 161 km is optimal, favoring capacity installations near demand. Inter-zone hydrogen flow trends from northern to southern zones due to price and transportation costs. There's a mild preference for building larger facilities earlier, suggesting economies of scale.

Sammendrag

Hydrogen presenterer en spennende mulighet som et nullutslippsdrivstoff, spesielt for tungtransport og langtransportkjøretøyer. Dette potensialet gjør det til en nøkkelspiller i reduksjonen av Norges klimagassutslipp. I de senere årene har den norske regjeringen investert betydelig for å initiere en norsk ren hydrogenforsyningskjede, og har gitt betydelige subsidier til relevant forsking og prosjekt innen privat industri. Følgelig planlegger nå mange beslutningstakere drift av hydrogenproduksjon, og står overfor kritiske valg om lokalisering, timing og tilnærming til etablering av produksjonsanlegg. Produsentenes mål er å møte fremtidig etterspørsel til lavest mulig kostnad. Merkbar er det at elektrisitetskostnader utgjør 70-88% av de totale kostnadene ved produksjon av utslippsfri hydrogen. Som sådan, kunne utnyttelsen av fleksibiliteten gitt av forskjellige produksjonsteknologier hjelpe med å optimalisere disse kostnadene.

Denne avhandlingen utforsker innflytelsen av fleksibiliteten som tilbys av hydrogenproduksjonsteknologier på investeringsbeslutninger for hydrogenanlegg i Norge, og tar hensyn til usikkerhetene ved elektrisitetspriser og fremtidig hydrogenbehov i transportsektoren.

Vi introduserer en flertrinns, flerhorisont stokastisk modell for anleggslokalisering for å innkapsle usikkerhet og variasjoner i elektrisitetspriser på et operasjonelt nivå, og langsiktige usikkerheter i etterspørsel på et strategisk nivå. Denne modellen søker å minimere totale forventede kostnader ved investering, produksjon, og transport. Den omfatter strategiske beslutninger relatert til anleggsinvesteringer, inkludert lokalisering, kapasitet, og teknologivalg. Modellen gir plass for trinnvise forbedringer i produksjonseffektivitet og investeringskostnader knyttet til forskjellige teknologier. Kapasitet installert i tidligere trinn kan brukes til å møte etterspørselen i senere trinn. Når elektrisitetspriser blir kjent, optimaliserer modellen tilsvarende produksjonen under den operasjonelle fasen. Ved å integrere flere tidsperioder på dette stadiet, fanger vår modell opp timeprisfluktuasjoner i elektrisitet, og vurderer dermed virkningen av operasjonell fleksibilitet, gitt av teknologi, på strategiske investeringsbeslutninger. Så vidt vi vet, er dette det første tilfellet av et flerstegs flerhorisont anleggslokaliseringproblem som blir brukt for et lokasjonsproblem.

For å forbedre løsningstider og håndtere større problemer, utviklet vi en Lagrange-relaksering. Imidlertid overgikk den kommersielle løseren Gurobi denne tilnærmingen for problemer som kan løses innen vår maksimale tidsramme på 48 timer (172 800 sekunder).

Våre funn antyder at produksjonsfleksibilitet har minimal innvirkning på investeringsbeslutninger i den norske konteksten på grunn av lav timevolatilitet i elektrisitetspriser. De primære bestemmelsesfaktorene er i stedet funnet å være produksjonseffektivitet og investeringskostnader. Alkalisk teknologi, som er mer kostnadseffektiv, dominerer derfor Norges hydrogenforsyningskjede i 2023 og 2028, mens den mer fleksible PEM-teknologien blir foretrukket innen 2033 ettersom kostnadsforskjellen smalner. Kostnadsfordelingen samsvarer med tidligere studier: 60-70% produksjon, 5-10% investering, 20-30% transport. En distribuert forsyningskjede med en gjennomsnittlig hydrogen transportavstand på 161 km er optimal, favoriserer kapasitetsinstallasjoner nær etterspørsel. Inter-regional hydrogen flyt trender fra nordlige til sørlige soner på grunn av pris og transportkostnader. Det er en mild preferanse for å bygge større anlegg tidligere, noe som antyder stordriftsfordeler.

Table of Contents

List of Figures

List of Tables

Chapter 1

Introduction

Climate change represents a profound challenge for humanity in the coming years. Significant political endeavors globally aim to curtail greenhouse gas (GHG) emissions. The most recent major international effort was the Paris Climate Accords in 2016, where 193 states agreed to an overall reduction in global GHG emissions. The aim is to limit the mean global temperature increase to below 2°C. For its part, Norway has committed to reducing GHG emissions by a minimum of 55% by 2030, compared to 1990 levels (The Norwegian Government, 2022b). Achieving this target necessitates significant emission reductions in the transportation sector, which accounted for 33% of Norway's GHG emissions as of 2021 (Miljødirektoratet, 2022).

In the pursuit of reducing emissions, Norway leads the way in the electrification of its vehicle fleet, including cars, trains, and ferries. It boasts the world's highest proportion of new electric car sales, reaching 79% in 2022 (SSB, 2023). However, some scenarios, such as longer-haul ferry journeys, are not suitable for electrification due to battery weight limitations and refueling times. Hydrogen, an energy carrier with the potential for zero emissions (green hydrogen), can offer a solution in these contexts and could be instrumental in reducing GHG emissions, particularly within the transportation sector and energy-intensive industries.

Norway's green hydrogen production is currently minimal (The Norwegian Government, 2022a), posing a barrier to the introduction of hydrogen-fueled vehicles. However, business interest has surged in the past decade, with several companies planning national green hydrogen production initiatives (Menon Economics, 2022). The government has fostered this interest through supportive hydrogen policies. For example, the agency *Enova* has disbursed billions in subsidies and grants. In 2022, Enova awarded over a billion Norwegian kroner to projects related to green hydrogen production and its use as a fuel (Enova, 2022a).

Despite the lack of substantial green hydrogen production from a Norwegian supply side, demand has already surfaced from the maritime sector. Notably, on March 31, 2023, the Norwegian company *Norled* commenced operations of the world's first green hydrogen-fueled ferry Statens vegvesen (2023). Currently, Norled sources its hydrogen from a German company Linde plc (2021) (Sjøfartsdirektoratet, 2023).

Given these developments, it's evident that green hydrogen, especially in the maritime sector, will increasingly serve as a fuel source in the coming years. However, the extent of its future prevalence remains unclear. A lag in domestic production relative to consumption could potentially delay otherwise promising projects, setting up a classic chicken-or-egg conundrum. This discrepancy adds an extra layer of uncertainty to hydrogen demand in terms of overall demand and regional variations across Norway. Consequently, prospective investors in Norway's green hydrogen production face a complex decision-making environment with uncertainty regarding future demand.

As hydrogen is a *fungible good*, being a commodity that is interchangeable with other hydrogen units, businesses' primary concern will be investing in production facilities that

can minimize total unit costs of hydrogen production and distribution. Given that electricity costs constitute a significant component in green hydrogen production (70-88% of total costs), companies are incentivized to establish production facilities in areas with low electricity prices. In Norway, such areas are predominantly in the northern regions. Conversely, the majority of the anticipated demand is expected from southern Norway, which is considerably distant from the cheap electricity available in the North. Thus, a trade-off exists between production and transportation costs when investing in green hydrogen production in Norway.

Green hydrogen is primarily produced using either Alkaline or PEM electrolyzers. While Alkaline technology is more mature with lower required investment costs, PEM offers superior flexibility in production throughput adjustment and a shorter ramp-up time. This paper aims to determine whether the increased flexibility provided by PEM can justify its higher investment costs. The optimal location for hydrogen production facilities in Norway will also be examined as decision support for potential green hydrogen producers.

Previous research on optimizing hydrogen supply chains has employed deterministic and stochastic programming. A recent paper investigates optimal hydrogen production facility locations for Norway's maritime sector up to 2035 using a multi-period facility location model with capacity extension (Stádlerová & Schütz, 2021). However, limited research has been conducted on how technological flexibility affects hydrogen supply chain design. Refsdal and Sindre (2022) investigates the value of production flexibility within a two-stage facility location problem, accounting for electricity price uncertainty but deterministic demand. To our knowledge, no research has analyzed the optimization of hydrogen supply chains using a multi-horizon model, considering technical and economic advancements over time, long-term demand uncertainty, and operational uncertainties for assessing the impact of production flexibility on strategic investment decisions. Neglecting sequential decision-making could lead to suboptimal solutions due to anticipated improvements in hydrogen production technologies' cost and efficiency and uncertainties in long-term demand levels. Ignoring the flexibility offered by production technologies could also result in suboptimal solutions, particularly in cases of high price volatility.

To address these considerations, we formulate a multi-horizon stochastic optimization model for determining where and when to invest in production plant facilities, their respective capacities, and production technology. The model encompasses two time periods: one for strategic facility investment decisions and the other for operational-level production planning. The strategic time period comprises several five-year stages with demand uncertainties. Over time, the investment and operational costs of hydrogen production decrease. For each demand realization at each strategic stage, an operational component models production planning across multiple time periods, thus capturing variability in stochastic parameters and assessing the flexibility in production technology. Due to a large number of scenarios and extensive solution times, we use Lagrangian relaxation. To our knowledge, this is the first instance of formulating and solving a multi-horizon facility location problem. The model is run generally, as well as for specific scenarios, to glean managerial insights.

The structure of this paper is as follows: Chapter 2 delves into technical and financial aspects pertaining to the green hydrogen value chain, with emphasis on PEM and Alkaline production technologies. Chapter 3 reviews pertinent literature on stochastic programming and facility location, supply chain network design, and hydrogen production flexibility. Chapter 4 provides a comprehensive description of the problem. A mathematical model for the problem is presented in Chapter 5. In Chapter 6, we introduce a Lagrangian

relaxation framework, which is then applied and tested on the model. Chapter 7 explains how the model is implemented

Chapter 2

Background

This chapter presents the reader with essential terminology and topics in order to understand hydrogen production and its future development, mainly from a technological and economic perspective. An emphasis is put on discussing the operational flexibility offered by different production technologies, and their economic implication. Section 2.1 presents the most widespread technologies used to produce hydrogen, their respective costs, and the operational flexibility that they offer. In Section 2.2, the future global demand for hydrogen across different segments of the transportation sector is discussed. Further, the distribution of hydrogen from the production facility to consumers is discussed in Section 2.3. Then the general cost functions of hydrogen production are discussed in Section 2.4, which is important for later modeling of production. Finally, the Norwegian electricity market is discussed in Section 2.5, including the economic impacts of operational flexibility.

2.1 Hydrogen production

In the process of energy generation via combustion, fuel cells, or turbines, hydrogen acts as a zero-emission fuel by solely releasing water during operation. However, its production can entail greenhouse gas emissions, the levels of which fluctuate depending on the input factors and production techniques used (IRENA, 2020a). These production methods are grouped into color-coded categories such as ”gray,” ”blue,” and ”green,” each reflecting specific input factors, primary energy sources, and the direct and indirect emissions produced over their life cycle, as displayed in Figure 2.1 and Table 2.1 and further explained in subsequent sections. Additionally, there are other categories like ”turquoise” and ”brown” hydrogen, of which the former is still in its early stages of development through methane pyrolysis (IRENA, 2020a), and the latter is disregarded in this report due to its coal-derived nature making it irrelevant from the Norwegian supply chain perspective.

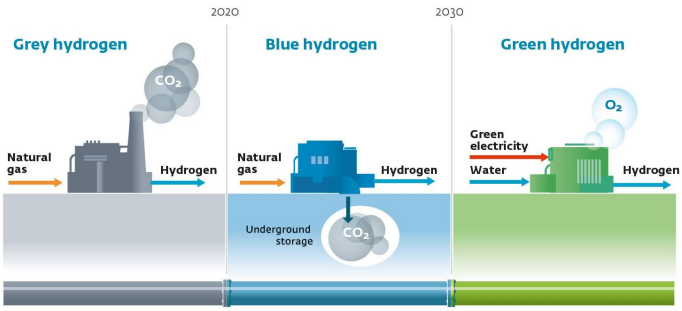

Figure 2.1: Schematic illustrating input and output factors, as well as CO2 emissions, from gray, blue and green hydrogen production (The World of Hydrogen, 2022).

Table 2.1: The colors of hydrogen adapted from Broadleaf (2021).

Characteristic	Grey	Blue	Green
Energy source	Fossil fuels	Fossil fuels	Renewables
Feedstock	Natural gas	Natural gas, coal, oil, biomass	Water
Technology	Reforming Gasification	Reforming + CSS Gasification + CSS	Electrolysis
By-products	CO_2	CO_2	Oxygen
Environmental footprint	High	Low	Minimal

2.1.1 Green Hydrogen

Green hydrogen is generated by means of electrolysis that employs electricity generated from renewable energy sources. As the production method only employs electricity to transform water (H_2O) into hydrogen (H_2) and oxygen (O_2), it does not discharge any greenhouse gases, and is therefore emission free, both directly and indirectly.

Several electrolysis technologies are available, namely Alkaline, Anion Exchange Membrane (AEM), Proton Exchange Membrane (PEM), and Solid Oxide Electrolyzer Cell (SOEC). However, this report will solely focus on Alkaline and PEM as they are the most established technologies and are commercially provided by major electrolyzer firms like NEL, ITM Power, and Thyssenkrupp (Nel, 2021, ITM-Power, 2022, Thyssenkrupp, n.d.). AEM, on the other hand, currently experiences issues with limited lifetimes, while SOEC has high CAPEX and prolonged start-up times (Andrenacci et al., 2022).

2.1.1.1 Alkaline Electrolysis

Figure 2.2 illustrates the fundamental principle of Alkaline electrolysis. An Alkaline electrolyzer is composed of two metallic electrodes immersed in a liquid electrolyte, typically an aqueous solution of KOH or NaOH. Water reduction occurs at the cathode, as indicated by the following equation:

$$H_2O + 2e^- \rightarrow H_2 + 2OH^- \tag{2.1}$$

And at the anode, oxidation of hydroxyl takes place:

$$2OH^- \rightarrow \frac{1}{2}O_2 + H_2O + 2e^- \tag{2.2}$$

Only water is consumed in the process, and the products are hydrogen (H_2) and oxygen (O_2) (Millet & Grigoriev, 2013).

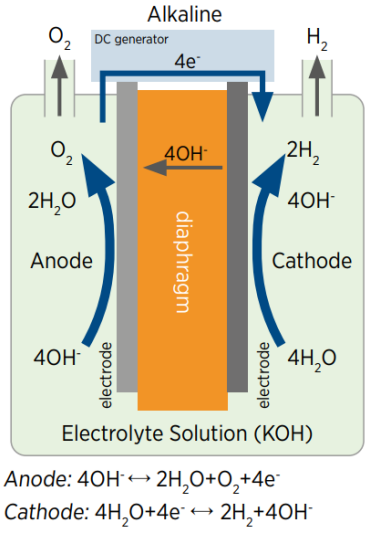

Figure 2.2: Alkaline hydrogen production schematic with half-reactions (IRENA, 2020b).

As reported by Andrenacci et al. (2022), alkaline electrolyzers present capacity utilization versatility, although their operational flexibility is somewhat limited due to a constrained load range of 20% to 100% of installed capacity. This implies a minimum operational threshold of 20% for these electrolyzers. Consequently, in situations requiring less than 20% utilization, the system would generate surplus hydrogen, leading to unnecessary consumption of electricity.

Nel (2021) states that the duration for initiating an alkaline electrolyzer startup hinges on its design and configuration. Startups can be broadly classified into two types - a full startup and a hot standby startup. The latter typically requires around 30 minutes, while the former might take up to 150 minutes. Operating in hot standby mode, a prerequisite for a hot startup, necessitates energy consumption. The extended startup period constrains the operational flexibility of alkaline electrolyzers, making them less suitable for environments with variable electricity availability or price fluctuations, as they would be unable to rapidly adjust to changes in power access or cost electricity prices.

When relying on dedicated renewable energy sources, like wind power, accessing electricity for hydrogen electrolysis can pose a challenge. Wind power is known for its volatility, and it's not uncommon for the amount of power generated to fluctuate significantly and rapidly, occasionally even dropping to zero if the wind stops blowing. In such cases, operational flexibility in terms of the being able to swiftly return to full utilization levels after turning production on, is crucial.

Andrenacci et al. (2022) report that alkaline electrolysis is an economically favorable option for hydrogen production due to its low dependence on costly raw materials which gives relatively low CAPEX of 600 €/kW, which is lower than other electrolysis technologies. Additionally, the expected CAPEX for alkaline electrolysis in 2030 is even lower at 480 €/kW. The operational costs associated with alkaline hydrogen production are estimated to be around 50 €/(kg/d)/y in 2020, with further reductions anticipated to bring the cost down to 48 €/(kg/d)/y by 2030. Alkaline electrolyzers are a well-established technology, having been used commercially for over a century. While economies of scale may bring some reductions in the CAPEX, significant decreases are not expected (IEA, 2019). Table 2.2 provides an overview of the critical KPIs associated with alkaline hydrogen production.

Table 2.2: KPIs of Alkaline electrolyzers (Andrenacci et al., 2022).

No.	Parameter	Unit	State of the art	Target
			2020	2030
1	Electricity consumption	kWh/kg	50	48
2	CAPEX	€/kW	600	480
3	O&M	€/(kg/d)/y	50	35
4	Hot idle ramp up	sec	60	30
5	Cold idle ramp up	min	60	30
6	Lifespan	h	90 000	180 000

2.1.1.2 Proton Exchange Membrane Electrolysis (PEM)

Figure 2.3 illustrates the fundamental principle of a PEM electrolyzer. The device comprises two electrodes separated by a proton-conducting polymer electrolyte, forming a membrane electrode assembly (MEA). The anode is immersed in water, and at this electrode, oxygen evolution occurs.

At the anode oxygen evolution takes place:

$$H_2O \rightarrow \frac{1}{2}O_2 + 2e^- + 2H^+ \tag{2.3}$$

The hydrogen electrons are transported across the membrane, and hydrogen gas is created at the anode:

$$2H^+ + +2e^- \rightarrow H_2 \tag{2.4}$$

Only water is consumed in the process, and the products are hydrogen (H_2) and oxygen(O_2) (Millet & Grigoriev, 2013).

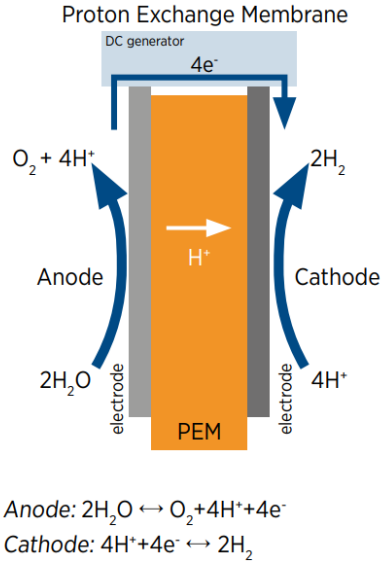

Figure 2.3: PEM hydrogen production schematic with half-reactions (IRENA, 2020b).

According to Andrenacci et al. (2022), PEM electrolyzers are not subject to a lower bound on the load range and can operate at rates between 0% and 160% of their capacity.

Although some vendors claim that overloading the system up to 160% is possible, this capability is reliant on appropriate power supply and thermal management tailored to the specific load, and it is not the industry standard. Hence, this capability will not be considered in this report.

Nel (2021) states that the startup time for PEM electrolyzers varies depending on whether it is a cold start (i.e., $\geq$ 6 hours since the last startup) or a warm start. A cold start takes approximately 23 minutes, while a warm start requires only 8 minutes. In contrast, other sources indicate that the response time for PEM electrolyzers is less than a few seconds, and the energy needed to maintain a warm state for the system during startup is negligible (Andrenacci et al., 2022). This enhanced flexibility in startup times makes PEM electrolyzers a suitable option to pair with volatile electricity prices or availability, as the system can be quickly turned off during periods of high prices or electricity unavailability and in cases where prices drop significantly.

The production of PEM electrolyzers requires expensive materials for both the cathode (such as iridium and platinum) and membrane materials, resulting in a higher CAPEX compared to alkaline electrolyzers. However, ongoing research on cathode and membrane technology is expected to lower the CAPEX of PEM electrolyzers. Despite this disadvantage, PEM electrolyzers offer the benefit of producing hydrogen at higher pressures than alkaline electrolyzers, eliminating the need for compression during storage or delivery. Currently, the lifespan of PEM electrolyzers is shorter than that of alkaline electrolyzers, but future research is expected to address this issue (IEA, 2019).

Table 2.3: KPIs of PEM from Andrenacci et al. (2022).

No.	Parameter	Unit	State of the art	Target
			2020	2030
1	Electricity consumption	kWh/kg	55	48
2	CAPEX	€/kW	900	500
3	O&M	€/(kg/d)/y	41	21
4	Hot idle ramp up	sec	2	1
5	Cold idle ramp up	sec	30	1
6	Lifespan	h	60 000	180 000

2.1.1.3 Cost of Green Hydrogen Production

The production cost of green hydrogen is heavily influenced by technology selection, capacity utilization, and electricity prices. The Levelized Cost of Hydrogen (LCOH) estimates for Alkaline and PEM technologies are illustrated in Figure 2.4, which breaks down the costs into CAPEX, Operations & Maintenance (O&M), and electricity expenses, using data from (Andrenacci et al., 2022).

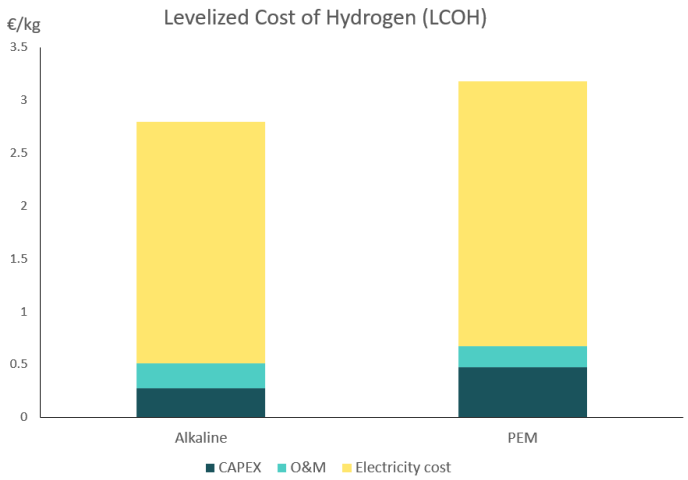

Figure 2.4: Cost of hydrogen with CAPEX and O&M assumptions from Andrenacci et al. (2022), based on the framework of UK Government (2022) and an electricity price of 40 €/MWh.

The Levelized Cost of Hydrogen (LCOH) for Alkaline and PEM are presented in Figure 2.4, and the cost largely depends on the technology choice, utilization rate, and electricity price. Alkaline has a LCOH of 2.8 €/kg, while PEM has a LCOH of 3.2 €/kg. Electricity is the most significant cost driver, contributing 80% of the total hydrogen production cost. The reduction of LCOH is primarily driven by lower electricity prices. Alkaline has the lowest CAPEX and electricity consumption, as shown in Section 2.1.1.1 and Section 2.1.1.2, while PEM has the lowest O&M cost, leading to the price differences between the two technologies.

Scaling up hydrogen production through electrolyzers can result in significant economies of scale. According to IRENA (2020b) estimates, the cost per kilowatt (kW) of capacity for alkaline electrolyzers decreases as the size of the electrolyzer increases, as shown in Figure 2.5. For example, a 1 MW alkaline hydrogen stack has a capital expenditure (CAPEX) of $1000/kW, whereas a 10 MW stack has a CAPEX of $600/kW, and a 100 MW stack has a CAPEX of $400/kW.

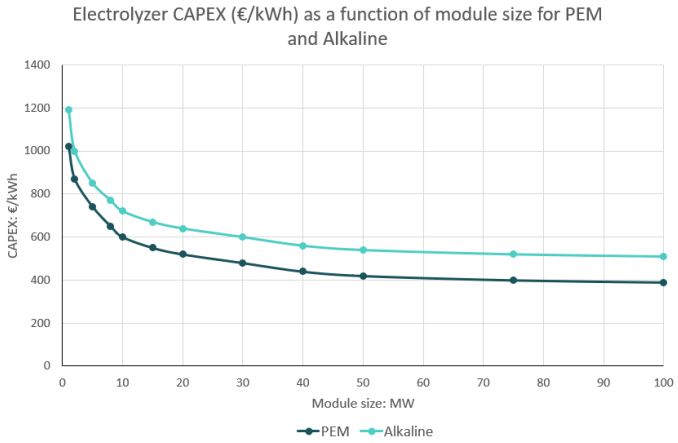

Figure 2.5: Economies of scale in the investment cost of hydrogen production adapted from IRENA (2020b).

2.1.2 Blue and Gray Hydrogen Production

Gray hydrogen is produced from natural gas using either Steam Methane Reforming (SMR) or Autothermal Reforming (ATR) processes. However, gray hydrogen emits significant amounts of greenhouse gases and is not a suitable option for a zero-emission future, as stated by IEA (2019)

Blue hydrogen is a type of hydrogen produced from coal or natural gas with carbon capture and storage (CCS). In Norway, natural gas is the only viable source for blue hydrogen production, as there is no coal industry. However, since only 85-95% of the CO2 can be captured, blue hydrogen is not completely emission-free (Moseman & Herzog, 2021). Additionally, the production of natural gas involves emissions of methane and CO2, which can result in higher GHG emissions than direct burning of the natural gas in some cases, as demonstrated by Howarth and Jacobson (2021) for the USA. Nevertheless, this is not the case with Norwegian gas production (Gardarsdottir, 2021).

This report does not consider blue and gray hydrogen technologies for hydrogen production, as gray hydrogen may not be a suitable for a zero-emissions future. Additionally, Stádlerová and Schütz (2021) show in their study that blue hydrogen technology is not a preferred choice for a Norwegian supply chain in the maritime sector

2.2 Future Demand

The hydrogen industry is already significant, with fertilizer and chemical feedstock production being the main drivers of demand. Unfortunately, the hydrogen used for these industries is not sourced from low-emission production methods, resulting in approximately 900 million tonnes of CO2 emissions in 2020. This amount surpasses the combined emissions of Germany and France, as reported by DNV (2022). Despite the industry's size, only 4% of global hydrogen production was sold on an open market in 2017, according to DNV (2019). Additionally, most hydrogen production is integrated with the supply chain and serves as an input factor, being located close to the consumption point.

Hydrogen is poised to have a significant impact in various industries, including transportation, building heating, electricity generation, and manufacturing (DNV, 2022). The open market for hydrogen is projected to surge from 3 to 240 MtH2/year between 2020 and 2050, with an average annual growth rate of 15.7%. This trend is expected to account for 5% of the world's total energy demand.

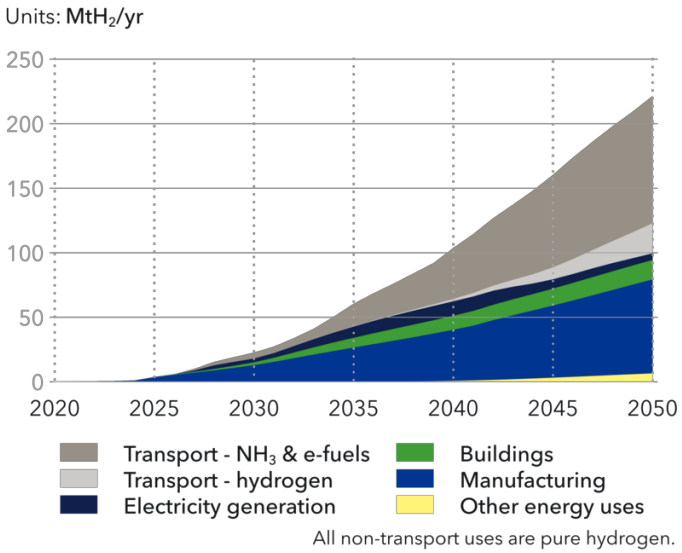

Figure 2.6: Global hydrogen and its derivatives production for energy purposes by usage route (DNV, 2022).

According to DNV (2022) and IEA (2019), there is significant uncertainty surrounding the anticipated demand for hydrogen leading up to 2050, with a wide range of potential projections. Moreover, as there is presently no existing supply chain to facilitate the utilization of hydrogen, the creation of such a system will be necessary from the ground up.

The scope of this report is limited to analyzing the demand for hydrogen solely within the transportation sector of Norway. This decision is based on the fact that the transportation industry is expected to account for the majority of hydrogen demand globally, as illustrated in Figure 2.6. Furthermore, demand from other sectors is typically incorporated into more extensive production processes and does not contribute to the hydrogen sold on the open market. As of 2021, the transportation sector in Norway was responsible for 33% of the country's total CO2 emissions (Miljødierktoratet, 2022).

2.2.1 Road Transport

According to Miljødierktoratet (2022), road transportation accounts for around 50% of the energy consumption in the transportation sector of Norway. This energy consumption is further divided equally between passenger traffic and the transportation of goods, each accounting for 50% of the total.

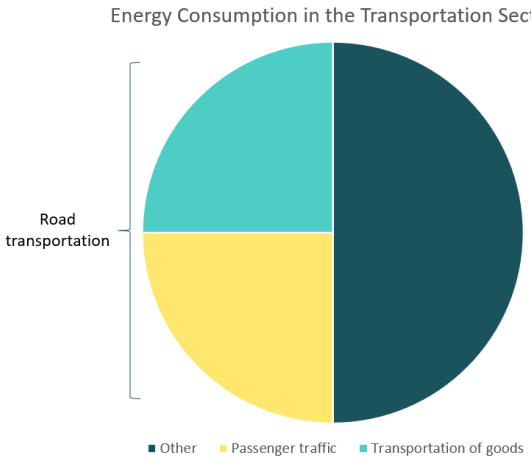

Figure 2.7: Energy consumption in the transportation sector (Miljødierktoratet, 2022).

The majority of energy consumption in road transport is derived from fossil fuels, however, effective policies implemented by the Norwegian government have led to a reduction in emissions from private cars in recent years, as more individuals are transitioning to electric cars. Electric vehicles are not as suitable for longer-distance transportation of passengers or goods due to lengthy charging times and the high weight and space requirements for batteries, thus DNV (2019) has identified three segments in which hydrogen may serve as a more appropriate low-emission alternative: light-weight vehicles, bus transportation, and heavy-weight vehicles.

2.2.1.1 Light Weight Vehicles

At present, light-weight hydrogen cars (FCEVs) are more costly than electric vehicles (EVs), and it is anticipated that EVs will prevail in this segment until 2050. Nonetheless, FCEVs can be competitive in certain segments where there are lengthy gaps between charging stations, high range requirements, or prolonged usage periods, as noted by DNV (2019). However, the report does not provide any estimates regarding the magnitude of this demand.

2.2.1.2 Bus Transportation

The degree of competitiveness of hydrogen buses is contingent on their application. In the case of buses that have short travel distances and a limited number of daily routes within urban areas, such as school buses, electric buses are projected to be the predominant technology. On the other hand, for routes that cover greater distances and have lower population densities, hydrogen buses are expected to be able to compete with electric buses. Various countries have already implemented hydrogen buses, including the USA, France, and Japan (DNV, 2019).

2.2.1.3 Heavy Weight Vehicles

Hydrogen is projected to be a viable alternative to electric vehicles for heavy vehicles because of the limitations in range that electric vehicles currently face. Regarding competition with diesel vehicles, DNV (2019) refers to studies that suggest FCEVs will be competitive by 2025.

2.2.2 Rail Transport

A significant proportion of trains in Norway already incorporate zero-emission technology, with over 80% of train traffic being serviced by electric trains. However, the reason for not electrifying the remainder of the railway in Norway is due to the high infrastructure expenses associated with low-traffic routes. Looking toward a zero-emission future, hydrogen-driven trains will likely compete against battery-electric trains. Hydrogen trains benefit from a longer range and are lighter, while electric trains are expected to have a lower price. This competition between electric and hydrogen trains is likely to divide the rail sector, which is unsuited for contact wire, between hydrogen and battery-driven trains (DNV, 2019).

2.2.3 Maritime Passenger Transport

Public tenders play a crucial role in Norway's maritime passenger transportation sector as they determine the operation of various routes. These tenders may specify the use of zero- or low-emissions technology in contracts, such as the upcoming Bodø-Moskenes-Værøy-Røst ferry connection which requires the use of hydrogen as fuel starting from 2025 (Samferdselsdepartementet, 2022). Using public tenders, the Norwegian government can help promote the hydrogen market and boost demand. This can be anticipated beforehand as public tenders are typically announced years in advance.

2.3 Distribution of Hydrogen

The transportation of hydrogen presents a range of technological and economic challenges. Despite being the lightest element, hydrogen has a low volumetric energy density, measuring between 0.8-2.1 kWh/L depending on pressure, state, and temperature. As depicted in Figure 2.8, this is approximately four to five times lower than gasoline and diesel.

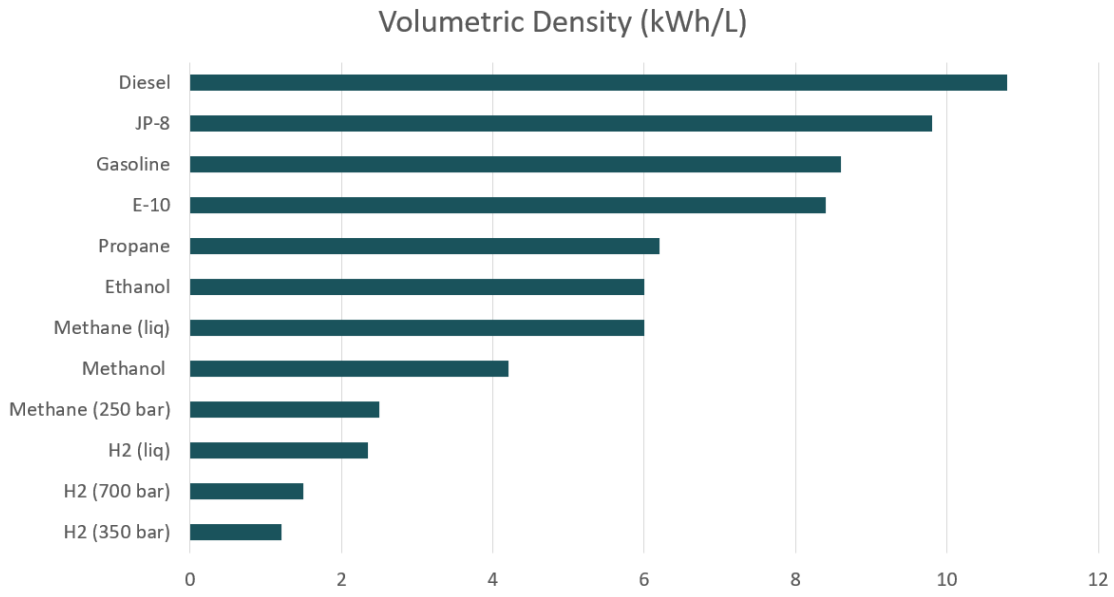

Figure 2.8: Volumetric energy density for different fuels based on lower heating values (US. Department of energy, 2022).

The limiting factor in transporting hydrogen is its volumetric energy density (Danebergs & Aarsskog, 2020b). Due to this limitation, large volumes of hydrogen are required for transportation, resulting in higher prices per kWh compared to other energy sources. Additionally, hydrogen must be handled at high pressures or low temperatures to be transported as a liquid. This process incurs additional costs, such as compression or cooling expenses, which further increases the overall expense of transporting hydrogen.

Transporting hydrogen can be achieved through various means, including compressed or liquid form, or as a derivative with a higher volumetric density, such as ammonia or liquid hydrogen organic carriers (LHOCs). However, if the final demand is for pure hydrogen, converting it into these derivatives incurs energy losses that make it economically unviable for transportation within Norway (Ishimoto et al., 2020). Moreover, hydrogen transportation through its derivatives is still in its early stages of development, leading to uncertainties (Damman et al., 2020). Hence, this report excludes the option of transporting hydrogen through its derivatives.

The transportation method for hydrogen depends on the distance and volume to be transported. For low volumes, trucks are the most suitable option. Compressed form is preferable for short distances, whereas liquefaction is more cost-effective for longer distances. Pipelines are the cheapest option for large volumes and short distances, while shipping is the most economical means of transportation for long distances and large volumes. Figure 2.9 illustrates the costs and cheapest mode of transport for a specific set of volumes and distances.

Specific minimum cost mode for hydrogen transport

Production volume (tpd) \ Distance (km)	10	50	100	250	500	750	1000	2000	3000
1	CT	CT	CT	CT	CT	LT	LT	LT	LT
5	CSP	CT	CT	CT	LT	LT	LT	LT	LS
10	CSP	CT	CT	LT	LT	LT	LT	LS	LS
20	CSP	CSP	CSP	LT	LT	LS	LS	LS	LS
30	CSP	CSP	CSP	CSP	CS	CS	CS	CS	LS
40	CSP	CSP	CSP	CSP	CS	CS	CS	LS	LS
50	CSP	CSP	CSP	CSP	CS	CS	CS	LS	LS
60	CPP	CSP	CSP	CSP	CS	CS	CS	LS	LS
70	CPP	CSP	CSP	CSP	CS	CS	LS	CS	LS
80	CPP	CSP	CSP	CSP	CS	CS	CS	LS	LS
90	CPP	CSP	CSP	CSP	CS	CS	CS	LS	LS
100	CPP	CSP	CSP	CSP	CS	CS	CS	CS	LS

Specific minimum cost for hydrogen transport

Production volume (tpd) \ Distance (km)	10	50	100	250	500	750	1000	2000	3000
1	2.92	4.25	5.91	10.89	19.18	24.65	26.99	37.74	47.18
5	2.03	3.79	5.57	10.66	18.72	21.33	23.68	33.88	38.40
10	1.05	3.79	5.51	10.59	13.20	15.67	18.15	20.77	21.33
20	0.56	2.53	4.99	10.42	12.96	14.11	14.25	14.82	15.38
30	0.39	1.71	3.35	8.27	11.63	11.63	11.63	11.63	13.40
40	0.31	1.30	2.53	6.22	8.97	8.97	8.97	11.85	12.41
50	0.26	1.05	2.03	4.99	7.37	7.37	7.37	11.25	12.95
60	0.23	0.89	1.71	4.17	6.30	6.30	6.30	10.85	12.36
70	0.21	0.77	1.47	3.58	5.54	5.54	10.01	10.03	11.95
80	0.19	0.68	1.30	3.14	4.97	4.97	8.90	11.07	11.63
90	0.18	0.61	1.16	2.80	4.53	8.02	8.02	10.82	11.39
100	0.16	0.56	1.05	2.53	4.17	7.31	7.31	10.45	11.76

CT Compressed truck | LT Liquid truck | CSP Compressed steel pipeline | CS Compressed ship | LS Liquid ship

Figure 2.9: Specific minimum cost in NOK/kg and mode for hydrogen transport (Madsen, 2019)

Figure 2.9, as presented by Madsen (2019), fails to consider the strict Norwegian regulations requiring a 45-minute resting period after a truck has been driven for 4.5 hours, which necessitates the employment of additional drivers for longer journeys. The cost of transportation increases significantly in Norway due to the high labor costs associated with employing more drivers (Arbeidslivet.no, n.d.). As a result, Figure 2.9 does not reflect the cost spike that occurs due to this regulation, making the cost of hydrogen transportation above 1000 km appear lower than it actually is.

2.4 General Cost Functions of Production Plants

The costs of building and operating hydrogen production facilities are expensive, and can be divided into two categories: short-term and long-term costs. Long-term costs are associated with expenses that extend over several years, and involve a trade-off between capital and labor input factors. The goal is to minimize these costs while maximizing production levels, resulting in an optimal combination of capital and labor that can be identified at the intersection of isoquant and isocost curves (Mathis & Koscianski, 2002). Figure Figure 2.10 demonstrates this concept, where the ideal combination of capital and labor for a given production quantity, q_1, is located at the intersection of line AB and the isocost curve for q_1. Once a capital and labor combination is determined, the capital is fixed and adjustments to production can only be made by modifying the labor input. For example, to increase production to q2, labor input must be adjusted to L3, however, this is not optimal as the ideal combination of labor and capital for q_2 can be found at the intersection of curve CD and the cost isocost for q_2, with L_2 and K_2.

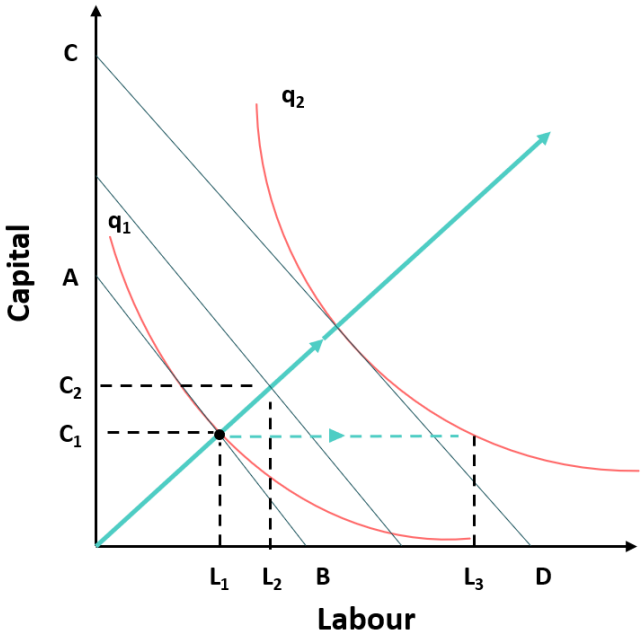

Figure 2.10: Long- and short-term expansion paths adapted from Pindyck and Rubinfeld (2018).

At a specific capacity, the short-term cost function is linked to the long-term cost function, with the short-term cost curves tangent to the long-term cost curve. In the short-term, labor is the only input factor that can be adjusted, while capital remains constant. Assuming that the marginal returns of input factors are decreasing, the short-term cost function is convex in shape (Mathis & Koscianski, 2002), as illustrated in Figure 2.11. The shape of the function is due to increasing economies of scale (Pindyck & Rubinfeld, 2018).

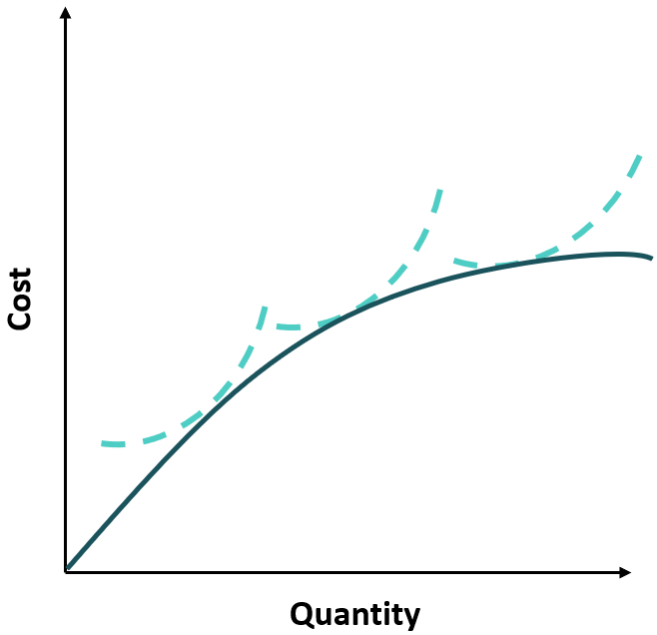

Figure 2.11: Long- and short-term cost functions for production facilities, adapted from (Pindyck & Rubinfeld, 2018).

When it comes to hydrogen production, the primary long-term decision involves determining the capacity to invest in and later making adjustments to that capacity. On the other hand, decisions such as production quantities and transportation, which may require daily adjustments, are associated with short-term costs. In the short-term, it is necessary to keep at least one input factor constant, which is typically the capital for hydrogen production, while labor inputs such as electricity and employees can be adjusted. As demonstrated in Section 2.1.1.1 and Section 2.1.1.2, it is not possible to increase production beyond the installed capacity for hydrogen production. As a result, the short-term cost curve is only valid to the left of the long-term cost curve in Figure 2.11.

2.5 The Norwegian Electricity Market

As indicated in Section Section 2.1.1.3, the cost of electricity is the most significant factor in determining the levelized cost of hydrogen (LCOH). Consequently, the cost of electricity in Norway has a considerable impact on the optimal production planning and the choice of regions for locating hydrogen production plants.

In Norway, there are five distinct regional electricity trading areas: NO1 (based in Oslo), NO2 (based in Kristiansand), NO3 (based in Trondheim), NO4 (based in Tromsø), and NO5 (based in Bergen) (Statnett, 2022). These regions have varying power generation and consumption requirements, with the three southern regions being more interconnected with the continental European power market. As a result, there are often significant discrepancies in power prices between the northern and southern regions of Norway, as illustrated in Figure 2.12. The regional division of the bidding zones is displayed in Figure 2.13.

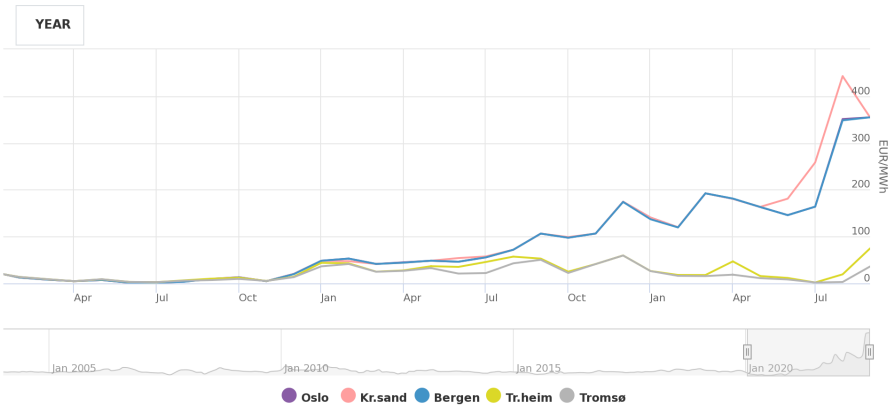

Figure 2.12: Prices of power between the five Norwegian balancing regions, from January 2021, until September 2022 (Nord Pool, 2022a).

Figure 2.13: This map show the five electricity price bidding areas in Norway (Statnett, 2022).

Hydropower is Norway's primary electricity production source, accounting for 90% of the country's power generation (Statkraft, 2022). The remaining 10% primarily consists of wind power, which contributes 7.5% to the power supply. Norway leads the world in the share of renewable energy production, with 99% of its electricity coming from renewable sources (Enerdata, 2022), owing to its favourable mountainous topography for hydropower. As a result, the price of electricity in Norway is heavily influenced by the water volume in its reservoirs. This, combined with higher energy consumption during the winter months, creates seasonal variation in power prices, as depicted in Figure 2.14. Typically, power prices are at their lowest around July and peak during the winter months.

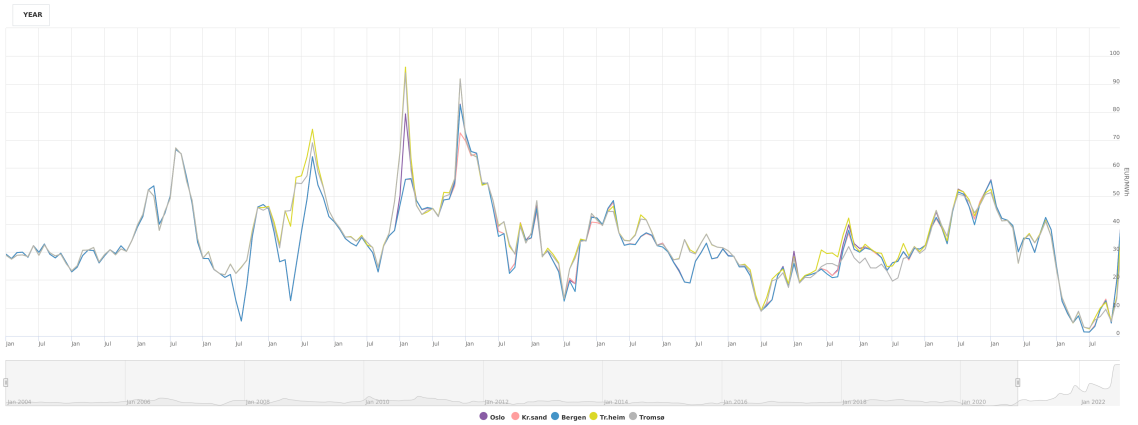

Figure 2.14: Power prices in Norway's five bidding zones between Q1 2004 to Q4 2020. (Nord Pool, 2022b).

Electricity procurement often occurs a day in advance of delivery and consumption via the *day-ahead market*, where hourly electricity prices are set according to the previous day's supply and demand dynamics (Olje- og energidepartementet, 2022). Despite the relatively flat daily price profile in the Norwegian power system, due to low costs of adjusting production, there are instances where the price can fluctuate significantly from hour to hour Figure 2.15. Such price dynamics present challenges for industries like hydrogen production, as electricity costs are the main cost component. If the start-up time exceeds an hour, producers may not fully exploit potential hourly price drops, given the electricity required for warming up during the preceding hours. Moreover, shorter start-up times result in a larger proportion of actual production time within the hour, thereby increasing the potential for exploiting price drops. This underscores the value of operational flexibility offered by PEM to Alkaline in cases of high price volatility, as it enables greater utilization of price drops, thereby reducing production costs.

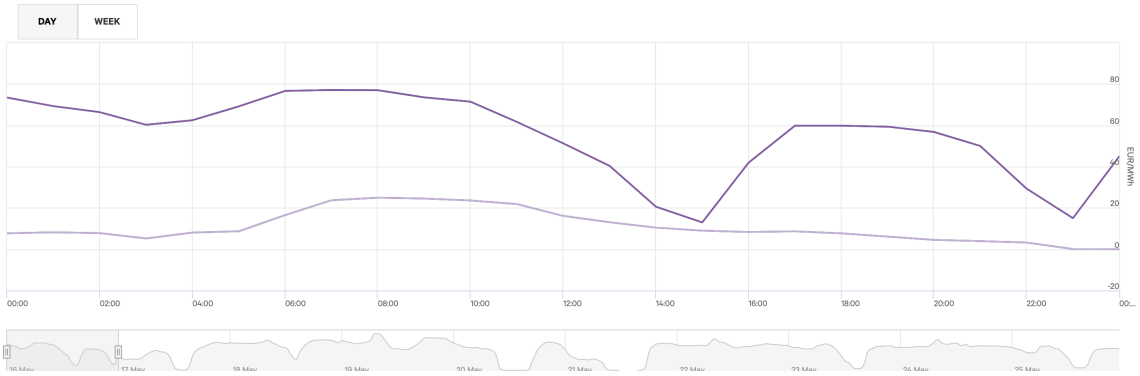

Figure 2.15: Hourly day-ahead prices between for the bidding zones of Norway 16.05.2023. One can see price spikes of over a 100%at 15:00-16:00 and 23:00 - 24:00.

Chapter 3

Related Literature

This chapter discusses the literature that studies problems relevant to stochastic programming, facility location, supply chain network design, and hydrogen production. We begin in Section 3.1 by introducing the facility location problem for deterministic problems and under economies of scale. After this, we discuss relevant concepts within stochastic programming in Section 3.2, such as multi-period and multi-stage stochastic facility location programs, as well as multi-horizon stochastic programming. Next, we study supply chain network design in Section 3.3, where a special emphasis is put on hydrogen supply chain networks. Last, in Section 3.4, we cover literature that captures the modeling of hydrogen production at the operational level.

3.1 Facility Location

Decisions pertaining to the location and configuration of production facilities and warehouses are critical for industrial companies, typically having a significant impact on production and transportation costs, as well as the demand one can serve. Given their substantial cost and long-term nature, these decisions must be thought through carefully. The Facility Location Problem (FLP) focuses on finding the optimal locations for facilities or equipment to serve a specific set of customers or demand points (Saldanha-da-Gama, 2022). In its simplest form, which includes no restrictions on capacity and transportation, the FLP is known as the uncapacitated facility location problem (UFLP). In real life, however, both lower and upper bounds on the capacities typically exist. The version of FLP that considers such constraints is known as the capacitated facility location problem (CFLP). For both problems, the investment, production, and transportation costs can be location dependent. Sridharan (1995) provides a review of the CFLP and proposes a generic model for solving this problem, as seen below:

$$z = min \sum_{i=1}^{m} \sum_{j=1}^{n} c_{ij} x_{ij} + \sum_{i=1}^{n} f_j y_j \tag{3.1}$$

subject to

$$\sum_{j=1}^{n} x_{ij} = 1. \qquad i = 1, ..., m \tag{3.2}$$

$$\sum_{i=1}^{m} d_i x_{ij} \leq q_j y_j, \qquad j = 1, ..., m \tag{3.3}$$

$$0 \leq x_{ij} \leq y_j, \qquad i = 1, ..., m; j = 1, ..., n \tag{3.4}$$

$$\sum_{i=1}^{n} q_j y_j \geq \sum_{i=1}^{m} d_i, \qquad j = 1, ...n \tag{3.5}$$

$$y_j \in \{1, 0\}, \qquad j = 1, ..., n \tag{3.6}$$

Where c_{ij} is the total cost of transportation from facility j to serve customer i; d_i is the demand of customer i: q_j is the capacity of facility j; f_j is the fixed cost associated with plant j; x_{ij} is the fraction of the demand of customer i supplied from plant j; $y_j = 0$ or 1, depending on whether plant j is closed or open; $I = \{1, ..., m\}$: the set of customers; $J = \{1, ..., n\}$: set of potential locations.

The model considers fixed costs and capacities for each location, with the choice of locations being the only decision variable. One can use a continuous investment variable when dealing with linear investment costs. However, if the investment costs are nonlinear, an alternative approach is to have a discrete set of capacities to choose from. In this case, a variable is generated for each capacity at each location to decide the capacity to install. As the number of capacities to choose from increases, the number of variables will grow polynomially.

3.1.1 Facility Location Under Economies of Scale

As noted in Section 2.1.1.3, hydrogen production benefits from economies of scale, causing non-linear increases in investment costs as capacity expands.To manage this aspect, many Facility Location Problem (FLP) studies employ Staircase Costs (FLSC). According to Holmberg (1994), the staircase cost function is a finite, piecewise linear, and increasing function with a discrete set of discontinuities.

The modular capacitated plant location model (MCPL) is a generalized version of the FLSC. This model selects capacities from a finite and discrete set of options without limiting them to multiples of a particular size. Correia and Captivo (2003) used this model to study healthcare facility locations in Portugal. Their study includes investment and production costs related to specific capacities and facility locations and a set of customers whose demand must be met by particular production facilities.

In their study, v.d. Broek et al. (2006) address an FLP involving slaughterhouse locations in Norway, incorporating economies of scale. They utilize a discretized investment cost function with multiple breakpoints to represent non-linear investment costs as a piecewise linear function. Their model also includes transportation costs and demand requirements. Here, transportation costs refer to the cost of moving animals from farms to slaughterhouses, and demand represents the total number of animals that must be slaughtered.

3.2 Stochastic programming

Uncertainty is a critical factor in decision-making. Variables such as customer demand, energy prices, and technological advancements, among others, all carry inherent uncertainty. Stochastic programming addresses these uncertainties in optimization problems by employing known or estimated probability distributions for the parameters.

Stochastic programming originated with Dantzig (1955), who introduced the two-stage stochastic linear program with recourse aimed at minimizing expected total costs. The model incorporates stochastic cost coefficients in the objective function, each with a specific probability distribution. Dantzig (1955) also demonstrated how to manage variance, drawing on Markowitz's mean-variance analysis. A comprehensive two-stage stochastic linear program formulation is presented by Birge and Louveaux (2011):

$$\min z = c^T y + E_\xi[\min q_s^T x_s] \tag{3.7}$$

subject to:

$$Ay = b \tag{3.8}$$

$$T_s y + W x = h_s \tag{3.9}$$

$$y \geq 0, x_s \geq 0 \tag{3.10}$$

This formulation comprises two stages and presumes a finite discrete set of possible scenarios, $\mathcal{S}$, each representing a complete realization of all uncertain parameters (Correia & Saldanha-da-Gama, 2019). In the first stage, decisions, y, are made under uncertainty about future, ξ, realizations. These first-stage decision variables are present in the objective (3.7), in constraint (3.8), and in (3.9), where they connect to second-stage variables, x_s. The second stage, after the realization of a random event $s \in \mathcal{S}$, allows decision-making with known second-stage data q_s, h_s, and T_s. The vector $\xi_\omega^T = (q_\omega^T, h_\omega^T, T_\omega^T)$ represents the random variables in the second stage data. The first-stage variables y are independent of s, while x depends on s, which adds complexity as the second-stage decisions can differ per scenario. Though the problem involves two stages, this formulation can extend to accommodate multiple stages, forming a multi-stage stochastic programming problem.

The flow of information is crucial in stochastic problems. Decisions made in one stage can not be based on information one receives after the decision has been made. These decisions are said to be made *ex-ante*, whereby all first-stage decisions remain consistent across all scenarios. Decisions made after the uncertainty is revealed are said to be *ex-post* decisions and typically react to realized values of uncertain parameters. For instance, in a facility location problem, facility locations often constitute *ex-ante* decisions due to their strategic nature (Correia & Saldanha-da-Gama, 2019).

3.2.1 Two-stage Stochastic Facility Location Problems

Long-term investment decisions in production facilities need consideration of location-influencing factors like customer demand, production, and transportation costs. Given the inherent uncertainty of these factors, informed decision-making poses a challenge. In a two-stage facility location problem, facility location decisions are made during the first stage without knowing the actual values of uncertain parameters until the second stage. This necessitates anticipating potential scenarios to ensure decision robustness under varying circumstances.

Ravi and Sinha (2004) explore a particular instance of a two-stage uncapacitated stochastic facility location problem. This problem, formulated below, focuses on an initial stage with unknown demand and aims to minimize the sum of the anticipated fixed and variable costs. The uncertain demand varies across multiple scenarios, each associated with distinct probabilities:

$$z = \sum_{i \in F} f_i y_i^0 + \sum_{k=1}^{m} p_k \Big(\sum_{i \in F} f_i^k y_i^k + \sum_{i \in F, j \in D} d_j^k c_{ij} x_{ij}^k \Big) \tag{3.11}$$

subject to:

$$\sum_{i \in F} x_{ij}^k \geq d_j^k, \qquad j = 1, ..., |D|; k = 1, ..., m \tag{3.12}$$

$$x_{ij}^k \leq y_i^0 + y_i^k, \qquad i = 1, ..., n; j = 1, ..., |D|; k = 1, ..., m \tag{3.13}$$

$$x_{ij}^k, y_{ij}^k \in 0, 1, \qquad i = 1, ..., n; j = 1, ..., |D|; k = 1, ..., m \tag{3.14}$$

In this formulation, F denotes the set of facilities, D is the set of clients, and c_{ij} represents the distance between each facility and client. Each scenario k carries a specific probability p_k and demand d_j^k. Every facility i has an opening cost f_i^0 for the first stage and a recourse cost f_i^k. The variable x_{ij}^k equals one if, and only if, facility i serves customer j in scenario k. According to constraint (3.13), if $x_{ij}^k = 1$, then facility i must open either in the first stage, implying $y_i^0 = 1$, or in the recourse scenario k, meaning $y_i^k = 1$, or in both. This single-period problem doesn't specify costs for the second stage. Risk neutrality is assumed, as demonstrated by minimizing the expected costs. However, the model can incorporate risk aversion by adding a penalty for variance (Correia & Saldanha-da-Gama, 2019).

Schütz et al. (2008) developed a model that incorporates both uncertainties in the demand and the short-term costs, with an S-shaped long-term cost function. The model considers transportation costs and costs related to investing, maintaining, and operating facilities, expressed through general and non-linear facility costs that capture economies and diseconomies of scale. In the first stage, capacity decisions are made to establish a range where variable costs are linear and equal to long-run costs. However, production volumes outside this range are allowed and are subject to a piecewise linear short-term cost function. Thus, this model presents a hybrid approach that combines features of both capacitated and uncapacitated facility location problems.

As far as we know, Snyder (2006) is the most comprehensive review of facility location under uncertainty. In addition, Melo et al. (2009) provides a review of facility location in the context of supply chain management. Correia and Saldanha-da-Gama (2019) also cover some of the more recent literature on facility location under uncertainty, following Snyder (2006).

3.2.2 Multi-Period Stochastic Facility Location Problems

So far, we have explored facility location problems where influential parameters like investment costs, demand, and production costs are assumed constant. However, real-world problems often exhibit temporal variations in these parameters. To accommodate predictable changes, a dynamic model is frequently necessary (Nickel & Saldanha-da-Gama, 2019).

The concept of a *planning horizon*, the timeframe over which decisions are made, becomes essential when considering facility location over time. Problems incorporating a multi-period planning horizon are termed as multi-period. Thus, multi-period facility location problems (MPFLPs) determine where and what types of facilities to establish and when to do so within the planning horizon. This allows for potential capacity expansions in periods following the facility's establishment, often in response to increasing demand. Nickel and Saldanha-da-Gama (2019) introduce a standard multi-period pure phase-in CFLP (facilities can only be opened):

$$\min \sum_{t \in T} \sum_{i \in I} f_{it} y_{it} + \sum_{t \in T} \sum_{j \in J} (\sum_{i \in I} c_{ijt} x_{ijt} + o_{jt} d_{jt} v_{jt}) \tag{3.15}$$

subject to:

$$\sum_{i \in I} x_{ijt} + v_{jt} = 1, \qquad t = 1, ..., |T|; j = 1, ..., |J| \tag{3.16}$$

$$\sum_{i \in I} y_{it} \leq m_t \qquad t = 1, ..., |T| \tag{3.17}$$

$$\sum_{j \in J} d_{jt} x_{ijt} \leq Q_i y_{it} \qquad i = 1, ..., I; t = 1, ..., T \tag{3.18}$$

$$y_{it} \geq y_{i(t-1)} \qquad t = 2, ..., |T|; i \in I^c \tag{3.19}$$

$$x_{ijt} \geq 0 \qquad t = 1, ..., |T|; i = 1, ..., |I|; j = 1, ..., |J| \tag{3.20}$$

$$y_{it} \in 0, 1 \qquad t = 1, ..., |T|; i = 1, ..., |I| \tag{3.21}$$

In the above formulation, y_{it} denotes whether a facility operates at location i in time period t, and f_{it} represents a fixed cost incurred from operating a facility. The decision variable x_{itj} represents the fraction of the demand of customer $j \in J$ in period $t \in T$ that is supplied by facility $i \in I$, with c_{ijt} being its corresponding unit cost. The parameter o_{jt} represents the unit costs of unmet demand in cases where the total customer demand is unsatisfied, with v_{jt} representing the proportion of unmet customer demand from time period t. Demand satisfaction of the customers, including potential unmet demand, is accounted for in (3.18). Only a given number of facilities m_t can be operated at time t, which is handled in restriction (3.17). Restriction (3.21) enforce capacity restrictions.

The above multi-period model allows for facility investments at any location across the whole planning horizon, given that no existing facility was built beforehand. It does not allow for capacity expansions, however. By assuming that capacity expansions occur at the beginning of the time periods, the problem can be adjusted to allow for expansions in the following way:

$$\min \sum_{t \in T} \sum_{i \in I} \sum_{p \in P_i} f_{ipt} y_{ipt} + \sum_{t \in T} \sum_{j \in J} \sum_{i \in I} \sum_{p \in P_i} (c_{ijpt} x_{ijpt} + o_{jt} d_{jt} v_{jt}) \tag{3.22}$$

subject to:

$$\sum_{i \in I} \sum_{p \in P_i} x_{ijpt} + v_{jt} = 1, \qquad t = 1, ..., |T|; j = 1, ..., |J| \tag{3.23}$$

$$\sum_{i \in I} \sum_{p \in P_i} y_{ipt} \leq m_{pt} \qquad t = 1, ..., |T| \tag{3.24}$$

$$\sum_{j \in J} d_{jt} x_{ijpt} \leq n_{ip^0} Q_p + \sum_{\tau=1}^{t} Q_p y_{ip\tau} \qquad i = 1, ..., I; t = 1, ..., T; p = i = 1, ..., |P| \tag{3.25}$$

$$y_{ipt} \geq y_{ip(t-1)} \qquad t = 2, ..., |T|; i \in I^c \tag{3.26}$$

$$x_{ijpt} \geq 0 \qquad t = 1, ..., |T|; i = 1, ..., |I|; j = 1, ..., |J|; p = i = 1, ..., |P| \tag{3.27}$$

$$y_{ipt} \in 0, 1 \qquad t = 1, ..., |T|; i = 1, ..., |I|; p = i = 1, ..., |P| \tag{3.28}$$

The above model considers a set of facility types P. For each location, a subset of these types $P_i \in P$ can be progressively established during the planning horizon, such that

operational capacity can be adjusted. The parameter n_{ip^0} denotes the number of facilities of type p operating at location i before the beginning of the planning horizon. Therefore, the problem does not capture initial investments and further capacity expansions at the same location but rather adjustments to a system that has already been built.

Stádlerová et al. (2023) present a multi-period stochastic facility location problem for planning the Norwegian hydrogen supply chain for transportation. This model includes various demand scenarios, each representing demand realizations across multiple years. Capacity extensions are permitted to meet the demand for all years in a scenario, with economies of scale assumed for both investment and operational costs. The former is modeled in a staircase fashion. The model also imposes constraints on the maximum transportation distance, ensuring facilities only meet a subset of the customer demand. Due to the computational difficulty of the model, Lagrange Relaxation was applied to relax the restrictions connecting facilities and customers. The resulting Lagrangian subproblem optimizes the opening and expansion schedule for each facility across all scenarios, minimizing total expected costs. The scheduling of capacity expansions for a specific location is formulated and solved as a shortest-path problem via dynamic programming. Furthermore, for a given capacity, time period, and location, the customer allocation problem is solved as a continuous knapsack problem.

Multi-period problems add time as a complexity dimension, making models more challenging and time-consuming to solve. Therefore, there is a trade-off between the value of formulating the problem as a multi-period model and the computational complexity. The value of a multi-period solution is often case-dependent when compared to a static counterpart. The latter uses the available data within the planning horizon to seek a time-invariant solution, focusing on the optimal setup in the first period to fulfill all future periods' needs. Under capacity restrictions and changing parameters such as demand, a static solution may require assuming maximum demand levels for every stage within the planning horizon. This can lead to high costs and suboptimal solutions, particularly when capacity expansions can exploit economies of scale. If investment costs decrease over time, a reference cost must be established, such as the maximum or average cost, to balance current expenditure against future adjustments for optimal planning (Nickel & Saldanha-da-Gama, 2019). To the knowledge of this thesis writers, Nickel and Saldanha-da-Gama (2019) is the most comprehensive review on multi-period facility location.

3.2.3 Multi-stage Stochastic Programming

In two-stage stochastic programming, it's assumed that uncertainties realize only once after first stage decisions have been made. However, many practical problems require sequential decision-making in response to outcomes that unfold over time (Birge & Louveaux, 2011). To address this complexity, *multi-stage stochastic programming* extends the two-stage approach to accommodate sequential decision-making and the progressive realization of uncertainties. A general linear multi-stage stochastic program with fixed recourse is provided by Birge and Louveaux (2011). The model uses implicit nonanticipativity constraints:

$$\min z = c^1 x^1 + E_{\xi}^2[\min c^2(\omega)x^2(\omega^2) + ... + E_{\xi^H}[\min c^H(\omega)x^H(\omega^H)]...] \tag{3.29}$$

subject to:

$$W^1 x^1 = h^1 \tag{3.30}$$

$$T^{t-1}(\omega^t)x^{t-1} + W^t x^t(\omega^t) = h^t(\omega) \quad t = 2, ..., H; \tag{3.31}$$

$$\dots \vdots \tag{3.32}$$

$$T^{H-1}(\omega^H)x^{H-1} + W^H x^H(\omega^{H-1}) = h^H(\omega); \tag{3.33}$$

$$x^1 \geq 0; x^t(\omega^t) \geq 0 \quad t = 2, ..., H; \tag{3.34}$$

As depicted in (3.29), the model's objective is to minimize the sum of expected costs $c^t(\omega^t)$ associated with all decisions $x^t(\omega^t)$ taken at each stage $t \in H$. Here, W^t is a known parameter, whereas T^t, h^t, and $c^t(\omega^t)$ are stochastic parameters, accommodating variations in cost coefficients, constraint coefficients, and right-hand-side values. These stochastic parameters can encapsulate variability in future investment costs, operational costs, and demand. The decision variable x depends on the history up to time t, represented as ω^t, which is determined by the random process ξ^t.

3.2.3.1 Multi-stage Stochastic Facility Location Problems

Multi-stage facility location problems (MSFLPs) can offer more flexibility than their two-stage multi-period counterparts, as new decisions can be made after the gradually revealed information. This could be relevant for making adjustments such as capacity expansions and new investments when new information about customer demand is revealed. To our knowledge, however, only a handful of papers address MSFLPs. Yu et al. (2021) assesses the value of multi-stage facility location with risk aversion by comparing two two-stage multi-period CFLPs to a multi-stage one. The following mathematical formulation is introduced:

$$\min \sum_{t=1}^{T}\sum_{i=1}^{M} f_{ti} \sum_{\tau=1}^{t} x_{\tau i} + \sum_{t=1}^{T}\sum_{i=1}^{M}\sum_{j=1}^{N} c_{tij} y_{tij} \tag{3.35}$$

subject to:

$$\sum_{i=1}^{M} y_{tij} = d_{tj}, \qquad j = 1, ..., N; t = 1, ..., T \tag{3.36}$$

$$\sum_{j=1}^{N} y_{tij} \leq h_{ti} \sum_{\tau=1}^{t} x_{\tau i} \qquad i = 1, ..., M; t = 1, ..., T \tag{3.37}$$

$$\sum_{j=1}^{t} x_{\tau i} \leq 1, \qquad i = 1, ..., M; t = 1, ..., T \tag{3.38}$$

$$x_{ti} \in \mathbb{Z}_+ \qquad i = 1, ..., M; t = 1, ..., T \tag{3.39}$$

$$y_{tij} \in \mathbb{R}_+ \qquad i = 1, ..., M; t = 1, ..., T \tag{3.40}$$

The problem involves $|T|$ stages, where in each stage $t \in T$, the decision to rent $1, ..., M$ potential facilities is made. The coefficient c_{tij} signifies the unit cost of shipping a product from facility i, and f_{ti} is the fixed rental cost for facility i at stage t. The objective function in (3.35) seeks to minimize total rental and operational costs across all stages. Facility capacity at location i in stage t is represented by h_{ti}. Demand $d_{tj}, t \neq 1$ is considered stochastic, following a known probability distribution, whereas the first stage demand

d_{1j} is deterministic. The constraint in (3.36) ensures demand satisfaction, while (3.37) restricts product shipment not to exceed production capacity. Constraint (3.38) limits facility openings to a single instance per location.

Traditional two-stage FLPs are NP-hard, which require a long runtime for large decision spaces. Expanding a two-stage FLP to become multi-stage further increases the complexity and runtime exponentially, and are thus difficult problems to solve. It is, therefore, useful to use either heuristics, meta-heuristics, or approximation methods to solve such problems within a reasonable time. Lai et al. (2019) solves the following multi-objective four-stage CFLP using simplified swarm optimization:

$$\begin{aligned}\min \sum_{i=1}^{Nsup}\sum_{j=1}^{Nplt} s_{ij}x_{ij} + \sum_{j=1}^{Nplt}\sum_{k=1}^{Ndtc} t_{ij}y_{jk} \\ + \sum_{k=1}^{Ndtc}\sum_{l=1}^{Ncus} u_{kl}z_{kl} + \sum_{j=1}^{Nplt} f_j v_j + \sum_{k=1}^{Ndtc} g_k r_k\end{aligned} \tag{3.41}$$

$$\max \sum_{j=1}^{Nplt} Uplt_j y_{jk} + \sum_{k=1}^{Ndtc} Udtc_k z_{kl} \tag{3.42}$$

Subject to:

$$sum_{j=1}^{Nplt} x_{ij} \leq a_i \qquad i = 1, ..., |I|; \tag{3.43}$$

$$\sum_{k=1}^{Ndtc} y_{jk} \leq b_j v_j \qquad j = 1, ..., |J|; \tag{3.44}$$

$$\sum_{l=1}^{Ncus} z_{kl} \leq c_k z_k \qquad k = 1, ...|K|; \tag{3.45}$$

$$\sum_{k=1}^{Ndtc} z_{kl} \geq d_l \qquad l = 1, ..., |L|; \tag{3.46}$$

$$v_j, z_k = \{0, 1\} \forall j \qquad k = 1, ..., |K|; \tag{3.47}$$

$$x_{ij}, y_{jk}, z_{kl} \geq 0 \qquad i = 1, ..., |I|; j = 1, ..., |J|; k = 1, ...|K|; l = 1, ..., |L|; \tag{3.48}$$

In the model discussed in the referenced paper, the objective function shown in Equation (3.41) is designed to minimize the overall cost of a supply chain network (SCN), incorporating both transportation and fixed costs. In contrast, Equation (3.42) is purposed to maximize the total utility derived from all operational facilities, which includes plants and distribution centers. The calculation of facility utility leverages the Fuzzy Analytic Hierarchy Process (FAHP), a method that employs qualitative factors outlined in the paper. Each weight indicated as $wplt_{jm}$ or $wdtc_{km}$ for instance, is determined through expert opinion as presented in this model by Lai et al. (2019). Constraints pertaining to capacity for suppliers, plants, and distribution centers are respectively represented by Equations (3.43)–(3.45). Meanwhile, equation (3.46) is designed to ensure customer demand satisfaction.

This model relates to the capacitated facility location problem (CFLP), which is recognized as a special case of the multi-stage CFLP. Due to the NP-hard nature of CFLP, it is necessary to apply heuristic or meta-heuristic strategies to solve the problem effectively. Given that multiple non-dominated solutions exist for multi-objective problems, providing a spectrum of compromise alternatives for decision-makers, the authors propose a multi-objective evolutionary algorithm (MOEA). This algorithm is intended to generate a set of Pareto-optimal solutions, offering flexibility in decision-making.

3.2.3.2 Multi-horizon Multi-stage Stochastic Programming

Infrastructure planning and models are challenging due to the combination of time scales. While planning and building infrastructure are strategic decisions, with time horizons spanning multiple years, one needs an operational time scale to get a clear picture of the infrastructure's performance and profitability. Similarly, it is also important to assess the operational impact of investment decisions for facility location decisions, especially for hydrogen facility locations, where operational costs account for the majority of total costs.

Strategic and operational levels are fraught with uncertainties. On the strategic level, future demand and technological evolution introduce uncertainty. These strategic decisions subsequently restrict the range of operational recourse and influence operational-level decisions. The operational uncertainties can be for instance, future spot prices of commodities. The confluence of uncertainties across different time scales complicates the traditional multistage stochastic programming formulation, leading to an exponential growth in model size (Kaut et al., 2014). This scenario explosion results from the approach of branching operational scenarios for every strategic scenario at each strategic stage, given the independence of strategic and operational events, as depicted in figure Figure 3.1a.

Kaut et al. (2014) propose an innovative modeling approach that significantly curbs model size compared to the traditional approach. They argue that strategic decisions depend not on individual operational scenarios but on the overall operational performance of the respective strategic decision. Consequently, branching is only necessary between strategic stages, while operational nodes are embedded within their respective strategic nodes. This checks the feasibility and performance of the decisions at the respective strategic nodes without the scenario explosion, as demonstrated in Figure 3.1, where Figure 3.1a illustrates the traditional approach, and Figure 3.1b displays the multi-horizon approach.

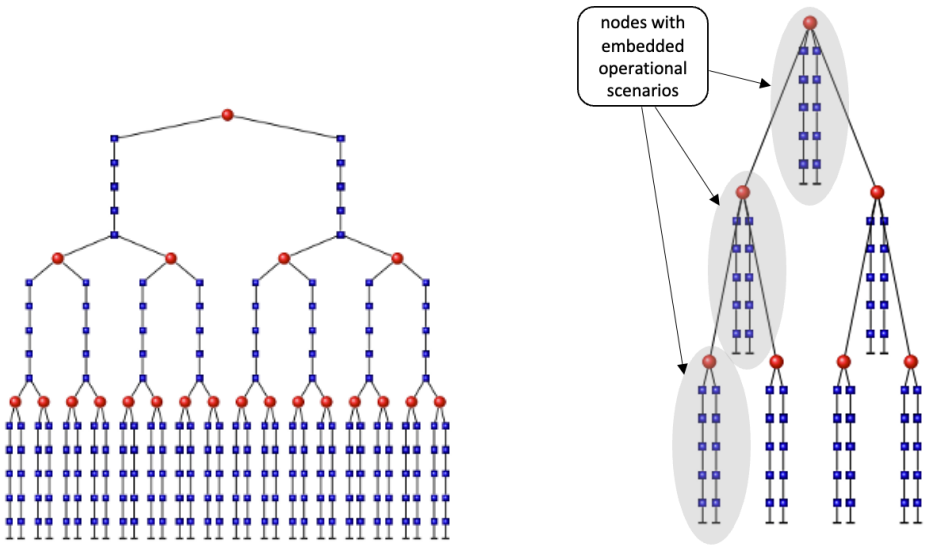

(a) both strategic and operational uncertainty **(b)** multiple operational scenarios per node

Figure 3.1: Illustrations provided by Maggioni et al. (2020a). To the left (a) we see a scenario tree arising from the traditional way of modeling stochastic problems with both strategic and operational uncertainty. The illustration to the right (b) show the corresponding multi-horizon approach.

In the proposed multi-horizon structure by Kaut et al. (2014), there is no connection between operational scenarios of two consecutive strategic nodes. This structure is exact if the following two conditions are satisfied. Firstly, the strategic uncertainty must be independent of the operational uncertainty, and the strategic decisions must not depend on any particular operational decisions. Secondly, the first operational decision in a strategic node cannot depend on the last operational decision from the previous period.

The first condition is reasonable and can be expected to be met in many situations, mainly when the gap between strategic and operational time scales is significant (years versus hours). However, the second condition is more challenging to meet precisely. For instance, considering strategic periods that align with calendar years and one-hour operational periods, we would need the operational decisions at 00:00 on January 1 to be independent of those at 23:00 on December 31 of the previous year. This implies that the proposed structure will most likely approximate the 'standard trees' from the previous section, and the degree of approximation is case-dependent. For example, consider a power producer owning hydropower plants; water reservoirs introduce a temporal aspect to the operational model, contravening the second condition. Nevertheless, in regions with cold winters, reservoirs are generally at their minimum levels at the end of winter in most scenarios. Hence, the approximation error will be relatively insignificant if strategic decisions are positioned at winter's end.

Maggioni et al. (2020b) presents a formulation for a multi-horizon stochastic program based on a multi-horizon scenario tree and node notation, which is given as follows:

$$\min_{x,y} \sum_{t=1}^{H} \sum_{l \in \mathcal{N}_t} \pi_l (c_l x_l + \sum_{s \in \mathcal{S}_t} w_l^s \sum_{\tau \in T_t} q_l^{s,\tau} y_l^{s,\tau}) \tag{3.49}$$

subject to:

$$Ax_l = h_l \quad l \in \mathcal{N}_1 \tag{3.50}$$

$$T_l x_{a(l)} + W_l x_l = h_l \quad l \in \mathcal{N}_t, t \in \mathcal{H} \setminus \{1\} \tag{3.51}$$

$$T_l^{s,1} x_l + W_l^{s,1} y_l^{s,1} = h_l^{s,1} \quad l \in \mathcal{N}_t, s \in \mathcal{S}_t, t \in \mathcal{H} \tag{3.52}$$

$$T_l^{s,\tau} y_l^{s,\tau-1} + W_l^{s,\tau} y_l^{s,\tau} = h_l^{s,\tau} \quad l \in \mathcal{N}_t, \tau \in \mathcal{T} \setminus \{1\}, s \in \mathcal{S}_t, t \in \mathcal{H} \tag{3.53}$$

$$x_l \in \mathbb{R}_+^{n_t} \quad l \in \mathcal{N}_t, t \in \mathcal{H} \tag{3.54}$$

$$y_l^{s,\tau} \in \mathbb{R}_+^{n_t^\tau} \quad l \in \mathcal{N}_t, \tau \in \mathcal{T}_t, s \in \mathcal{S}_t, t \in \mathcal{H} \tag{3.55}$$

In the equations, c_l, h_l, T_l, and W_l represent vectors and matrices at a strategic node $l \in \mathcal{N}t, t \in \mathcal{H} \setminus 1$. For $l \in \mathcal{N}1$, we set $\mathcal{T}_l = A, W_l = 0$, and assume c_l and h_l as known vectors. Each strategic node l at stage t has a unique *ancestor*, $a(l)$, at stage $t-1$, excluding the root node. The probability of reaching node l through strategic event realizations is denoted by π_l, and its conditional probability at the ancestor node is $\pi_{a(l),l}$. Analogously to ancestor nodes, each non-leaf node at stage t has successors at stage $t+1$.

3.3 Supply Chain Network Design

Supply chain network design (SCND) is an operations research discipline that determines the most efficient location and capacity for facilities and the flow of goods through those facilities (Li et al., 2019). When dealing with uncertainty, the goal of SCND is to create a configuration that performs well regardless of the specific outcomes of uncertain parameters.

Supply chain management (SCM) comprises three planning levels that vary based on the time frame: strategic, tactical, and operational. The strategic level is responsible for decisions that have long-term impacts on the firm, typically spanning over several years (Simchi-Levi et al., 2004). These decisions revolve around the quantity, location, and capacities of facilities, which are related to the facility location discussed in Section 3.1.

The primary expansion of supply chain research beyond traditional facility location problems is the examination of how tactical and operational decisions impact optimal strategic decisions. Numerous studies have developed stochastic models with multiple tactical or operational periods (Govindan et al., 2017). In these models, the second stage encompasses several time periods, enabling the capture of variations in stochastic parameters and the ability to modify tactical and operational decisions in different periods.

Schütz et al. (2009) investigate a two-stage stochastic program that involves a strategic location decision in the first stage and operational decisions in the second stage, spanning multiple time periods to capture variations in stochastic parameters. The authors examine the impact of the level of aggregation in the second stage on the first-stage solution and find that disaggregated problem instances result in lower expected costs than aggregated instances. This suggests that solutions with higher temporal resolution lead to lower costs for the given problem instances.

3.3.1 Hydrogen Supply Chain Network Design

Li et al. (2019) conducted a review of the literature on hydrogen supply chain network design and found that linear and mixed-integer linear programming models (LP/MILP) are commonly used for modeling hydrogen supply chain networks.

Almansoori and Shah (2006)'s paper that introduces a model which accounts for production, storage, and transportation under deterministic demand, serves as a foundation for many subsequent papers cited in Li et al. (2019). Almansoori and Shah (2009) extended this model to address multiple periods. The authors applied their model to design a hydrogen supply chain in Great Britain and considered the entire value chain, including technology selection, facility location, production and storage capacities, and transportation mode.

Li et al. (2019) categorized modifications of Almansoori and Shah (2006) hydrogen supply chain model into four types: multi-objective, multi-period optimization, introducing uncertainty, and integration with other supply chains. The paper selected for analysis in this report focuses on uncertainty and multi-period modification. Most of these papers examine uncertainty in demand, but Sabio et al. (2010) explore uncertainty in operating costs and raw material prices. They propose a computationally intensive multi-scenario, multi-period MILP to model the uncertainty. However, to handle the complexity of the model, a decomposition strategy is introduced. A case study on a hydrogen supply chain in Spain is used to illustrate the effectiveness of the decomposition strategy for up to eight time periods, as opposed to six time periods without it, considering 18 potential production locations, four technologies, and 50 scenarios

Myklebust et al. (2010) examine a hydrogen supply chain problem in Germany with deterministic parameters. The study aims to investigate how demand and input costs influence technology selection. The model considers three options for hydrogen production from natural gas and only one for electrolysis. Regions with demand and the potential for production capacity are included in the model, allowing demand and production to coincide in many cases. The model also accounts for the option of exporting hydrogen to other regions using pipelines or trucks.

Stádlerová and Schütz (2021) investigate the location of hydrogen facilities to cater to the maritime transportation industry in Norway. Their research proposes a multi-period model for facility location, featuring capacity expansion for developing the hydrogen supply chain towards 2035. The model incorporates economies of scale in investment and production costs, provides a choice of hydrogen technologies, and enables customer allocation decisions.

3.4 Hydrogen Production flexibility

Electrolysis plant operators face a significant challenge related to the cost of electricity, which accounts for 70-88% of the cost of hydrogen production. To overcome this challenge, plants need to have the ability to operate dynamically, enabling them to take advantage of lower electricity prices at certain times (Matute et al., 2021). The flexibility to efficiently switch production on and off in response to significant price volatility can be advantageous. However, there are no papers available that address the optimization of both short-term hydrogen production in relation to electricity prices and the strategic decision of where to locate hydrogen production plants.

Matute et al. (2021) have created a model that considers the fluctuating prices of electricity and determines the best plan for hydrogen production at a specific facility. The model has limitations on the number of cold starts permitted within a given period to prevent undue stress on the technology. It also ensures that production and power consumption have minimum partial loads if the electrolyzer goes into standby mode. The proposed model is a mixed-integer non-linear optimization problem (MINLP). The researchers used Alkaline as a case study, and the model does not compare different technologies.

As previously mentioned, Alkaline has a significantly longer ramp-up time than PEM before reaching full utilization potential after production is initiated. To model factors such as this, different production modes can be implemented for a facility over a specific time period. Leo and Engell (2018) used a two-stage stochastic program to determine optimal day-ahead electricity procurement and production scheduling by incorporating production modes. In the first stage, the program chooses different operation modes (Off, Startup, and On), which determine the planned production throughput and electricity consumption for a given time period. After a mode switch, a certain number of time periods must elapse before the next switch can occur.

Corengia and Torres (2022) investigate the impact of time-varying power on the selection of hydrogen production technologies at a specific location. The paper compares the Alkaline, PEM, and SOEC technologies for two scenarios: small-scale and large-scale hydrogen production plants, which are defined as producing 500 kg/day and 2.5 tons/day, respectively. According to their findings, Alkaline technology offers a more cost-effective solution in both cases, while PEM technology's higher investment cost offsets its flexibility advantages. However, the study does not explore the benefits of flexibility in start-up times.

Seljom and Tomasgard (2015) distinguish between short-term and long-term uncertainty in their analysis of the impact of wind power's short-term uncertainty on long-term energy investments. Long-term uncertainty involves factors that affect parameters over an extended period, usually spanning years, such as future greenhouse gas reduction commitments. Short-term uncertainty, on the other hand, refers to recurring conditions, including wind conditions and commodity price fluctuations. To model energy investments under short-term uncertainty, the authors utilize stochastic programming. The investment decision is made in the first stage and implemented in the second stage, where uncertain parameters are revealed. The objective of operational decisions is to meet demand at the lowest cost. The second stage follows an operational time structure, divided into four seasons, each with 12 two-hour steps. This model captures the variability between every two-hour step at the operational level, allowing for investment decisions that provide appropriate flexibility.

Chapter 4

Problem Description

This chapter presents our facility location problem under demand and electricity price uncertainty, with the choice to invest in multiple production technologies. The problem consists of making sequential strategic and operational decisions over multiple stages, with the objective of making an overall optimal investment scheme, as defined by having the lowest expected total costs, i.e., the sum of expected investment, production, and transportation costs over all the stages.

The decision process for a given stage is illustrated in Figure 4.1, where for each stage, strategic decisions and subsequent operational recourse decisions are made in response to realization in the event space. The overall decision process takes place over multiple stages, with decisions at one stage being influenced by previous decisions and realizations and expectations over future realizations. The problem, therefore, entails a sequential decision process and can be modeled as a multi-stage problem. Further, the operational level consists of multiple time periods as well, each corresponding to a specific hourly electricity price realization. We, therefore, have two time scales, one for strategic investment decisions and one for operational production decisions. Such a multi-stage problem can be formulated as a multi-horizon problem as seen in Figure 4.2, where the operational stages and decisions are embedded in the strategic ones.

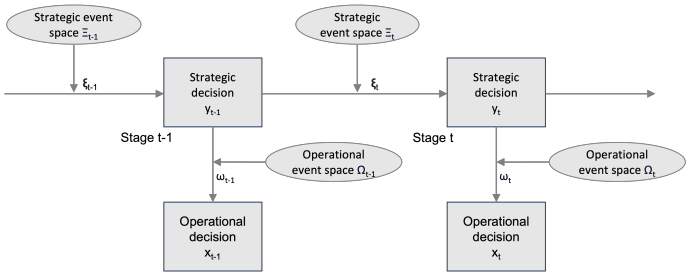

Figure 4.1: Overview of the sequential decision process, each stage involves a strategic event (demand level), a strategic investment decision, an operational event (electricity price), and an operational recourse decision (production schema). This sequence occurs for every stage.

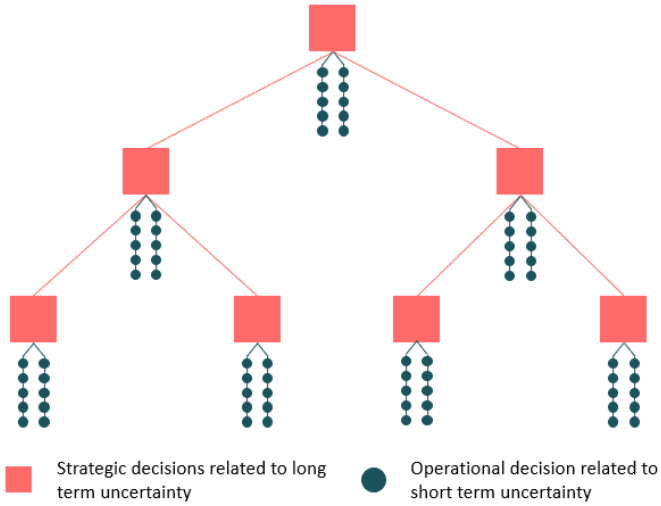

Figure 4.2: A three-stage multi-horizon stochastic problem. Strategic decisions are made along the red squares, each corresponding to a specific demand realization. The blue represents the operational decisions to be made, and are embedded into the strategic decisions.

We are given a set of possible facility locations, production technologies, a set of customers, and production capacities one can invest in. A set of strategic stages is given where one can invest. The stage has associated nodes where each node has a realization of demand for each customer. In addition, each node, except the root node at the first strategic stage, has a parent node on which it depends on the previous investments done at a location. At each node, one decides whether to invest or not and, if so, which combinations of production technology and capacity to invest in. The chosen investment restricts the production throughput and flexibility at a location. The installed capacity is an upper limit on the production throughput of hydrogen for each location, and the chosen technology influences the production plan in two ways. The technology determines the range of feasible capacity utilization levels, where PEM has a broader interval to choose from than Alkaline. In addition, the choice of technology affects production ramp-up time, where PEM offers an almost instant ramp-up, whereas Alkaline spends over an hour in ramp-up mode. There are thus different degrees of production-related flexibility between PEM and Alkaline, with the former having the greatest flexibility. Once you have made an investment decision or lack thereof, it cannot be undone, but additional investments can be made at later stages. The investment and production costs are expected to drop over time due to technological and economic advancements. The costs related to a specific production technology depend on what stage it was acquired at.

At the operational level, one has a set of production periods, which consists of a set of time periods. One needs to decide on a production plan for hydrogen, fulfilling the demand at the given node while minimizing the production and transportation cost, given the invested capacity at that given node. The production planning consists of deciding production quantities for all opened facilities at all time periods for each realization of the different strategic stages and electricity prices. Production is done according to the restrictions that come from the capacity and technology chosen. The electricity price is stochastic and is the only parameter variable over each operational horizon. Thus, it will influence production planning: When the electricity price is high, one should produce at low utilization rates, while if the electricity price is low, one should produce at high utilization rates.

The transportation costs are a function of the distance between the customer in the production facility and the amount of hydrogen transported. The costs increase strictly with the distance and weight. Each production facility can only reach the customers within a maximum distribution range.

Chapter 5

Mathematical Model

5.1 Sets

$\mathcal{H} = \{1, ..., \|H\|\}$	-	Set of strategic stages
$\mathcal{N}_h$	-	Set of ordered nodes of the strategic tree at stage $h \in \mathcal{H}$
$\mathcal{S}_h$	-	Set of operational scenarios (or profiles) at strategic time $h \in \mathcal{H}$
$\mathcal{I}$	-	Set of possible facility locations
$\mathcal{J}$	-	Set of customer locations
$\mathcal{K}$	-	Set of possible discrete capacities
$\mathcal{P}$	-	Set of possible production technologies
$\mathcal{E}$	-	Set of epochs for different seasons
$\mathcal{T}$	-	set of time periods in each epoch

$\mathcal{P}_W \subseteq \mathcal{P}$	-	Subset of production technologies requiring stay time in off mode after production shutdown

5.2 Parameters

5.2.1 Strategic Parameters

B_p	-	Lower bound of production for technology $p \in \mathcal{P}$
C^l_{kp}	-	Annualized investment and operational costs for technology $p \in \mathcal{P}$ at capacity level $k \in \mathcal{K}$ at strategic node $l \in \mathcal{N}_h$, $h \in \mathcal{H}$
D^l_{je}	-	Demand at port $j \in \mathcal{J}$ in epoch $e \in \mathcal{E}$ at strategic node $l \in \mathcal{N}_h, h \in \mathcal{H}$ in the scenario tree
K_k	-	Production capacity level $k \in K$
$a(l)^\omega$	-	Ancestor to the node l of degree $\omega \in \{0, ..., h-1\}$, where degree indicates number of preceding stages. Degree 0 corresponds to the current stage, degree 1 correspond to it's immediate ancestor (i.e., parent node), degree 2 corresponds to the ancestor of it's immediate ancestor degree $h-1$ corresponds to the root node, $l \in \mathcal{N}_h$, $h \in \mathcal{H}$
π_l	-	Probability of strategic node $l \in \mathcal{N}_h$, $h \in \mathcal{H}$

5.2.2 Operational Parameters

$E^{hl}_{is\tau e}$	-	The cost of electricity at location $i \in \mathcal{I}$ at a given time period τ in epoch e, as defined by scenario $s \in \mathcal{S}_h$, derived at strategic node $l \in \mathcal{N}_h$, $h \in \mathcal{H}$
F^{hl}_p	-	Production efficiency of technology p at the strategic time period h.

w_s^l - Weight (probability) of operational scenario $s \in \mathcal{S}_h$, derived at strategic node $l \in \mathcal{N}_h$, $h \in \mathcal{H}$

W_p - minimum stay time in off mode after turning production off for technology $p \in \mathcal{P}^{\mathcal{W}}$

T_{ij} - Distribution costs from facility i to customer j, $i \in \mathcal{I}, j \in \mathcal{J}$

L_{ij} - 1 if demand at location j can be served from facility i, 0 otherwise, $i \in \mathcal{I}, j \in \mathcal{J}$

U - Penalty cost per unit of hydrogen not supplied

O - Penalty cost per unit of hydrogen overproduced

5.3 Decision variables

5.3.1 Strategic Decision Variables

y_{ikp}^l - 1 if a facility is opened at location i at the k-th capacity level for technology p at strategic node l, 0 otherwise, $l \in \mathcal{N}_h$, $h \in \mathcal{H}$, $i \in \mathcal{I}, k \in \mathcal{K}, p \in \mathcal{P}$

5.3.2 Operational Decision Variables

$d_{ikps\tau e}^{hl}$ - 1 if there is production at location i, at the k-th capacity level for technology p acquired in strategic period h, at time period τ in epoch e for scenario s, derived from strategic node l, 0 otherwise, $i \in \mathcal{I}, k \in \mathcal{K}, p \in \mathcal{P}, \tau \in \mathcal{T}, e \in \mathcal{E}, s \in \mathcal{S}_h, h \in \mathcal{H}$

o_{ise}^l - Amount of excess produced hydrogen at facility i in epoch e in scenario s, derived from strategic node $l \in \mathcal{N}_h$, $i \in \mathcal{I}, e \in \mathcal{E}, s \in \mathcal{S}_h, h \in \mathcal{H}$

$q_{ip\tau se}^{hl}$ - Production volume at facility i by technology of type p acquired in stage h, at time period τ in epoch e of scenario s, derived from strategic node $l \in \mathcal{N}_h$, $h \in \mathcal{H}$, $i \in \mathcal{I}, \tau \in \mathcal{T}, e \in \mathcal{E}, s \in \mathcal{S}_h$

u_{jse}^{hl} - Amount of unsatisfied demand after supply of non-imported hydrogen to customer j for epoch e at scenario s, derived at strategic node $l \in \mathcal{N}_h$, $h \in \mathcal{H}$, $j \in \mathcal{J}, e \in \mathcal{E}, s \in \mathcal{S}_h$

x_{ijse}^l - Amount of customer demand at location j satisfied from facility i in epoch e and scenario s, derived at strategic node $l \in \mathcal{N}_h$, $h \in \mathcal{H}$, $j \in \mathcal{J}, i \in \mathcal{I}, e \in \mathcal{E}, s \in \mathcal{S}_h$

5.4 Objective function of investment planning master problem

$$\min_y \sum_{h \in \mathcal{H}} \sum_{l \in \mathcal{N}_h} \pi_l \Big(\sum_{i \in \mathcal{I}} \sum_{p \in \mathcal{P}} \sum_{k \in \mathcal{K}} C_{kp}^l y_{ikp}^l (|\mathcal{H}| + 1 - h) + \sum_{s \in \mathcal{S}_h} w^s \psi^s(y) \Big) \tag{5.1}$$

Equation 5.1 minimizes the total expected annualized costs of both the strategic decisions and their respective operational costs, for all stages. The first expression of the objective function captures the expected strategic investment cost made at every stage of the model, $h \in \mathcal{H}$, broken down by the respective strategic scenarios at each strategic stage, $l \in \mathcal{N}_h$. As capacity investments made in one stage will also be available for use in subsequent stages, the annualized investment costs are multiplied by the number of strategic stages for

which they will be modeled operationally. That is, investments made at the strategic nodes in the first stage will be multiplied by $|\mathcal{H}|$, as these investments are modeled operationally for all the strategic stages. Similarly, investments made at the last stage, i.e., leaf nodes, will only be modeled operationally for one strategic period and are thus only multiplied by a factor of 1.

The second expression of the objective function captures the expected operational costs made at every stage. That is, the weighted sum of the expected production and transportation costs from a strategic investment decision y^l made in node l. The aim is not to engage in actual operational planning but to adequately represent the anticipated operational impacts of long-term investment decisions. The set of operational scenarios $\mathcal{S}_h$ and its corresponding probability vector w^s is the same for all the strategic nodes within a strategic stage. The function $\psi^s(y)$ denotes the operational costs tied to a specific investment decision at a strategic node l for a given operational scenario, s. It is important to note that this is a recourse function consisting of scenarios and costs arising after the investment decisions, y^l, have been made. The objective function operates in a recursive way, where for each stage h, strategic investment decisions y^l made for each respective demand realization, along with the current stage h and strategic node l are passed into the operational recourse function.

5.5 Strategic Restrictions

$$\sum_{k\in\mathcal{K}}\sum_{p\in\mathcal{P}} y^l_{ikp} \leq 1, \qquad h \in \mathcal{H}, l \in \mathcal{N}_h, i \in \mathcal{I}; \tag{5.2}$$

$$y^l_{ikp} \in \{0,1\}, \qquad h \in \mathcal{H}, l \in \mathcal{N}_h, i \in \mathcal{I}, k \in \mathcal{K}, p \in \mathcal{P}; \tag{5.3}$$

Restriction 5.2 ensures that you only can invest in one capacity and technology at a location for each node in a stage. Restriction 5.3 is the binary constraint on the investment variable.

5.5.1 Strategic Nonanticipativity constraints

$$y^{a(l)}_{ikp} = y^{a(l')}_{ikp}, \qquad l, l' \in \mathcal{N}_h, h \in \mathcal{H} \setminus \{1\}, a(l) = a(l'), k \in \mathcal{K}, p \in \mathcal{P}, i \in \mathcal{I}; \tag{5.4}$$

Restriction 5.4 ensures non-anticipativity of strategic nodes, such that for any pair of nodes, l and l', with the same strategic parent node, their respective parent nodes have to have made the same investment decision. Thus, knowledge about future realizations cannot be exploited.

5.6 Objection function of the operational subproblem

$$\psi^s(y) = \min \sum_{\delta=1}^{h}\sum_{i\in\mathcal{I}}\sum_{p\in\mathcal{P}}\sum_{\tau\in\mathcal{T}}\sum_{e\in\mathcal{E}} E^{\delta l}_{is\tau e}F^{\delta l}_p q^{\delta l}_{ip\tau se} + \sum_{i\in\mathcal{I}}\sum_{j\in\mathcal{J}}\sum_{e\in\mathcal{E}} T_{ij}x^l_{ijse} + \sum_{j\in\mathcal{J}}\sum_{e\in\mathcal{E}} Uu^l_{jse} + \sum_{i\in\mathcal{I}}\sum_{e\in\mathcal{E}} Oo^l_{ise}; \tag{5.5}$$

Equation (5.5) represents the operational stage objective functions, which consists of the sum of production costs, distribution costs, and penalty costs for not fulfilling demand at a given operational scenario, s. $F^{\delta l}_{ips\tau e}$ denotes the production costs of the short-term cost function, which is the production unit costs. It encapsulates, among other things, the cost of electricity for a specific production location i at a specific hour τ in a given season e. Further, the term captures the electricity required to produce a unit of hydrogen for production technology p acquired a strategic time period h. $q^{\delta l}_{ip\tau se}$ denotes the production volume at a given technology, location, and moment of time. As available production capacity investments can have been made in previous stages as well, not only in the current stage, it is indexed by δ. In this way, potential technological improvements with respect to the efficiency of electricity usage during hydrogen production is captured. In this way, capacity acquired at later stages can have improved electricity and cost efficiency compared to capacity acquired at later stages. Thus, a given location can contain available production capacity of the same technology type p, where the newer capacity has a higher production efficiency than the older capacities while still being able to use the older capacity. The rest of the objective function includes transportation costs, and underage and overage costs, respectively.

5.7 Operational Restrictions

$$d^{\delta l}_{ikps\tau e} \leq y^{\omega}_{ikp}, \qquad \delta = \{1, ..., h\}, \omega = \{a(l)^{(h-1)}, ..., a(l)^1, l\}, \\ i \in I, \tau \in \mathcal{T}, p \in \mathcal{P}, k \in \mathcal{K}, e \in \mathcal{E}, s \in \mathcal{S}_h, h \in \mathcal{H}; \tag{5.6}$$

Restriction (5.6) makes sure that one can only produce hydrogen from available installed capacity at a given location and a given strategic stage. Similar to the production volume variable $q^{\delta l}_{ip\tau se}$, the "production on or off"-variable $d^{\delta l}_{ikps\tau e}$ is indexed by the strategic stage in which it's corresponding capacity was acquired. At a strategic node $l \in \mathcal{N}_h$, there are thus h such "on or off"-variables for each location, capacity, and production technology, corresponding to capacity acquired at the node l in the present strategic stage h and all the available capacity acquired by its ancestors in previous stages.

5.7.1 Demand Fulfillment

$$\sum_{i \in \mathcal{I}} x^l_{ijse} + u^l_{jse} \geq D^l_{je}, \qquad j \in \mathcal{J}, e \in \mathcal{E}, s \in \mathcal{S}_h, h \in \mathcal{H}, l \in \mathcal{N}_h; \tag{5.7}$$

$$\sum_{j \in \mathcal{J}} x^l_{ijse} + o^l_{ise} = \sum_{\delta=1}^{h} \sum_{\tau \in \mathcal{T}} \sum_{p \in \mathcal{P}} q^{\delta l}_{iptse}, \qquad i \in \mathcal{I}, e \in \mathcal{E}, s \in \mathcal{S}_h, h \in \mathcal{H}, l \in \mathcal{N}_h; \tag{5.8}$$

Restriction (5.7) ensures that demand is either satisfied or not satisfied. Restriction (5.8) ensures that the total amount of hydrogen produced at any location i in epoch e by all the available capacities acquired in the current and preceding stages, $q^{\delta l}_{iptse}$, is equal to the demand satisfied to all it's respective customers, x^l_{ijse}, and the excess produced hydrogen o^l_{ise}.

5.7.2 Transportation restriction

$$x^l_{ijse} \leq L_{ij} D^l_{je}, \qquad i \in \mathcal{I}, j \in \mathcal{J}, e \in \mathcal{E}, s \in \mathcal{S}_h, h \in \mathcal{H}, l \in \mathcal{N}_h; \tag{5.9}$$

Constraint (5.9) restrict which facilities i can satisfy demand from customer location j.

5.7.3 Production restrictions

$$q^{\delta l}_{ip\tau se} \leq \sum_{k \in \mathcal{K}} K_k d^{\delta l}_{ikps\tau e}, \qquad \delta = \{1, ..., h\}, i \in \mathcal{I}, p \in \mathcal{P}, \tau \in \mathcal{T}, e \in \mathcal{E}, s \in \mathcal{S}_h, h \in \mathcal{H}, l \in \mathcal{N}_h; \tag{5.10}$$

$$\begin{aligned} q^{\delta l}_{ip\tau se} \geq \sum_{k \in \mathcal{K}} B^{\delta}_p K_k d^{\delta l}_{ikps\tau e}, \\ \delta = \{1, ..., h\}, i \in \mathcal{I}, p \in \mathcal{P}, \tau \in \mathcal{T}, e \in \mathcal{E}, s \in \mathcal{S}_h, h \in \mathcal{H}, l \in \mathcal{N}_h. \end{aligned} \tag{5.11}$$

$$\begin{aligned} d^{\delta l}_{ikps\tau e} - d^{\delta l}_{ikps(\tau+1)e} \leq 1 - \frac{1}{W_p} \sum_{\sigma=\tau+2}^{\sigma=\tau+1+W_p} d^{\delta l}_{ikps\tau e}, \\ \delta = \{1, ..., h\}, i \in \mathcal{I}, k \in \mathcal{K}, p \in \mathcal{P}^{\mathcal{W}}, \tau \in \mathcal{T} \setminus \{|\mathcal{T}| - 1, |\mathcal{T}|\}, e \in \mathcal{E}, s \in \mathcal{S}_h, h \in \mathcal{H}, l \in \mathcal{N}_h; \end{aligned} \tag{5.12}$$

Restriction (5.10) force production volume from installed capacities to be zero if production is not possible, i.e., if a facility is not opened at location i or during the waiting period of the ramp up-stage, and force it to be less than or equal to the maximum installed capacity. Constraint (5.11) makes sure that hydrogen production is greater than or equal to the lower bound of allowable utilization for a technology p acquired in strategic stage δ, or zero. Constraint (5.12) forces production in the following W_p periods to be zero if you switch off production in one period for technology $p \in P^W$. The on-and-off mechanism is recorded for the strategic stage in the capacity was acquired. One can thus for instance, have two installed production capacities of technology type $p \in P^W$, respectively required at the strategic stages δ and δ', where only one of them is required to stay off, namely the one which was turned off in the previous operational time period $\tau - 1$.

5.7.4 Non-negativity and Binary Constraints

$$x^l_{ijse} \geq 0, \qquad i \in \mathcal{I}, j \in \mathcal{J}, e \in \mathcal{E}, s \in \mathcal{S}_h, h \in \mathcal{H} l \in \mathcal{N}_h; \tag{5.13}$$

$$q^{\delta l}_{ip\tau se} \geq 0, \qquad \delta = \{1, ..., h\}, i \in \mathcal{I}, p \in \mathcal{P}, \tau \in \mathcal{T}, e \in \mathcal{E}, s \in \mathcal{S}_t, h \in \mathcal{H} l \in \mathcal{N}_h; \tag{5.14}$$

$$u^l_{jse} \geq 0, \qquad j \in \mathcal{J}, e \in \mathcal{E}, s \in \mathcal{S}_h, h \in \mathcal{H} l \in \mathcal{N}_h.; \tag{5.15}$$

$$o^{l}_{ise} \geq 0, \qquad i \in \mathcal{I}, e \in \mathcal{E}, s \in \mathcal{S}_h, h \in \mathcal{H} l \in \mathcal{N}_h; \tag{5.16}$$

$$d^{\delta l}_{ikps\tau e} \in \{0,1\}, \qquad \delta = \{1,...,h\}, i \in \mathcal{I}, k \in \mathcal{K}, p \in \mathcal{P}, \tau \in T, e \in \mathcal{E}, s \in \mathcal{S}_h, h \in \mathcal{H}, l \in \mathcal{N}_h; \tag{5.17}$$

Constraint (5.13) to (5.17) include binary and non-negativity requirements on the variables.

Our model exhibits the *relatively complete recourse* property as we have penalty costs for producing too much hydrogen, but penalty costs for not fulfilling the demand due to (5.7) and (5.8). *Relatively complete recourse* means that for every solution of the strategic investment variables y we can construct a feasible solution for the operational stage. This makes it easier to implement acceleration techniques to the model as one does not need to take into account feasibility when relaxing constraints.

Chapter 6

Solution Method

The main idea behind Lagrangian relaxation is to transform the original constrained optimization problem into a simpler, more manageable form. This is achieved by integrating constraints directly into the objective function by introducing Lagrange multipliers. Each constraint is associated with a multiplier, and a new term is added to the objective function corresponding to the product of this multiplier and the constraint. This process relaxes the problem by expanding the feasible solution space, making it easier to solve.

The Lagrangian problem is solved over several iterations, yielding a solution for different values of the Lagrange multipliers. The set of best solutions forms the dual problem, the solution which offers a lower bound to the original problem's solution. An iterative method, such as the subgradient method, determines the optimal values of the Lagrange multipliers, fine-tuning them based on the extent of constraint violation.

As the process continues, the solution to the relaxed problem converges towards the original problem's solution, allowing us to solve the original complex optimization problem more effectively and manageably. This process culminates either when a feasible solution that satisfies the original constraints is identified or when an optimal solution is determined such that further changes to the multipliers cease to enhance the objective function.

While the Lagrangian relaxation does not guarantee an optimal solution to the original problem, it often offers an effective approximation, especially in cases where the direct approach is computationally prohibitive. Furthermore, the solution to the dual problem serves as a valuable indicator of the optimal solution's bounds. This framework's efficacy can be visualized effectively in a two-dimensional space, as illustrated in Figure 6.1, showing how sequential cuts (tangent lines) to a convex function converge to the function's minimum.

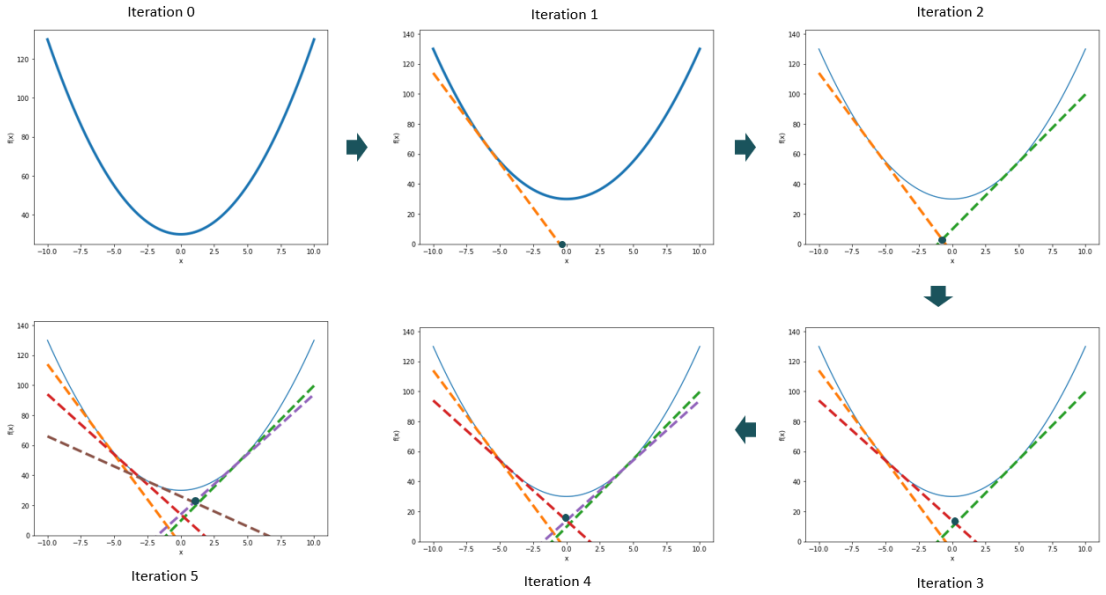

Figure 6.1: Illustration of five steps of a Lagrangre relaxation on 2D minimization problem.

The Lagrangian relaxation method has mainly been utilized in the field of facility location in deterministic situations as seen in works by Shulman (1991), Holmberg et al. (1999), Jena et al. (2016) and Jena et al. (2017), but also has some application to stochastic settings as seen in Schütz et al. (2008). Recently, Stádlerová et al. (2023) applied Lagrangian relaxation to a multi-period two-stage hydrogen facility location problem and found that it produced good bounds within short running times. This suggests that the Lagrangian relaxation method is a viable option to extend to this thesis's multi-stage facility location problem.

To do so, we relax the demand constraints (5.7): $\sum_{i\in\mathcal{I}} x^l_{ijse} + u^l_{jse} \geq D^l_{je}, \qquad j \in \mathcal{J}, e \in \mathcal{E}, s \in \mathcal{S}_h, h \in \mathcal{H}, l \in \mathcal{N}_h;$, which are the only constraints linking the decision variables among various facility locations and have been used in the literature as seen in works by Shulman (1991) in a deterministic setting, Schütz et al. (2008) in a single-period stochastic setting, and Jena et al. (2016) in a multi-period setting. We define the matrix of Lagrangian multipliers, λ^l_{jse}, and arrive at the following Lagrangian subproblem:

$$\begin{aligned}\min_{y} \sum_{h\in\mathcal{H}}\sum_{l\in\mathcal{N}_h} \pi_l\Big(\sum_{i\in\mathcal{I}}\sum_{p\in\mathcal{P}}\sum_{k\in\mathcal{K}} C^l_{kp} y^l_{ikp}(|\mathcal{H}|+1-h) + \\ \sum_{s\in\mathcal{S}_h} w^s\Big(\sum_{\delta=1}^{h}\sum_{i\in\mathcal{I}}\sum_{p\in\mathcal{P}}\sum_{\tau\in\mathcal{T}}\sum_{e\in\mathcal{E}} E^{\delta n}_{is\tau e} F^{\delta n}_{p} q^{\delta l}_{ip\tau se} + \sum_{i\in\mathcal{I}}\sum_{j\in\mathcal{J}}\sum_{e\in\mathcal{E}}(T_{ij}-\lambda^l_{jse})x^l_{ijse} \\ + \sum_{j\in\mathcal{J}}\sum_{e\in\mathcal{E}}(U-\lambda^l_{jse})u^l_{jse} + \sum_{i\in\mathcal{I}}\sum_{e\in\mathcal{E}} Oo^l_{ise} + \sum_{j\in\mathcal{J}}\sum_{e\in\mathcal{E}}\lambda^l_{jse} D^l_{je}\Big)\Big)\end{aligned} \tag{6.1}$$

subject to constraints (5.2) - (5.6) and (5.8) - (5.17). In this relaxed problem, u^l_{jse} is unbounded and is not connected to any other decision variable, as the only constraint related to u^l_{jse} in the original problem is the relaxed constrain (5.7). As this is a minimization problem, the term $\sum_{j\in\mathcal{J}}\sum_{e\in\mathcal{E}}(U-\lambda^l_{jse})u^l_{jse}$ can be disregarded as it will be equal to zero in any optimal solution. Additionally, the expression $\sum_{j\in\mathcal{J}}\sum_{e\in\mathcal{E}}\lambda^l_{jse}D^l_{je}$ is constant for

a given set of multipliers λ^l_{jse}, and can be disregarded as well. Since all constraints are specified individually for each facility location $i \in \mathcal{I}$, the problem can be decomposed and solved independently for each location $i \in \mathcal{I}$. This allows us to decompose the problem for each location, and define:

$$LR = \sum_{i\in\mathcal{I}} g_i(\lambda) + \sum_{h\in\mathcal{H}} \sum_{l\in\mathcal{N}_h} \sum_{s\in\mathcal{S}_h} \sum_{j\in\mathcal{J}} \sum_{j\in\mathcal{J}} \pi_l w^s \lambda^l_{jse} D^l_{je} \tag{6.2}$$

Where g_i for each location, i, is defined as:

$$\begin{aligned} g_i(\lambda) = \sum_{h\in\mathcal{H}} \sum_{l\in\mathcal{N}_h} \pi_l \Big(\sum_{p\in\mathcal{P}} \sum_{k\in\mathcal{K}} C^l_{kp} y^l_{ikp}(|\mathcal{H}| + 1 - h) + \\ \sum_{s\in\mathcal{S}_h} w^s \Big(\sum_{\delta=1}^{h} \sum_{p\in\mathcal{P}} \sum_{\tau\in\mathcal{T}} \sum_{e\in\mathcal{E}} E^{\delta l}_{is\tau e} F^{\delta l}_p q^{\delta l}_{ip\tau se} + \sum_{j\in\mathcal{J}} \sum_{e\in\mathcal{E}} (T_{ij} - \lambda^l_{jse}) x^l_{ijse} \\ + \sum_{j\in\mathcal{J}} \sum_{e\in\mathcal{E}} (U - \lambda^l_{jse}) u^l_{jse} + \sum_{e\in\mathcal{E}} Oo^l_{ise}\Big)\Big) \end{aligned} \tag{6.3}$$

subject to (5.2) - (5.6) and (5.8) - (5.17) for the given facility $i \in \mathcal{I}$

6.1 Solving the Lagrangian Subproblem

The optimal solution to the Lagrangian subproblem represents the optimal investment decisions for each facility over all stages, all scenarios, and all epochs such that the total expected costs are minimized. In deterministic problems, this has been identified by solving the shortest path problem through the use of dynamic programming techniques (Shulman, 1991, Jena et al., 2016). Further, Stádlerová et al. (2023) has shown it to be a feasible method for solving a similar problem in the two-stage setting. Our problem has a substantially more complex production planning problem, where we need to plan the selected production level for several time periods t and epochs e. As well as having binary variables d restricting if we can produce at a facility given if we have shut-down production in previous time periods (5.12). In comparison, Stádlerová et al. (2023) only needs to decide what percentage of the installed capacity one should produce, with a lower bound on how low you can go. Therefore we will check if solving the problem through the shortest path problem with dynamic programming is better than solving it with a commercial solver.

6.2 Shortest path

As noted earlier, determining the best decisions for opening and expansion can be framed as a shortest path issue within a single graph, which can then be resolved using dynamic programming techniques as seen in deterministic settings in Shulman (1991), Holmberg (1994) and Jena et al. (2016), and stochastic setting Schütz et al. (2008). For some multi-period settings using a single graph might not be suitable, as seen in Stádlerová et al. (2023). To the best of our knowledge, this has not been applied to a stochastic multi-stage multi-horizon problem such as ours. For our problem, the graph where you can perform the shortest-path algorithm will become very large due to the previous investment decisions

needing to stay the same for nodes, and the production planning is dependent on the previously installed capacity as you can use previously installed capacity to fulfill demand in a later stage. This means that one needs to create a three-dimensional graph for each facility. One dimension of this graph is the capacity layer, where you need connections between each possible capacity you can install in one stage to all the possible capacities in the next stage. This is illustrated in Figure 6.2. Further, as one has different production technologies one can choose from and one is not restricted to sticking to the same over all stages, one also needs a layer that connects all possible combinations of capacities and technologies, $|P| * |K|$ to the same combinations for each stage. Finally, as we have more and more realizations for the demand as we move forward in time (stages), one needs a layer that represents this. As one can use the previously installed capacity to fulfill demand, this layer grows exponentially with the number of possible combinations of previously installed capacity and technology. For example, if you have eight possible capacities and two technologies, one would need $2 * 8 = 16$ nodes to represent the possible solutions in the first stage. For the second stage, one would need $16 * 16 = 256$ nodes for each realization of the demand in that stage, Figure 6.3 tries to illustrate this.

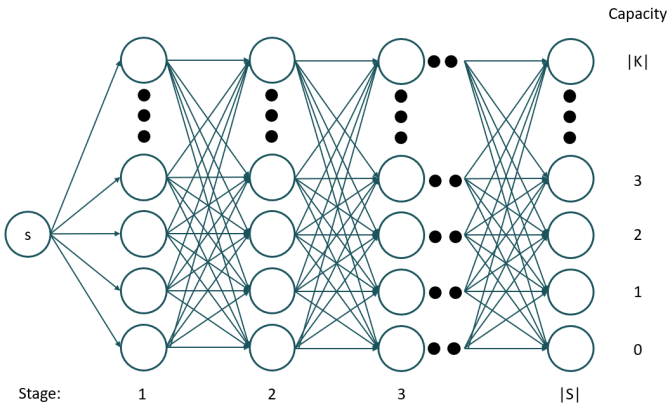

Figure 6.2: Illustration of the shortest path problem for given facility in the stages vs. capacity dimension

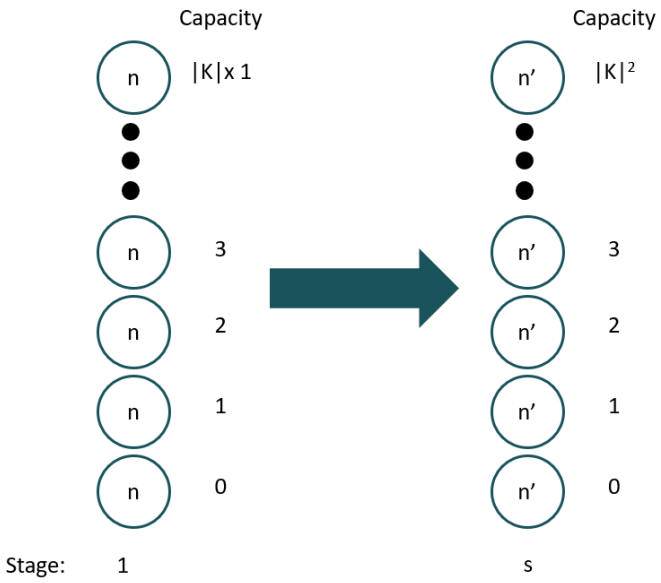

Figure 6.3: Illustration of the shortest path problem for given facility in the stages vs. nodes dimension

6.2.1 Operational Production Cost

In order to find the transition cost from one node to the next, one needs to compute the expected cost of fulfilling demand in the next node with the capacity installed thus far plus the intended installed capacity. To do this, we need to define a problem where you are given $i \in \mathcal{I}$, $h \in \mathcal{H}$ and $n \in \mathcal{N}_h$, where the y^l_{ikp} is given for all the ancestors of node n and for the node n it also is given with the vector $\mathbf{y}$ with dimensions (i, k, p, l) with ones where there have been installed capacity:

$$\begin{aligned} P^{nh}_{ik'p'}(\lambda, y) = \min \sum_{\delta=1}^{h} \sum_{p\in\mathcal{P}} \sum_{\tau\in\mathcal{T}} \sum_{e\in\mathcal{E}} E^{\delta l}_{is\tau e} F^{\delta l}_{p} q^{\delta n}_{ip\tau se} + \\ \sum_{i\in\mathcal{I}} \sum_{j\in\mathcal{J}} \sum_{e\in\mathcal{E}} (T_{ij} - \lambda^n_{jse}) x^n_{ijse} \\ + \sum_{j\in\mathcal{J}} \sum_{e\in\mathcal{E}} U u^n_{jse} + \sum_{i\in\mathcal{I}} \sum_{e\in\mathcal{E}} O o^n_{ise} \end{aligned} \tag{6.4}$$

S.T

$$d^{\delta l}_{ikps\tau e} \leq y(i, k', p', \omega), \qquad \begin{aligned} \delta = \{1, ..., h\}, \omega = \{a(n)^{(h-1)}, ..., a(n)^1, n\}, \\ \tau \in \mathcal{T}, p \in \mathcal{P}, k \in \mathcal{K}, e \in \mathcal{E}, s \in \mathcal{S}_h \end{aligned} \tag{6.5}$$

$$\sum_{j\in\mathcal{J}} x^n_{ijse} + o^n_{ise} = \sum_{\delta=1}^{h} \sum_{\tau\in\mathcal{T}} \sum_{p\in\mathcal{P}} q^{\delta n}_{iptse}, \qquad e \in \mathcal{E}, s \in \mathcal{S}_h \tag{6.6}$$

$$x^n_{ijse} \leq L_{ij} D^n_{je}, \qquad j \in \mathcal{J}, e \in \mathcal{E}, s \in \mathcal{S}_h \tag{6.7}$$

$$q^{\delta n}_{ip\tau se} \leq \sum_{k\in\mathcal{K}} K_k d^{\delta n}_{ikps\tau e}, \qquad \delta = \{1, ..., h\}, p \in \mathcal{P}, \tau \in \mathcal{T}, e \in \mathcal{E}, s \in \mathcal{S}_h \tag{6.8}$$

$$q^{\delta n}_{ip\tau se} \geq \sum_{k \in \mathcal{K}} B^{\delta}_{p} d^{\delta n}_{ikps\tau e}, \tag{6.9}$$
$$\delta = \{1, ..., h\} p \in \mathcal{P}, \tau \in \mathcal{T}, e \in \mathcal{E}, s \in \mathcal{S}_h.$$

$$d^{\delta n}_{ikps\tau e} - d^{\delta n}_{ikps(\tau+1)e} \leq 1 - \frac{1}{W_p} \sum_{\sigma=\tau+1}^{\sigma=\tau+1+W_p} d^{\delta n}_{ikps\tau e}, \tag{6.10}$$
$$\delta = \{1, ..., h\}, k \in \mathcal{K}, p \in \mathcal{P}^{\mathcal{W}}, \tau \in \mathcal{T} \setminus \{|\mathcal{T}| - 1, |\mathcal{T}|\}, e \in \mathcal{E}, s \in \mathcal{S}_h,$$

$$x^{l}_{ijse} \geq 0, \qquad j \in \mathcal{J}, e \in \mathcal{E}, s \in \mathcal{S}_h; \tag{6.11}$$

$$q^{\delta n}_{ip\tau se} \geq 0, \qquad \delta = \{1, ..., h\}, p \in \mathcal{P}, \tau \in \mathcal{T}, e \in \mathcal{E}, s \in \mathcal{S}_h; \tag{6.12}$$

$$u^{n}_{jse} \geq 0, \qquad j \in \mathcal{J}, e \in \mathcal{E}, s \in \mathcal{S}_h \tag{6.13}$$

$$o^{n}_{ise} \geq 0, \qquad , e \in \mathcal{E}, s \in \mathcal{S}_h \tag{6.14}$$

$$d^{\delta n}_{ikps\tau e} \in \{0, 1\}, \qquad \delta = \{1, ..., h\}, k \in \mathcal{K}, p \in \mathcal{P}, \tau \in T, e \in \mathcal{E}, s \in \mathcal{S}_h \tag{6.15}$$

$$x^{n}_{ijse} \geq 0, \qquad , j \in \mathcal{J}, e \in \mathcal{E}, s \in \mathcal{S}_h, \tag{6.16}$$

$$q^{\delta n}_{ip\tau se} \geq 0, \qquad \delta = \{1, ..., h\}, \tau \in \mathcal{T}, p \in \mathcal{P}, e \in \mathcal{E}, s \in \mathcal{S}_h; \tag{6.17}$$

$$u^{n}_{jse} \geq 0, \qquad j \in \mathcal{J}, e \in \mathcal{E}, s \in \mathcal{S}_h \tag{6.18}$$

$$o^{n}_{ise} \geq 0, \qquad e \in \mathcal{E}, s \in \mathcal{S}_h \tag{6.19}$$

$$d^{\delta n}_{ikps\tau e} \in \{0, 1\}, \qquad \delta = \{1, ..., h\}, k \in \mathcal{K}, p \in \mathcal{P}, \tau \in T, e \in \mathcal{E}, s \in \mathcal{S}_h; \tag{6.20}$$

In addition to the value of this, one also needs to add the cost of installing the capacity in the next node given by C^{n}_{kp}. Combining this one get the following expansion cost from $(a(n)^1, k, p, \mathbf{y})$ to $(n, k, \mathbf{y} \cup y^{a(n)^1}_{kp} = 1)$:

$$(a(n)^1, k, p, \mathbf{y})(n, k', p', \mathbf{y} \cup y_k p^{a(n)^1} = 1) = C^{n}_{kp} + P^{nh}_{ikp}(\lambda, y) \tag{6.21}$$

6.2.2 Dynamic programming solution

In order to find the optimal solution from the graph created, one needs to find the path in the tree which minimizes the expected costs over all demand realizations, which means you need to find the expected shortest path from a source s to all of the leaf nodes representing the final demand realizations where you respect the non-anticipavity constraint. This means that starting from the bottom of the tree at stage $h = |H|$ you find the optimal decision $(k, p)k \in \mathcal{K}p \in \mathcal{P}$ for all possible realizations of $\mathbf{y}$, which represent a possible configuration of investments in ancestor node realizations, for each realization of demand $n \in N_h$

$$E_{nh}(\mathbf{y}) = \pi_n min_{k,p} C^{n}_{kp} + P^{nh}_{ikp}(\lambda, \mathbf{y}) \tag{6.22}$$

You then obtain the optimal solution in the last stage for each given $\mathbf{y}$. You then move up to the next stage where you repeat the procedure for all given $\mathbf{y}$ for that stage and obtain E_{nh}s for $h = |H| - 1, n \in N_h$ where you need to add $\sum_{l \in c(n)^h} E_{l|H|}(\mathbf{y} \cup (n, p, k))$, where $c(n)^h$ is the set of children of node n in strategic stage h. This continues upward the tree until you reach the source node and find the minimum. This procedure is illustrated

in Figure 6.4, where you have an illustration case with two possible technologies, two realizations of demand per parent, and one possible production technology. Each tree represents how one finds the optimal path for each stage, where the red circles signal that it is the optimal solution.

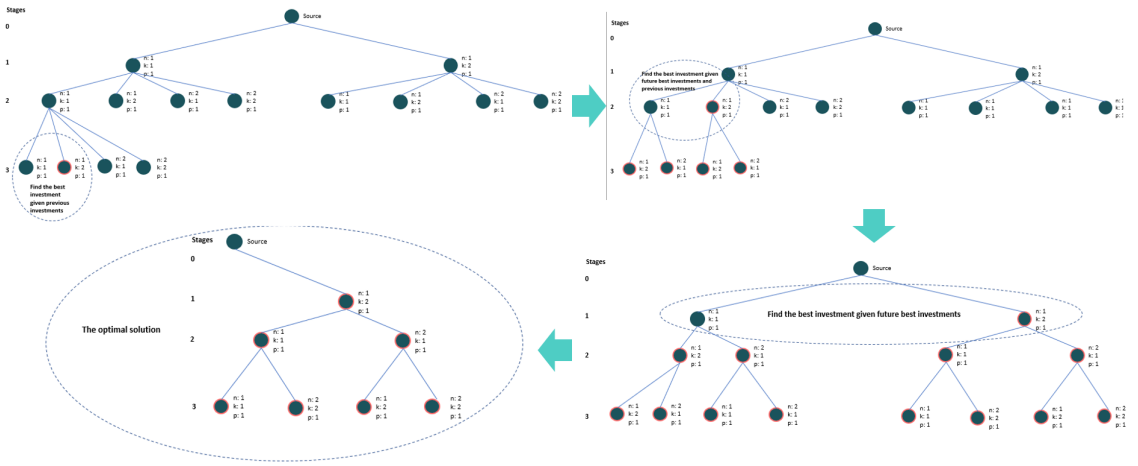

Figure 6.4: Illustration of how one finds the optimal solution with the shortest path for a small problem instance.

6.2.2.1 Curse of Dimentionality

The curse of dimensionality is a key challenge when applying dynamic programming to complex problems. Introduced in Bellman (1952) the term highlights an issue that arises as the number of decision variables in a problem increases: the computational complexity grows exponentially, making high-dimensional problems difficult, if not impossible, to solve within reasonable computational time and resource constraints.

Specifically, in dynamic programming, every potential state in the state space must be examined to determine the optimal policy. With each additional dimension, the number of possible states multiplies, rapidly increasing computational requirements. For instance, in a simple 10x10 grid navigation problem, there are 100 states. Doubling the grid dimensions to 20x20 raises the state count to 400, illustrating the exponential growth.

This phenomenon, the so-called "curse of dimensionality," is particularly relevant to our study. Given the multi-dimensional nature of our problem, we must recognize that dynamic programming could potentially be hampered by this computational hurdle when solving the Lagrange subproblem with shortest-path and dynamic programming.

6.3 Updating the Lagrangian multiplier

One finds a lower bound of the objective (5.1) subject to (5.2) - (5.6) and (5.8) - (5.17) by solving it for a given λ^l_{jse}. To find the highest possible lower bound, one needs to find the λ that maximizes the Lagrangian dual problem: $LD = max_\lambda LR(\lambda)$. The method utilized to solve this LD in this thesis is iteratively updating the multiplier by a box step method (Marsten et al., 1975), similar to Schütz et al. (2009) and Stádlerová et al. (2023). This method makes it possible to compute a lower bound without computing an upper bound. The subgradient ∇^{ml}_{jt} is calculated as $\nabla^{ml}_{jt} = D^s_{jt} - \sum_{i \in \mathcal{I}} x^l_{ijse}$ in each iteration m for each node l. We subsequently establish L^m as:

$$L^m = LR(\lambda^m) - \sum_{j\in\mathcal{J}}\sum_{h\in\mathcal{H}}\sum_{s\in\mathcal{S}_h}\sum_{e\in\mathcal{E}}\sum l \in \mathcal{N}_h \pi_l w_s \nabla_{jt}^{ml} \lambda_{jse}^{ml} \tag{6.23}$$

and determine the updating multipliers by solving the ensuing linear optimization problem:

$$max \quad \phi \tag{6.24}$$

$$\phi \leq L^i + \sum_{j\in\mathcal{J}}\sum_{h\in\mathcal{H}}\sum_{e\in\mathcal{E}}\sum_{s\in\mathcal{S}_h}\sum_{l\in\mathcal{S}_h} \pi_l w_s \nabla_{jt}^{ml} \lambda_{jse}^{m+1,l}, \qquad i = 1, ..., m \tag{6.25}$$

$$\lambda_{jse}^{m+1,l} \leq \lambda_{jse}^{ml} + \delta_{jse}^{ml}, \qquad j \in \mathcal{J}, h \in \mathcal{H}, s \in \mathcal{S}_h, l \in \mathcal{N}_h, e \in \mathcal{E} \tag{6.26}$$

$$\lambda_{jse}^{m+1,l} \geq \lambda_{jse}^{ml} - \delta_{jse}^{ml}, \qquad j \in \mathcal{J}, h \in \mathcal{H}, s \in \mathcal{S}_h, l \in \mathcal{N}_h, e \in \mathcal{E} \tag{6.27}$$

$$\phi \in \mathbb{R}, \lambda_{jse}^{m+1l} \in \mathbb{R} \tag{6.28}$$

This method limits how much the Lagrangian multiplier can change in each iteration using the constraints 6.26 and 6.27. The box sizes δ_{jse}^{ml}'s are unique for each λ_{jse}^{ml}. These λ's are initialized to a value based on domain knowledge. The δ_{jse}^{ml}'s are updated if the sign of the subgradient ∇_{jt}^{ml} changes according to $\delta_{jse}^{m+1,l} = \alpha * \delta_{jse}^{ml}$ where $0 < \alpha < 1$, similar to Stádlerová et al. (2023). Minimizing the box size aims to accelerate the process of identifying the optimal multipliers (Marsten et al., 1975), where the idea is that you prevent the model from jumping back and forth between very negative and positive multipliers illustrated in Figure 6.5. When multipliers remain unchanged for five iterations, we reset the box size, permitting larger multiplier adjustments to evade being trapped in a local optimum. Figure 6.5 illustrate the concept of the box size in a two-dimensional setting.

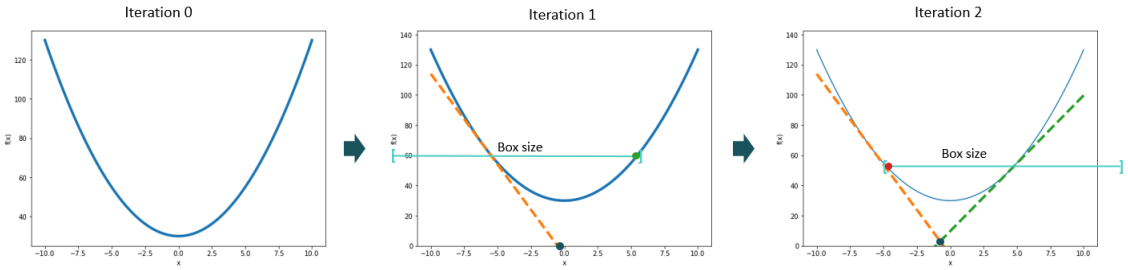

Figure 6.5: Illustration of the updating of Lagrange multipliers with box sizes.

6.4 Upper bound

The Lagrangian relaxation presented above gives a valid lower bound. Still, it does not produce an upper bound since one is not guaranteed that the solution from the Lagrange relaxation gives a feasible solution. To build a feasible upper-bound solution, we utilize a greedy heuristic. Since we have a model with complete recourse due to the penalty cost of producing too much and too little hydrogen, the relaxed problem will always be feasible. But this solution might have very high penalty costs. In our upper bound heuristic, we aim to find a feasible solution with minimum penalty costs. The main steps of the heuristic are presented in Figure 6.6 where n represents the stage you are in ordered from 0 to the

total number of demand realizations in all stages, $|N|$. E.g., if you have three stages and four children per parent, you will have $|N| = 1 + 4 + 16 = 21$. You iterate from the first node to the last and expand the demand until all demand is satisfied. This iterative way of expanding demand is utilized since you can use the previously installed capacity to satisfy demand.

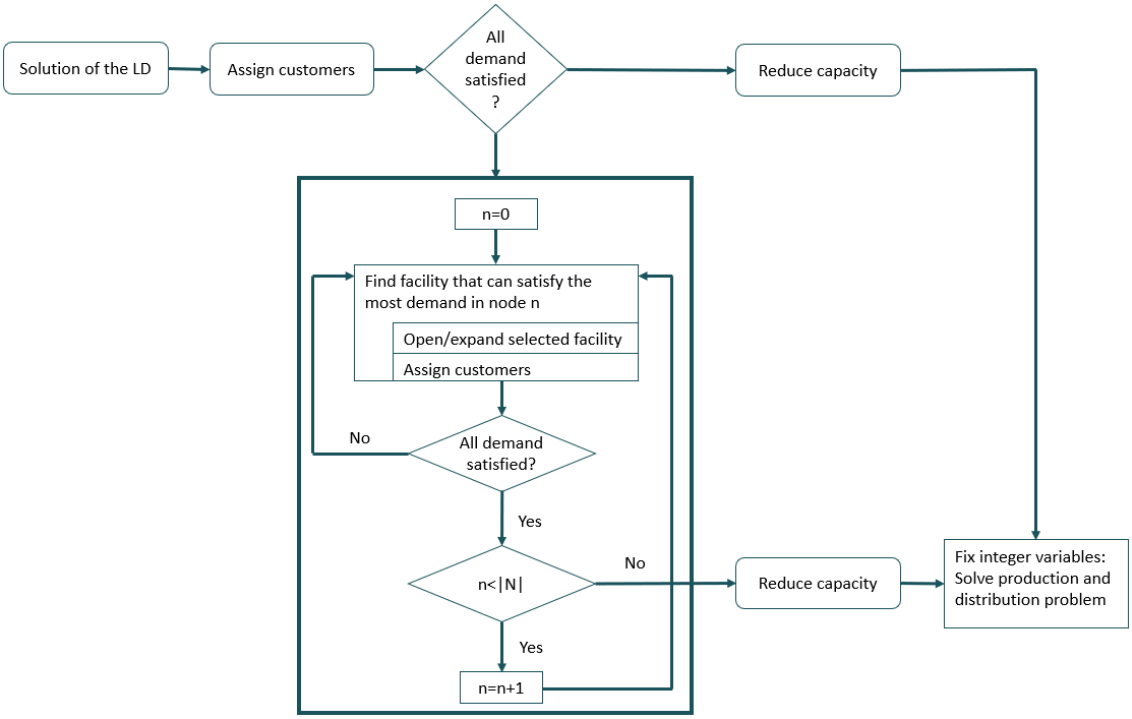

Figure 6.6: Schemtic showing the process of producing an upper bound

First, we initialize the solution with the installed capacity from the solution of the Lagrangian dual problem, LD. We ignore the production and distribution solution from the LD when we progress to the next steps of the heuristic.

Then we progress to the *Assign Customer* step. Here we create a list of pairs of facilities i and customers with unfulfilled demand j, for the given node we find ourselves in. The pairs are sorted based on their reduced transportation cost $T_{ij} - \lambda^n_{jse}$. Then, we start with the pair with the lowest reduced cost and serve the customers from the given facility until all capacity has been used to serve customers. This is repeated until there is no more demand to assign or all demand has been satisfied. Since we have relatively complete recourse, we do not need to solve the production plan optimization to ensure that this is a valid allocation of customers.

After the initial *Assign Customer* stage, we check whether we have excess production or unfulfilled demand. The solution from the LD probably installs too little demand to satisfy the demand in all nodes. To accommodate this, we introduce a procedure for increasing the capacity. As the installed capacity in previous stages can be utilized to satisfy demand in a stage, we iterate through all the nodes from the first one when increasing the capacity. In a given node, we find the facility that can serve the most unsatisfied customers. If two facilities can serve the same amount of unsatisfied customers, we choose randomly between these. Then we increase the capacity of this facility by one step with the technology already installed. If there is no installed capacity at the given facility, we choose the most popular technology for that given stage. We do this based on the assumption that given

our Lagrange relaxation, has decided that this technology is the dominating technology in that node. This procedure is repeated until all demands in that node have been satisfied. Then we progress to the next node and repeat the processes. This is done until we have iterated through all nodes.

If the solution from the LD or the procedure of increasing demand has installed excess capacity, we try to decrease the capacity. This is done by iterating through all the excess capacity found for each facility and node in the *Assign Customer* step and checking if the excess capacity at that node is greater than the capacity gap between the capacity installed and the capacity one step below $excess_{in} > K_k * y^n_{ikp} - K_{k-1} * y^n_{ikp}$.

Finally, we fix the investment variables, y^l_{ikp}, and solve the remaining optimization problem of production planning and demand allocation with Gurobi. This is the problem presented in Chapter 5 with the y^l_{ikp}'s fixed such that the restrictions 5.2 to 5.4 can be disregarded.

Chapter 7

Case Study

This chapter presents the data used as input data for our case study. In Section 7.1, we present the demand data, specifically focusing on land-based transport and the maritime transportation sector, as well as how this data is employed to generate demand scenarios. Moving on to Section 7.2, we discuss the infrastructure data, including facility and customer locations. Section 7.3 focuses on the cost data, covering investment costs, operation and maintenance costs, hydrogen production specifications, distribution costs, electricity costs, and penalty costs. Next, Section 7.4 outlines the process of generating electricity cost scenarios, such as epoch generation, normal electricity scenarios, high variance scenarios, very volatile scenarios, and high- and low-cost scenarios. Finally, Section 7.5 establishes the instance nomenclature to ensure consistency throughout the computational study.

7.1 Demand

In this section, we showcase the demand data utilized within our model. As the future hydrogen demand remains uncertain, we anticipate it to experience a gradual increase leading up to 2025. The data sources include DNV (2019), Danebergs and Aarsskog (2020a) and Ocean Hyway Cluster (2020b), offering demand projections up to 2030, 2035, and 2035, respectively. Figure 7.1 illustrates the progression of demand from these studies, divided into land-based and maritime sectors and the overall demand. Furthermore, Figure 7.2 depicts the same demand distribution across Norway's five electricity bidding zones for 2035.

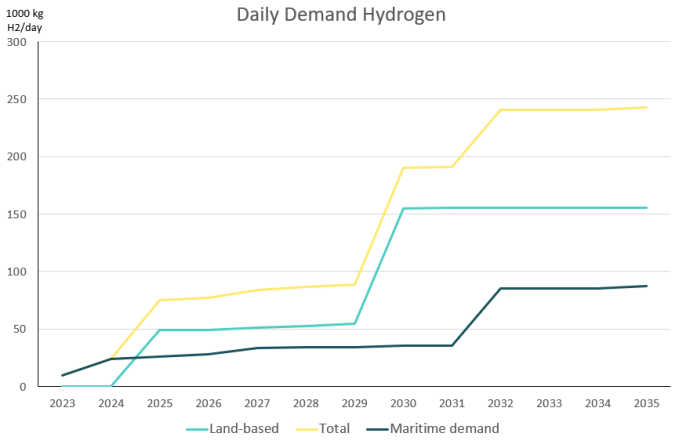

Figure 7.1: Daily demand evolution of hydrogen from 2022 towards 2035

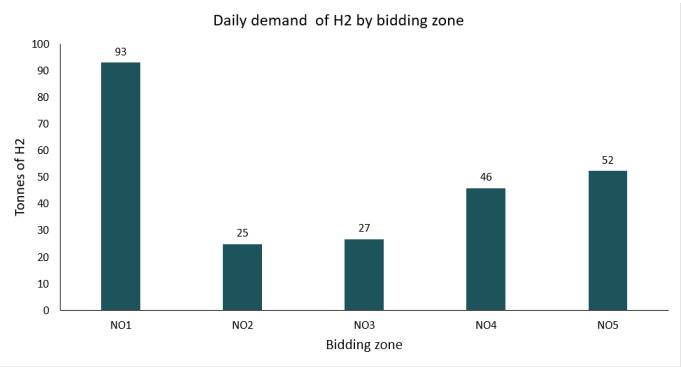

Figure 7.2: Daily demand of H2 in tonnes per bidding zone: NO1 (Oslo), NO2 (Kristiansand), NO3 (Trondheim), NO4 (Tromsø) and NO5 (Bergen
in 2035

7.1.1 Land-based Transport

Land-based transportation encompasses both rail and road transport. Road transport can be categorized into bus, light, and heavy road transportation. The demands employed in this report are derived from DNV (2019), which posits that light road transport will predominantly consist of electric vehicles. Consequently, light road transportation will not be considered a potential customer segment.

The land-based demand is allocated to customers described in Section 7.2.3 according to their road traffic volumes of the municipality of the customer location.

7.1.1.1 Bus Transportation

Bus demand estimation is grounded in the objectives outlined by Samferdselsdepartementet (2020), which call for 75% of all new long-distance buses to be zero-emission vehicles by 2030. DNV (2019) approximates a total of 6,000 long-distance buses in Norway. Assuming a 10-year lifespan for buses and a 50% share of new hydrogen-fueled buses, there will be 2,200 hydrogen buses in operation by 2030. These buses are expected to consume 7,000 tonnes of hydrogen annually.

7.1.1.2 Heavy Road Transportation

The projection for heavy road transportation is derived from the objectives set by Samferdselsdepartementet (2020), which aim for 50% of new heavy-duty trucks to be zero-emission by 2030. Assuming a 10-year lifespan for trucks and a 40% share of new hydrogen-fueled trucks, 5,000 heavy-duty hydrogen trucks will be on the road by 2030. These trucks are anticipated to consume 29,000 tonnes of hydrogen annually (DNV, 2019).

7.1.1.3 Rail Transportation

DNV (2019) outlines the total potential demand for hydrogen in the rail transportation sector if all non-electrified routes (Solørbanen, Rørosbanen, Raumabanen, Nordlandsbanen) were to transition to hydrogen. However, this scenario is not highly probable. DNV (2019) suggests that hydrogen trains will most likely be used for passenger transportation. Under this assumption, Rørosbanen and Raumabanen emerge as the most probable routes for hydrogen trains. By 2030, DNV (2019) projects that 60% of the traffic on these routes will be powered by hydrogen, resulting in an annual demand of 1,900 tonnes of hydrogen.

7.1.2 Maritime Transportation Sector

The maritime transportation sector comprises domestic car ferries, high-speed passenger ferries, and coastal routes. This section details the hydrogen demand for each of these customer segments, with estimates based on Ocean Hyway Cluster (2020b) and the following assumptions:

- Liquid hydrogen is deemed suitable only for vessels with consumption exceeding 1,000 kg between bunkering events. For lower consumption, compressed hydrogen is considered the optimal solution.
- By 2030, hydrogen fuel cells are expected to be fully mature, taking into account bunkering, storage, conversion, regulations, and integration.
- Fuel cell efficiencies are based on 2020 technology standards.
- No significant advancements are anticipated in ship performance.
- Timetables and vessel capacities for new contracts on established routes will remain unchanged.
- All future public tenders for car ferries, high-speed passenger ferries, and coastal routes will mandate zero emissions if technically feasible.

7.1.2.1 High-speed Passenger Ferries

Norway has approximately 100 high-speed passenger ferries, collectively consuming 56 million liters of diesel annually, which accounts for 0.7% of the country's petroleum sales. Danebergs and Aarsskog (2020a) examine the potential for hydrogen in this sector, focusing on quantity, demand timing, and routes. The study compares hydrogen fuel cells and battery electric solutions as competing low-carbon alternatives in this segment. Results indicate that hydrogen is suitable for 51 routes, while battery electricity is appropriate for 30 routes.

The study employs conservative yet realistic estimates of diesel consumption, considering only routes with an annual consumption above 20,000 liters. Demand timing is based on information from public tenders and contract periods, assuming that all ferries will switch to low-carbon fuels upon the expiration of their current contracts.

7.1.2.2 Domestic Car Ferries

Domestic car ferries represent a potential hydrogen demand segment in Norway. This sector encompasses over 130 ferry connections, operated by over 250 vessels, which transport nearly 20 million cars and 40 million passengers annually. The data employed in this report is sourced from the non-publicly available Ocean Hyway Cluster (2020d) study. This report outlines three distinct scenarios, reflecting uncertainties in the transition to hydrogen. We utilize the medium scenario from this case study.

7.1.2.3 Coastal Route

The Norwegian coastal route spans between Bergen and Kirkenes. Ocean Hyway Cluster (2020a) seeks to estimate the hydrogen demand along this route by 2030. The study features three scenarios, with demand fluctuations based on the number of hydrogen-powered vessels. While the results are not publicly accessible for presentation in this report, we utilize the medium scenario as input for the demand analysis.

7.1.3 Generation of Demand Scenarios

To create demand scenarios for our model, we need a procedure to create a demand scenario tree. We do this by creating bounds on the maximum and minimum demand in a given stage/level of the three. The minimum demand is based on the demand from the Maritime Transportation sector described in Section 7.1.2. To a large degree, this demand can be fulfilled by successful policies by the Norwegian government in public tenders. The maximum demand is the sum of the Maritime Transportation Sector and Land-Based Transportation demand, described in Section 7.1.1. As we want demand strictly to increase, we pass down a *growth_rate* that makes sure that the *min_limit* is at least a bit higher than the demand of the parent node. Further, we limit how much the demand can grow from a parent to a child by. This is done with the assumption that it is limited how much demand can grow from one period to the next and make sure that the further away leaf nodes are, the less likely they are to have the same demand. I.e., the nodes in the right-most part of the three have, in general, a higher demand than in the leftmost. This is done by setting a maximum growth rate based on domain knowledge. This is done by setting the $max\_limit = max\_demand * \frac{demand_{parent}}{max\_demand_{parent}} * growth\_rate$

After defining the maximum and minimum demand and the growth rate. The algorithm creates the three by going down the three randomly, creating demand in the next children in the range: $[min(current\_demand * growth\_rate, min\_demand), min(max\_demand * \frac{current_{demand}}{max\_demand_{current}} * growth\_rate, max\_demand)]$, with equal probability for all values in this range. This ensures that the demand doesn't decrease from one stage to the next, as we assume that the demand for hydrogen will increase strictly. The algorithm is described in pseudo-code in Algorithm 1, while Figure 7.3 shows how one a three of four levels/stages with to children per parent could look like, within the given maximum and minimum demands. We use a growth rate of 10% in this thesis.

Algorithm 1 Demand generation

```
function GENERATE_DEMAND_TREE(start_demand, demand_limits, n_children, m_levels, growth_rate)
    root ← start_demand
    demand_tree ← [root]
    for i ← 0 to m_levels − 1 do
        level ← []
        min_demand, max_demand ← demand_limits[i]
        min_demand × 0.95
        max_demand × 1.05
        for all parent in demand_tree[−n_children^i :] do
            for j ← 0 to n_children − 1 do
                if len(level) < n_children^(i+1) then
                    Calculate min_percent, max_percent, min_limit, and max_limit
                    demand ← random_integer(min_limit, max_limit)
                end if
                level.append(demand)
            end for
        end for
        demand_tree.extend(level)
    end for
    return demand_tree
end function
```

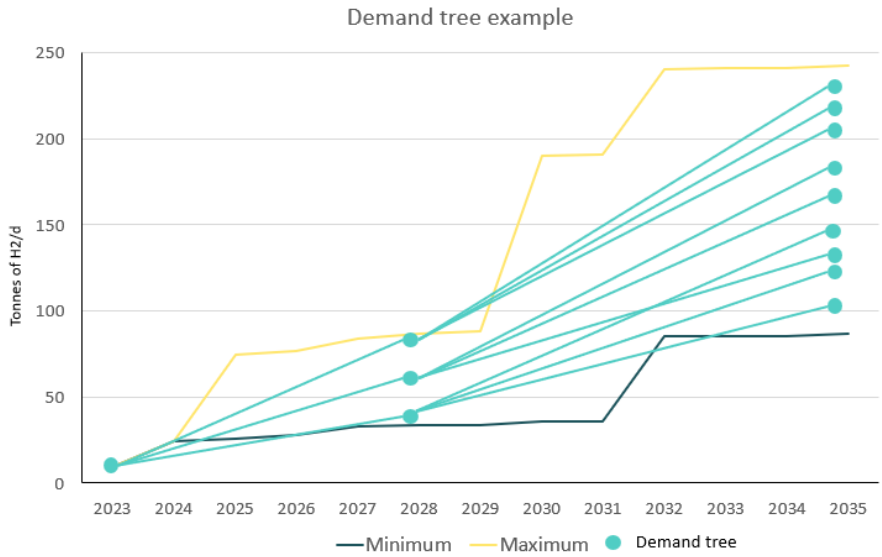

Figure 7.3: Example of how Algorithm 1 can produce a demand three for three levels and three nodes per parent.

In Chapter 8 we use a three-stage model to represent the years from 2023 to 2032. Each stage in the tree corresponds to a possible demand realization from 2023, 2028, or 2032. In our model, the production decisions in each node are multiplied by five in order to make it correspond to 5 years. Further, we create a balanced three, with equal probabilities for each node in a given level.

7.2 Infrastructure data

This section introduces the data related to facility and customer locations. The information on facility locations and customer locations is derived from the research conducted by Stádlerová and Schütz (2021) as well as Aglen and Hofstad (2022).

7.2.1 Facility Locations

The possible facility locations are based on the interactive map of 17 potential sites provided by Ocean Hyway Cluster (2020c). This map was later expanded to incorporate additional locations with assigned production technologies. However, we do not consider these modifications in our case study, particularly because choosing the production technology is a decision within our model. We supplement the initial 17 locations with those that received funding from Enova for hydrogen production in the maritime sector in 2022 (Enova, 2022b) and were not already included. This results in a total of 20 potential facility locations. Figure 7.3 showcases these possible locations for large-scale hydrogen production, indicating the electricity bidding zone each site belongs to, adapted from Ocean Hyway Cluster (2020c) and expanded with Enova (2022b).

Figure 7.4: Facility location candidates adapted from Ocean Hyway Cluster (2020c) and expanded with Enova (2022b), marked with the electricity bidding zone it belongs in.

7.2.2 Reducing Facility Locations

We devise three strategies to reduce the facility location space to mitigate high run times for our model. These strategies are:

1. **K-means clustering**: We employ k-means clustering based on the longitude and latitude of the locations to decrease the number of facilities to 12. This number is chosen based on a visual inspection of the map displaying the complete facility space.
2. **Southern bidding zones with k-means reduction**: We only consider facilities in the bidding zones NO1 (Oslo), NO2 (Kristiansand), NO3 (Trondheim), and NO5 (Bergen), while also taking into account the k-means reduction. This approach results in a total of 6 possible facilities.
3. **Largest cities**: We exclusively focus on the three largest cities in Norway: Oslo (Slemmestad), Bergen (Kollsnes), and Trondheim.

Table 7.1 provides an overview of the facilities included in each of the three strategies.

Table 7.1: Overview of the facility space for different reduction strategies

Strategy	Facilities
1	Andnes, Berlevåg, Finnes, Florø, Glomfjord, Hellesylt, Kollsnes, Slemmestad, Stavanger, Storekorsnes, Svolvær, Trondheim
2	Florø, Hellesylt, Kollsnes, Slemmestad, Stavanger, Trondheim
3	Slemmestad, Kollsnes, Trondheim

7.2.3 Customer Locations

The customer locations comprise 71 distinct sites, extending from Arendal in the south to Berlevåg in the north. The 51 coastal locations are informed by Danebergs and Aarsskog (2020a) and Ocean Hyway Cluster (2020b), both of which offer estimates of hydrogen demand in the Norwegian domestic maritime transportation and high-speed ferry sectors. These sites function as bunkering ports for Norway's maritime sector. Additional inland locations relevant to the road transportation sector are included to encompass the entire transportation sector. These sites are based on the selection made by Stádlerová and Schütz (2021) and represent the 20 municipalities with the highest road traffic volumes, as reported by Statistisk Sentralbyrå (2021). Figure 7.5 shows this selection of customer locations. There are no customers in the central part of Norway, which is related to it not being any maritime demand there, in addition to it not having high volumes of road traffic due to unfavorable road infrastructure for transportation.

Figure 7.5: Customer locations for hydrogen in Norway.

7.2.4 Reducing Customer Locations

Similar to the facility space, we suspect the customer space might be too large to achieve solutions within acceptable timeframes when considering larger scenario spaces. To address

this issue, we introduce three strategies to decrease the customer space, corresponding to the same three strategies presented in Section 7.2.2.

1. **K-means clustering reduction** Reduction of the customer space by applying K-means clustering on longitude and latitude, resulting in 30 locations.
2. **Bidding zone-based reduction** Retaining only the K-means reduced space for bidding zones NO1 (Oslo), NO2 (Kristiansand), NO3 (Trondheim), and NO5 (Bergen).
3. **Further K-means clustering reduction** Further reducing the space to 13 locations by employing K-means clustering, where 13 is chosen based on inspection of the data.

For strategies 1 and 3, the total demand in a cluster is assigned to the location chosen from that cluster. Table 7.2 presents the remaining customers for each strategy, offering a clearer overview of the reduced customer spaces.

Table 7.2: Overview of the facilities included in the three strategies

Strategy	Customer locations
1	Alta, Andøya, Askvoll, Bergen, Brattvåg, Dyrøy, Dønna, Hasvik, Herøy, Kirkenes, Lødingen, Namsos, Os, Rosendal, Sogndal, Svolvær, Sør-Tverrfjord, Tromsø, Vannøy, Ørnes, Kongsvinger, Støren, Åndalsnes, Fredrikstad, Asker, Hamar, Larvik, Karmøy, Berlevåg, Arendal
2	Askvoll, Bergen, Brattvåg, Dønna, Herøy, Namsos, Os, Rosendal, Sogndal, Kongsvinger, Støren, Åndalsnes, Fredrikstad, Asker, Hamar, Larvik, Karmøy, Arendal
3	Askvoll, Bergen, Brattvåg, Herøy, Namsos, Os, Sogndal, Støren, Asker, Hamar, Larvik, Karmøy, Arendal

7.3 Cost Data

In this section, we discuss the cost data utilized in this theis. The investment and operational expenses for hydrogen production are derived from Andrenacci et al. (2022), which evaluates multiple key performance indicators (KPIs) for hydrogen electrolyzers, taking into account current technology and objectives for 2030. Electricity prices, a crucial input for hydrogen production, are sourced from Nord Pool (2023).

7.3.1 Investment Cost

The investment cost for both alkaline and PEM hydrogen production technologies is based on the 2020 costs and 2030 targets provided by Andrenacci et al. (2022), offering CAPEX estimates at a 1 MW scale. Since Andrenacci et al. (2022) do not account for economies of scale, we estimate economies of scale using the curve from IRENA (2020b), as discussed in Section 2.1.1.3, assuming that economies of scale beyond 100 MW are negligible.

Moreover, the installation and engineering costs associated with setting up production facilities are assumed to be 20% of the investment (Jakobsen & Åtland, 2016). A facility

can invest in 9 distinct capacity points for both technologies. These nine capacities were chosen based on a logarithmic graph, where the maximum is selected such that all facilities given the transportation restrictions, can satisfy the maximum amount of demand it can reach.

Table 7.3 presents a summary of the investment cost for the discrete capacity points using 2020 data from Andrenacci et al. (2022), while Table 7.4 provides the same information for 2030 data. As discussed in Section 7.1.3, we create a demand scenario three with stages in 2023, 2028, and 2032. Our model uses the 2020 data for 2023 and the 2030 data for 2033. For 2028, we create a linear approximation between these specifications to determine the costs. This is represented in Table 7.5.

Table 7.3: Investment and engineering cost of hydrogen technologies over the discrete capacities for 2023.

Discrete Capacities	1	2	3	4	5	6	7	8	9
Capacity [tonnes/day]	0.5	2.5	5	12.5	25	50	80	125	250
Investment PEM [mill €]	0.9	3.6	5.4	12.9	24.8	45	72	101.3	202.6
Engineering PEM [mill €]	0.2	0.7	1.1	2.6	5.0	9	14.4	22.5	45
Investment Alkaline [mill €]	0.6	2.4	3.6	8.6	16.5	30	48	75	150
Engineering Alkaline [mill €]	0.1	0.5	0.7	1.7	3.3	6	9.6	15	30

Table 7.4: Investment and engineering cost of hydrogen technologies over the discrete capacities for 2033.

Discrete Capacities	1	2	3	4	5	6	7	8	9
Capacity [tonnes/day]	0.5	2.5	5	12.5	25	50	80	125	250
Investment PEM [mill €]	0.5	2	3	7.2	13.8	25	40	62.5	125
Engineering PEM [mill €]	0.1	0.4	0.6	1.4	2.7	5	8	12.5	25
Investment Alkaline [mill €]	0.4	1.9	2.9	6.9	13.2	24	38.4	60	120
Engineering Alkaline [mill €]	0.1	0.38	0.58	1.38	2.6	4.8	7.7	12	24

Table 7.5: Investment and engineering cost of hydrogen technologies over the discrete capacities for 2028 interpolated data.

Discrete Capacities	1	2	3	4	5	6	7	8	9
Capacity [tonnes/day]	0.5	2.5	5	12.5	25	50	80	125	250
Investment PEM [mill €]	0.7	2.8	4.2	10.05	19.3	35	56	81.9	163.8
Engineering PEM [mill €]	0.15	0.55	0.85	2	3.85	7	11.2	17.5	35
Investment Alkaline [mill €]	0.5	2.15	3.25	7.75	14.85	27	43.2	67.5	135
Engineering Alkaline [mill €]	0.1	0.44	0.64	1.54	2.95	5.4	8.65	13.5	27

Since we need to have a correct ratio between investments done in the different stages of our model, we divide these costs by 15 to annualize them and then multiply the investment done in the first stage by 15, as it will produce hydrogen for 15 years, the second by ten and the last by 5. The decision to annualize these costs by dividing by 15 is a trade-off between the lifetime stated by the manufacturers of 90 000 hours (∼10 years) (IEA, 2019), and the fact that this often is a pessimistic estimate in order to avoid the chance of having to pay for early malfunctioning. In addition, we assume that producing at 100% for ten years is not optimal. Thus, investments in the first stage will probably have some of the 90 00 hours of lifetime left ten years after installation.

7.3.2 Operation and Maintenance Cost

Andrenacci et al. (2022) operates with yearly costs for operation and maintenance. We transfer these costs to the investment cost and multiply the number of years the facility will be in operation, similarly to how we handle the investment cost. The data from Andrenacci et al. (2022) is also only provided for 2020 and 2030, this is handled in the same way as for the investment costs, where 2020 data corresponds to the 2023 investments, 2030 data to the 2032 investments, and 2028 is interpolated between these to data points. Table 7.6, 7.7 and 7.8 shows this data.

Table 7.6: Operation and maintenance of hydrogen for the different technologies per year for 2023.

Discrete Capacites	1	2	3	4	5	6	7	8	9
Capacity [tonnes/day]	0.5	2.5	5	12.5	25	50	80	125	250
O&M PEM [mill €/ year]	0.02	0.1	0.21	0.51	1.0	2.1	3.3	5.1	10.2
O&M Alkaline [mill €/year]	0.03	0.13	0.25	0.625	1.25	2.5	5	6.25	12.5

Table 7.7: Operation and maintenance of hydrogen for the different technologies per year for 2033.

Discrete Capacites	1	2	3	4	5	6	7	8	9
Capacity [tonnes/day]	0.5	2.5	5	12.5	25	50	80	125	250
O&M PEM [mill €/ year]	0.01	0.05	0.11	0.26	0.53	1.1	1.7	2.6	5.2
O&M Alkaline [mill €/year]	0.02	0.09	0.18	0.44	0.86	1.8	2.8	4.4	8.8

Table 7.8: Operation and maintenance of hydrogen for the different technologies per year for 2028 interpolated data.

Discrete Capacites	1	2	3	4	5	6	7	8	9
Capacity [tonnes/day]	0.5	2.5	5	12.5	25	50	80	125	250
O&M PEM [mill €/ year]	0.015	0.075	0.16	0.385	0.765	1.6	2.5	3.85	7.7
O&M Alkaline [mill €/year]	0.025	0.11	0.215	0.535	1.055	2.15	3.9	5.325	10.65

7.3.3 Hydrogen Production Specifications

The efficiency data for hydrogen production technologies are sourced from Andrenacci et al. (2022). For production scales above 0.5 MW (equivalent to 0.25 tonnes/day H2), hydrogen electrolyzer efficiencies remain consistent (Andrenacci et al., 2022). As a result, in our use case, efficiency stays constant across different discrete investment capacities. While there are minor differences in electrolyzer efficiency based on load variation and degeneration under variable load (Andrenacci et al., 2022), these effects will not be considered in our study, resulting in a linear short-term hydrogen production cost.

PEM and Alkaline technologies differ in their flexibility regarding the dynamic production range. Alkaline has a production range of 20-100%, while PEM's range is 0-100% (Andrenacci et al., 2022). This sets a lower production limit for Alkaline at 20% of installed capacity. The production specifications for PEM and Alkaline are summarized in Table 7.9, with power consumption being the only changing parameter between 2020 and 2030. For investments done in 2023 we use the 2020 data, and for the 2032 investments, we use the 2030 data, and for 2028 we use the mid-point of 51.5 kWh/kg for PEM and 49

kWh/kg for Alkaline.

Based on Nel (2021), startup times for PEM and Alkaline affect the required shutdown duration before production can resume. For PEM, the startup time is less than one hour, which is the granularity of electricity prices. Consequently, PEM has no restrictions on shutdown time. Alkaline startup times can range between 30, 90, or 150 minutes, depending on the initial state. We set a minimum shutdown time of 120 minutes (two time periods in our model's operational stage) for Alkaline as a compromise between these estimates. Determining the electrolyzer state upon shutdown is a separate optimization issue, which we will not address here. This factor does not impact the ability to vary the electrolyzer load. For example, if an electrolyzer produces hydrogen at hour 0, experiences a price spike at hour 1, and a price drop at hour 2, the optimal strategy for PEM would be to shut down at hour 1 and restart at hour 2. For Alkaline, this is not possible, and the options are either to shut down for both hour 1 and hour 2 or reduce the load to 20% (the lower production limit) at hour 1 and return to 100% at hour 2.

Table 7.9: Production specification of hydrogen technologies.

	PEM	**Alkaline**
Power consumption (kWh/kg) 2020	55	50
Power consumption (kWh/kg) 2030	48	48
Dynamic production range	0-100%	20-100%
Start-up periods	0 (0 hours)	2 (2 hours)

7.3.4 Distribution Cost

In this case study, we focus solely on hydrogen transportation via road, as transporting by ship or pipeline necessitates substantial single-point demands. Consequently, hydrogen transportation depends only on distance, as trailers will always be fully loaded and incur a fixed cost per trailer without any decreasing costs for each additional trailer. We adopt the values from Madsen (2019) for 1-tonne hydrogen transportation, which is approximately equivalent to a 40-foot, 300-bar container that a truck can carry.

As discussed in Section 2.3, Norwegian labor regulations limit truck drivers' working hours before requiring rest. As a result, our transportation costs have a maximum distance of 1000 km. The general cost function for hydrogen distribution, illustrated in Figure 2.9, covers a range of distance intervals, Table 7.10 summarizes the data used in our model.

Table 7.10: Distribution cost per kg hydrogen as a function of distance (Madsen, 2019)

Distance [km]	**1-50**	**51-100**	**101-250**	**251-500**	**501-750**	**751-1000**
Cost [€/(km*kg)	0.00825	0.00573	0.00423	0.00372	0.00319	0.00262

7.3.5 Electricity Cost

The electricity cost in this thesis is collected from the historical data in the database of day-ahead prices from Nord Pool (2023), and is used to represent the possible future realizations of electricity prices. The data is collected for each bidding zone in Norway, and each facility location from Section 7.2.1 is assigned its correct electricity price.

The data is collected from 2022, 2021, and 2020 and have been used to sample scenarios from. Figure 7.6 illustrates a sample of the data for a specific date within the

Kristiansand, Trondheim, and Tromsø price areas. Meanwhile, Figure 7.7 displays the variations throughout the entire time frame, highlighting the average monthly price for Kristiansand, Trondheim, and Tromsø.

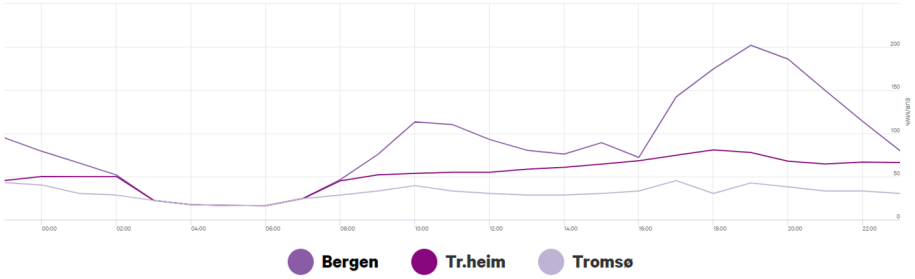

Figure 7.6: Daily fluctuations in the electricity price in Bergen, Trondheim, and Tromsø the 1st of October (Nord Pool, 2023).

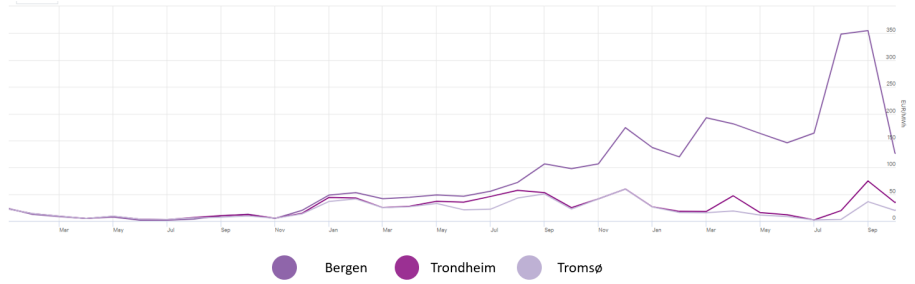

Figure 7.7: Monthly fluctuation in the electricity price in Bergen, Trondheim, and Tromsø between January 2020- December 2022 (Nord Pool, 2023).

7.3.6 Penalty Cost

To ensure relatively complete recourse, penalty costs are applied for the overproduction and underproduction of hydrogen. The penalty cost for overproduction is set at a relatively high rate of 20 €/kg, which approximates the cost of generating hydrogen in Lindesnes (the southernmost point in Norway) with an electricity price of 300 €/MWh and then transporting it to Nordkapp (the northernmost point in Norway). On the other hand, the penalty cost for underproduction is set at a comparatively low rate of 0.1 €/kg, assuming that the expense associated with managing surplus hydrogen is minimal.

7.4 Generation of Electricity Cost Scenarios

This section will present how we construct the input data that consists of epochs and daily electricity prices. Firstly explaining the epoch structure, and then explaining different schemas for sampling electricity data.

7.4.1 Epoch Generation

Our model processes information from electricity data, which is divided into scenarios. Each scenario consists of one or several epochs. An epoch, in turn, consists of a single day with 24 hours. This method of representing scenarios was chosen to effectively capture seasonal and daily electricity price variations. We will have 1, 2, or 4 epochs. The

four epochs represent the seasons of a year in Norway, which have differences in prices. Two epochs represent winter and summer, as these are the two seasons with the largest variations in price between themselves. Finally, for the one epoch instance, the data for one scenario is chosen from the pool of all the days in our electricity prices. For all the different epochs, we randomly sample electricity data through Monte Carlo sampling. The way this input data is generated is shown in Figure 7.8, 7.9, and 7.10, for 4, 2, and 1 epochs.

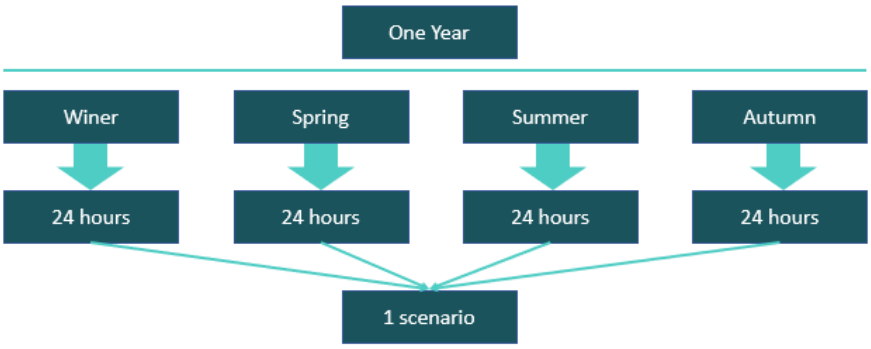

Figure 7.8: Illustration of how each scenario is generated for 4 epochs

.

Figure 7.9: Illustration of how each scenario is generated for 2 epochs

.

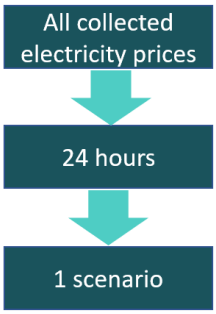

Figure 7.10: Illustration of how each scenario is generated for 1 epoch

.

7.4.2 Normal Electricity Scenarios

We employed a straightforward Monte Carlo sampling methodology in our model's limit testing. This approach leans on the "Law of Large Numbers," which posits that the scenarios will gradually align with a solid approximation of the data set given enough trials. The implementation involved selecting a random year from our available data without excluding it for subsequent picks and then picking a random date for each season, also without excluding it. These choices formed the basis for individual model scenarios.

The random numbers were generated using Python's randint function, which produces pseudo-random numbers rooted in the current millisecond timestamp (Python, 2023b). We establish our epochs based on the actual occurrences of electricity prices. Hence, all days and years have the same chance of occurrence, forming uniform probability distributions.

7.4.3 High Variance Scenarios

The choice to use PEM technology is often attributed to the high volatility of electricity prices (Abdollahipour & Sayyaadi, 2022). To determine if this factor similarly impacts our model, we establish scenarios that narrow our sampling pool to the top 10% of days exhibiting the greatest volatility, as determined by daily variance. We then use Monte Carlo sampling to create scenarios from these selected days.

As we see an increase in the construction of more variable renewable energy sources, such as onshore and offshore wind, along with solar PVs, the volatility of electricity prices could rise. Additionally, the new electricity cables connecting to Europe may also influence this trend in southern Norway as Europe's power grid transitions towards more renewable sources. Thus, exploring high-variance scenarios becomes crucial to determine the value of flexibility in hydrogen production.

7.4.4 Very Volatile Scenarios

We create a highly volatile scenario where Monte Carlo samples are taken from the top 1% of scenarios demonstrating the greatest total sum inter-hour electricity price variation, adjusted for the average daily price. This involves the absolute sum of the differences between each pair of hours in a day divided by the average electricity price. Equation (7.1) illustrates how this computation is done for a single day. This approach will provide us with scenarios depicting the most substantial relative daily price changes.

$$\frac{1}{\bar{p}} \sum_{i=0}^{23} \|p_{i+1} - p_i\| \tag{7.1}$$

where p_i is the electricity price in hour i and $\bar{p}$ is the average electricity price.

7.4.5 High- and Low-cost Scenarios

The impact of learning curve effects related to renewable energy generation could potentially reduce electricity costs. Conversely, increased electrification could create a demand scenario that leads to a spike in market prices. It remains uncertain which of these influences will primarily shape future electricity prices. Thus, it's intriguing to explore how various future scenarios might impact the design of the hydrogen supply chain.

To examine if high or low electricity prices influence the choice of hydrogen technology,

we employ an approach similar to generating high variance scenarios for high and low electricity cost scenarios. This involves only sampling from the days falling within the top or bottom 10% in terms of average electricity price. Monte Carlo sampling is then used to formulate scenarios from these particular days.

7.5 Instance Nomenclature

The model is solved for different pairs of customers and facilities, number of children per node, number of epochs, and number of electricity scenarios as described by the previous sections in this Chapter. We have three different facility-customer configurations (C) which we denote C1, C2, and C3. Further, we have either 1, 2, or 4 epochs, denoted as E1, E2, and E4. For the electricity scenarios, we use 2, 5, and 10, 25, 50, and 100 realizations of these, denoted S2, S5, S10, S25, S50, S100. We use 2, 4, 8, and X, denoted N2, N4, N8, and NX, for the demand scenarios described through the number of children per parent node. Finally, we have different characteristics of the electricity scenarios (T): n (normal), l (low), h (high), v (volatile), and vv (very volatile). This gives the following notation to distinguish between the instances CxExSxNxTx. For example, an instance with the largest customer space of 3, 1 epoch, 5 electricity scenarios, four nodes per parent, and normal electricity costs will be denoted C3E1S5N4Tn.

Table 7.11: Overview of all instances used in Chapter 8

Name	Customer-Facility config	Epochs	Scenarios	Number of children per parent	Electricity Scenario
C1E1S2N2Tn	Small	1	2	2	Normal
C1E2S5N2Tn	Small	2	5	2	Normal
C1E4S10N2Tn	Small	4	10	2	Normal
C1E2S5N4Tn	Small	2	5	4	Normal
C1E1S10N4Tn	Small	1	10	4	Normal
C1E4S10N8Tn	Small	4	10	8	Normal
C2E2S2N2Tn	Medium	2	2	2	Normal
C2E4S5N2Tn	Medium	4	5	2	Normal
C2E2S5N4Tn	Medium	2	5	4	Normal
C2E4S10N4Tn	Medium	4	10	4	Normal
C2E1S2N8Tn	Medium	1	2	8	Normal
C2E2S2N8Tn	Medium	2	2	8	Normal
C2E1S5N8Tn	Medium	1	5	8	Normal
C2E2S5N8Tn	Medium	2	5	8	Normal
C2E1S10N8Tn	Medium	1	10	8	Normal
C3E1S2N2Tn	Large	1	2	2	Normal
C3E2S10N2Tn	Large	2	10	2	Normal
C3E2S2N4Tn	Large	2	2	4	Normal
C3E1S5N4Tn	Large	1	5	4	Normal
C3E2S5N4Tn	Large	2	5	4	Normal
C3E1S10N4Tn	Large	1	10	4	Normal
C3E1S2N8Tn	Large	1	2	8	Normal
C3E2S2N8Tn	Large	2	2	8	Normal
C3E1S10N8Tn	Large	1	10	8	Normal
C1E4S25N2Tn	Small	4	25	2	Normal
C1E4S502Tn	Small	4	50	2	Normal
C1E2S50N2Tn	Small	2	50	2	Normal
C1E2S75N2Tn	Small	2	75	2	Normal
C1E1S75N2Tn	Small	1	75	2	Normal
C1E1S100N2Tn	Small	1	100	2	Normal
C1E1S150N2Tn	Small	1	150	2	Normal
C1E1S25N2Th	Small	1	25	2	High
C1E2S50N2Th	Small	2	50	2	High
C1E1S100N2Th	Small	1	100	2	High
C1E1S25N2Tl	Small	1	25	2	Low
C1E2S50N2Tl	Small	2	50	2	Low
C1E1S100N2Tl	Small	1	100	2	Low
C1E1S25N2Tv	Small	1	25	2	Volatile
C1E2S50N2Tv	Small	2	50	2	Volatile
C1E1S100N2Tv	Small	1	100	2	Volatile
C1E1S25N2Tvv	Small	1	25	2	Very Volatile
C1E2S50N2Tvv	Small	2	50	2	Very Volatile
C1E1S100N2Tvv	Small	1	100	2	Very Volatile
C3E1S2N8Th	Large	1	2	8	High
C3E1S2N8Tl	Large	1	2	8	Low
C3E1S2N8Tv	Large	1	2	8	Volatile
C3E1S2N8Tvv	Large	1	2	8	Very Volatile

Chapter 8

Computational Study

This chapter presents the results of the multi-horizon model applied, as detailed in Chapter 5, to the case studies presented in Chapter 7. It is structured into two sections: Model Performance Analysis (Section 8.1), and Managerial Insight (Section 8.2).

Section 8.1 initiates with the presentation of computational results using Lagrangian relaxation, both with and without the Shortest Path Heuristic, as introduced in Chapter 6. Subsequently, we compare the optimality gaps and runtimes derived from Lagrangian relaxation and commercial solver Gurobi. This comparison extends to the cases from Chapter 7 and larger problem instances in order to also examine the scalability of these methods in relation to our hardware capacity.

Section 8.2 emphasizes managerial implications. Here, we first explore the benefits of the problem's formulation as a stochastic multi-stage, multi-horizon program. This is followed by an evaluation of production flexibility's significance and, finally a discussion on the problem solutions derived from our implementation. In the former discussion, we present and discuss the insights gained from our problem solution with respect to production flexibility, investment decisions related to location, capacity and technology choice, cost factors, and the operational production schema.

In this chapter, all problem instances are solved on a computational cluster provided by the Department of Industrial Economics and Technology Management at NTNU, utilizing the same computational node. Gurobi, a commercial solver, is employed for these instances. The hardware and software specifications employed across all runs can be found in Table 8.1

Table 8.1: Hardware and software description.

Computer	HP bl685cG7
CPU	4x2.2GHz AMD Opteron 6274 - 16 core
RAM	128Gb
Disk	300Gb SAS 15k rpm
Python version	3.10.4
Gurobi version	10.0.0

8.1 Model Performance Analysis

This section focuses on the performance of the solution method for the problem, in particular, the comparison between solving the model with Gurobi and with our Lagrange Relaxation.

8.1.1 Implementation

We leverage multiprocessing to solve the Lagrangian subproblems for each facility location i in parallel, regardless of whether the subproblem is implemented as a shortest path problem or by the standard model representation. This parallel computation is carried out using the multiprocessing module within Python's standard library (Python, 2023a), a strategy deployed to reduce the runtime. This multiprocessing approach is visually represented in Figure 8.1.

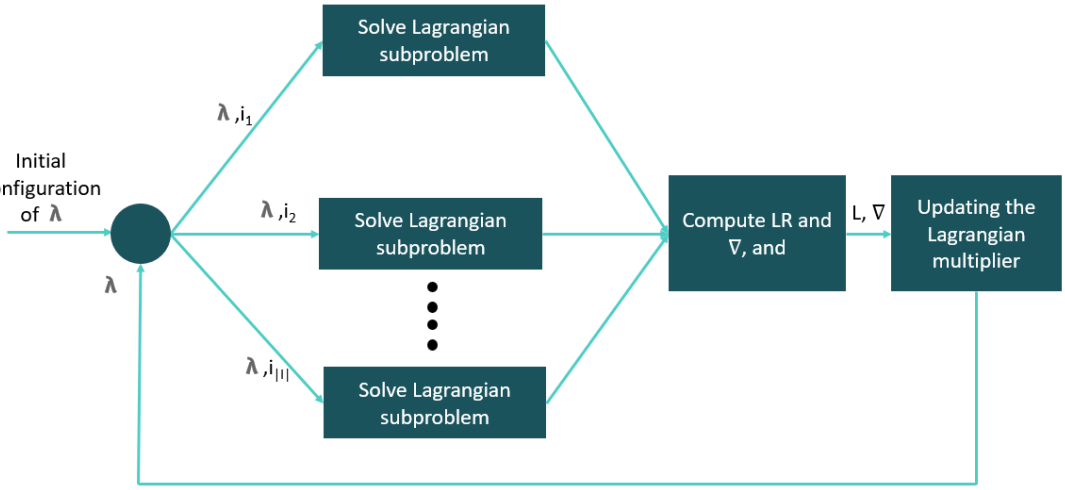

Figure 8.1: Illustration of the multiprocessing framework for solving the Lagrangian subproblem

8.1.2 Solving the Lagrangian Subproblem With Shortest Path

As discussed in Section 6.1 we have implemented two methods for solving the Lagrangian subproblem:

1. With dynamic programming and shortest path
2. With the commercial solver Gurobi

Our preliminary research involved comparing the two methods: method 1) the Shortest Path formulation and method 2) the commercial solver, Gurobi. We found that for problem sizes that fell within our established maximum solution time of 172,800 seconds (or 48 hours), the Shortest Path method exhibited significantly longer running times and yielded larger optimality gaps compared to the Gurobi method. The comparative analysis is detailed in Table 8.2, where the gap is defined the same way as by Gurobi:

$$Gap = \frac{UB - LB}{UB}, \tag{8.1}$$

Table 8.2: Table showing the gap, the time used and the number of iterations for solving the Lagrange subproblem with 1) shortest path and 2) Gurobi.

Inctance	Method 1			Method 2		
	Gap (%)	Time (s)	Lagrange iteration	Gap (%)	Time (s)	Lagrange iteration
C1E1S2N2Tn	25 %	42010	3	10 %	325	12
C2E2S5N4Tn	100 %	172 800	2	9 %	26071	17
C3E1S2N8Tn	100 %	172 800	1	7 %	51584	31

The challenges in terms of the large optimality gaps yielded by the shortest path method stem from the method's iterative nature and the complexity of the problem. A gap of 100% indicates that the Lagrange relaxation could not complete enough iterations to produce a lower bound better than the first LB obtained from installing no capacity and fulfilling no demand. The reason for why it is not able to complete enough iterations is largely due to the numerous *production optimization problems* necessitated by the investments, as seen in (6.4) - (6.20). These problems, though straightforward for Gurobi, are vast in terms of variables and constraints, rendering their construction computationally intensive.

The model build-time for the *production optimization problem* is considerably larger than the solve time, typically by a factor of 50 to 200. This vast discrepancy gives substantial overhead time usage, especially when solving the problem via the shortest path algorithm.

The number of times one needs to solve the production optimization problem scales with $|P||K|\frac{1-(|P||K||N|)^{|S|}}{1-(|P||K||N|)}$. This comes from the need to solve $|P||K|$ production optimization problems in the first stage. In the second stage, one needs to solve $|P||K||N|$ production optimization problems for each of the $|P||K|$ solutions from the first stage, a total of $(|P||K|)^2|N|$ problems. For the third stage, one also needs to solve $|P||K||N|$ production optimization for all the solutions from the second stage, a total of $(|P||K|)^3|N|^2$ problems. This development in the number of production optimization problems one needs to solve continues for the following stages. Here $|P|$, $|K|$, $|N|$, and $|S|$ denote the number of production technologies, capacities, child nodes per parent node, and stages in the problem, respectively This gives the following geometric sum $\sum_{s=1}^{s=|S|}(|P||K|)^s|N|^{s-1}$, which simplified is $|P||K|\frac{1-(|P||K||N|)^{|S|}}{1-(|P||K||N|)}$.

Consequently, even our smallest problem instance (nine capacities, two technologies, three stages, and two nodes per parent) leads to 23,994 problems. Additionally, inherent overhead accompanies the Gurobi model setup, incorporating model loading, variable and constant initialization, and parameter configuration.

Given the problem's complexity, our maximum solve time of 172,800 seconds (or 48 hours) may not suffice to fully benefit from solving the subproblem with the shortest path. Potential enhancements might lie in speeding up the run time for solving the production optimization problem in Gurobi. Techniques such as warm-starting could offer promising avenues for exploration and improvement.

8.1.3 Comparison with Commercial Solver

This section will compare our implementation of Lagrange relaxation with solving the model with a commercial solver. The two methods are defined as:

1. **Lagrange:** Solving the model with our Lagrange Relaxation as defiend in Chapter 6, but solving the Lagrange supproblem with Gurobi.
2. **Gurobi:** Solving the full model with the commercial solver Gurobi.

To be able to compare this we define the following numbers:

$$UB_{gap} = \frac{UB_{gurobi} - UB_{lagrange}}{UB_{lagrange}} \tag{8.2}$$

$$LB_{gap} = \frac{LB_{lagrange} - LB_{gurobi}}{LB_{lagrange}} \tag{8.3}$$

Equations (8.2) and (8.3) are established to determine whether the poorer performance is a trend specifically associated with the UB-heuristic or if the results from the lower bound produced by the Lagrange Relaxation. When doing this computational study, this time is set to be approximately equal to the time used for solving the model with Gurobi, to compare the gap provided by Gurobi with that of the Lagrange relaxation in similar time scales.

Our Lagrange relaxation has two termination criteria:

1. Time, which is set such that this criterion is a bit higher than the exact solution from Gurobi, in order to compare the gap provider by Gurobi wit that of Lagrange relaxation in similar time scales. It is checked after each iteration of solving the Lagrange subproblem.
2. If the Lagrange multipliers, λ, do not change more than 1%, defined as:

$$\frac{\overline{\lambda_{\mathbf{new}}} - \overline{\lambda_{\mathbf{old}}}}{\overline{\lambda_{\mathbf{old}}}} \leq 1\%.$$

Table 8.3 summarizes the gap and time use for using Gurobi and the Lagrange relaxation, as well as showing the UB-gap and LB-gap. For all instances, in Table 8.3, the Lagrange relaxation is terminated by reaching the time limit. Further, in Gurobi, the termination criteria were reaching an optimality gap below 1%.

Table 8.3: Results comparison between Gurobi and Lagrange relaxation. "*" denotes instances where Gurobi was prematurely terminated due to memory exhaustion prior to meeting the termination criteria. "n/a" signals termination during model construction.

Instance	Gurobi		Lagrange		Comparison	
	Gap (%)	Time (s)	Gap (%)	Time (s)	UB-gap (%)	LB-gap (%)
C1E1S2N2Tn	0.33	26	2.86	325	1.67	0.92
C1E2S5N2Tn	0.66	894	4.6	2568	4.6	0.66
C1E4S10N2Tn	0.75	5975	12.2	9121	13.2	-0.11
C1E2S5N4Tn	0.86	15841	4.3	20581	-0.64	4.3
C1E1S10N4Tn	0.80	10290	6.6	12220	4.2	2.03
C1E1S2N8Tn	0.5	1804	1.2	11531	-0.66	1.4
C1E2S2N8Tn	0.95	10252	1.2	20220	-1.0	1.1
C1E1S5N8Tn	2.57*	7995	0.84	11025	-1.74	-0.1
C1E1S10N8Tn	n/a	n/a	9.0	77059	n/a	n/a
C1E4S10N8Tn	n/a	n/a	7.98	127027	n/a	n/a
C2E2S2N2Tn	0.73	195	4.7	538	2.64	1.54
C2E4S5N2Tn	0.93	13516	9.5	26071	8.8	-0.33
C2E2S5N4Tn	0.94	16726	3.7	27910	2.5	0.14
C2E4S10N4Tn	n/a	n/a	8.5	51553	n/a	n/a
C2E1S2N8Tn	0.99	13179	5.2	20217	2.2	2.2
C2E2S2N8Tn	1.9*	27552	4.6	40821	2.5	0.14
C2E1S5N8Tn	8.9*	12745	8.1	50625	2.0	-2.9
C2E2S5N8Tn	n/a	n/a	15.7	103520	n/a	n/a
C2E1S10N8Tn	n/a	n/a	12.2	102832	n/a	n/a
C3E1S2N2Tn	0.96	325	1,9	886	0.5	0.5
C3E2S10N2Tn	1.1*	64661	7.5	70529	5.8	1.0
C3E2S2N4Tn	0.87	22929	3.1	26072	0.19	2.0
C3E1S5N4Tn	0.94	30315	7.8	36210	4.8	1.9
C3E2S5N4Tn	n/a	n/a	8.6	71451	n/a	n/a
C3E1S10N4Tn	n/a	n/a	5.8	50965	n/a	n/a
C3E1S2N8Tn	0.99	63201	4.3	51329	3.2	0.92
C3E2S2N8Tn	n/a	n/a	7.5	51684	n/a	n/a
C3E1S10N8Tn	n/a	n/a	100*	2421	n/a	n/a
Mean	1.67	19572	7.4	39985	2.9	0.88
Median	0.94	11517	5.8	27910	2.35	1.0
Min	0.33	26	0.84	325	-1.7	-2.9
Max	8.9	250000	37	127027	13	4.3

As we can see from Table 8.3, solving the model with Gurobi outperforms solving the model with our Lagrange relaxation for all instances that Gurobi can solve to optimality. However, when the instances get large enough for a combination of C, E, S and N, Gurobi either terminates before it reaches optimality or even solves the problem. This shows that the Lagrange relaxation can solve larger instances of the problem that more accurately represent the real world. However, the Lagrange relaxation also terminates for the largest instance C3E1S10N8Tn. This is related to the subproblem going out of memory. A possible workaround for this is not solving the sub-problems in parallel, as this would require less memory usage but would however substantially increase the running time.

As one can see in Table 8.3, the gap between the lower bound from the Lagrange relaxation

is, on average, 0.88% worse than that of Gurobi. Further, one can see that for some instances, the lower bound from the Lagrange relaxation is better than that of Gurobi, either due to the termination criteria of 1% for Gurobi or when Gurobi times out. This suggests that given sufficient time, our Lagrange relaxation provides good lower bounds for our problem.

At the same time, the upper bound from the Lagrange relaxation is, on average, 2.9% worse than the one from Gurobi. This gives a hint that the upper bound heuristic used is the main reason behind the Lagrange relaxation performing worse than Gurobi with respect to their optimality gaps. Further, the quality of the optimality gap derived from Lagrangian Relaxation shows more variation than the one derived from Gurobi. For certain problem instances, such as C1ES10N2Tn and C2E4S5N2Tn, the Lagrangian relaxation gap is relatively large, with 13.2% and 8.8%, respectively. Investigation of the results from the Lagrange Relaxation of these two instances shows that these are solutions with very little capacity installed, such that the heuristic has to install much capacity. I.e., the Lagrange Relaxation does not give solutions that have installed sufficient capacity in order to fulfill the demand but is rather punished through the Lagrangian multipliers for this behavior.

As we conclude this section, it becomes apparent that Lagrange Relaxation's upper bound calculation is the main reason behind the poor gaps. Its performance significantly lags compared to Gurobi, leading to considerable gaps optimality gaps. The upper bound provides a feasible solution, a critical element for gaining actionable managerial insights. However, due to its possible deviation from the actual optimal solution, the insights derived could suffer from inaccuracies when relying on the Lagrange Upper bound. Therefore, in Section 8.2, we have adopted Gurobi for the solution of the problem. This choice is driven by our intention to enhance the precision and value of our managerial insights.

8.1.4 Time Use for Lagrange Relaxation

Our Lagrange relaxation has three main steps that consume time:

- Solving the Lagrange subproblem
- Updating the Lagrange multipliers
- Computing the upper bound

Figure 8.2 shows the % distribution of the time spent between the three steps for C1E2S5N8Tn, C1E1S10N8Tn, C2E1S2N4Tn, C2E2S5N4Tn, C3E1S2N2Tn, and C3E2S10N2Tn.

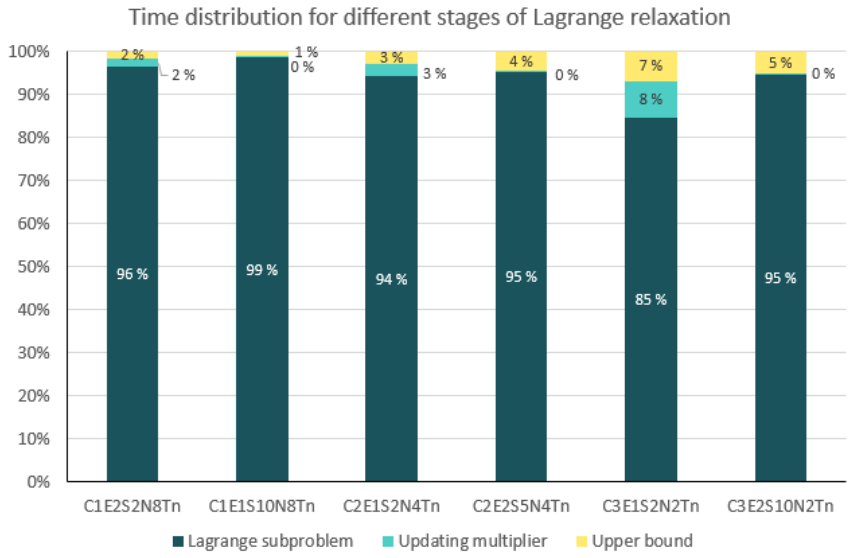

Figure 8.2: Time distribution for different stages of Lagrange relaxation

For all instances, the Lagrange subproblem consumes by far the most time. However, the timeshare used for computing the upper bound increases with larger facility-customer spaces. This is related to the way our heuristic is set up where you for each demand node in the demand scenario space you only expand one facility at a time. With the increasing number of facilities in the instance, this step takes more time. In addition, the complexity of the underlying production planning and distribution problem becomes more complicated.

Further, we find that for C3E1S2N2Tn, the "Updating multiplier" makes up a relatively larger share of the total time spent, compared to the other problem instances. This stems from the fact that instances with a low number of epochs, scenarios, and children per parent can do more iterations of the Lagrange algorithm before reaching the stopping criteria as the solution of the subproblem is easier to solve. This leads to more restrictions in the updating multiplier step, which increases the complexity of this problem.

8.1.5 Limit Test Number of Epochs and Electricity Scenarios

As seen in Section 8.1.3, there exists a trade-off when deciding the dimensions of the different input parameters to have a solvable model. To evaluate the value of production flexibility when choosing which production technology to use for a Norwegian hydrogen supply chain, one needs to evaluate the model over a high number of electricity scenarios. Therefore, we also limit tests of our model in Gurobi regarding the number of epochs and electricity scenarios while keeping the number of demand scenarios (N2) and customer-facility (C1) space to a minimum.

We only perform limit-test by solving the model with Gurobi, as our Lagrange relaxation proved to perform poorly in Section 8.1.3. Table 8.4 summarizes the findings from our limit testing.

Table 8.4: Results from limit testing the number of electricity cost scenarios. Instances with gap $\geq 1\%$ is terminated due to memory

Instance	Gap	Time (s)
C1E4S25N2Tn	0,87%	96112
C1E4S502Tn	3,90%*	179912
C1E2S50N2Tn	0,94%	115956
C1E2S75N2Tn	4,70%*	167382
C1E1S75N2Tn	0,97%	97213
C1E1S100N2Tn	0,98%	167382
C1E1S150N2Tn	15,20%*	102911

As we see from the above table, Gurobi already starts to struggle with solving problem instances with 50 electricity price scenarios for four epochs. For instances with two epochs, Gurobi does not reach the desired optimality gap of 1% when including 75 electricity price scenarios. In contrast, for one epoch, Gurobi does not reach the desired gap with 150 electricity price scenarios. Therefore, we will use E4S25, E2S50, and E1S100 for managerial insight, as they led to optimality gaps below 1%.

8.2 Managerial Insight

This subsection focuses on the managerial insight from the solutions we get when solving the selected problem instances. In Section 8.2.1, we present a framework for measuring the value of solving our outlined problem as a stochastic multi-stage multi-horizon problem. Section 8.2.2 analyzes the value of production flexibility under differing types of electricity price profiles, such as high price or volatile price scenarios. In Section 8.2.3, we focus on how the hydrogen production configuration will look, and in Section 8.2.4, how the hydrogen flows between electricity bidding zones.

For all instances in this section, we solve the model with Gurobi, as our Lagrange Relaxation was deemed unsuitable to provide good feasible solutions to gain managerial insight from.

8.2.1 Value of Stochastic Programming

In stochastic programming, one can evaluate the gains from modeling the problem as a stochastic program through the *Value of Stochastic Solution*. This is defined as the discrepancy between the expected objective value derived from using the expected value solution (EEV) and the result from the stochastic problem, also known as the recourse problem (RP) (Birge & Louveaux, 2011). This difference can be seen in (8.4).

$$VSS = EEV - RP \tag{8.4}$$

This is not straightforward in the multi-stage multi-horizon setting, as the VSS depends on whether you use the expected value in the strategic and operational decisions. If you lock the strategic decisions for all stages or only for a subset of these. Escudero et al. (2007) have extended the value of stochastic programming to the multi-stage setting. This approach was extended to the multi-horizon multi-stage setting by Maggioni et al. (2020a).

Maggioni et al. (2020a) presents the general multi-horizon stochastic program (MHSP) given by (3.49) - (3.55). They then define the *Multi-Horizon Expected Value problem* (MHEV), which is obtained by replacing both strategic uncertain parameters (c_l, h_l, T_l, W_l) and operational uncertain parameters $(q_l^{s,\tau}, h_l^{s,\tau}, T_l^{s,\tau}, W_l^{s,\tau})$ with their expected values,

$$(\sum_{l\in\mathcal{N}_t} \pi_l c_l, \sum_{l\in\mathcal{N}_t} \pi_l h_l, \sum_{l\in\mathcal{N}_t} \pi_l T_l, \sum_{l\in\mathcal{N}_t} \pi_l W_l) := (\overline{c}_t, \overline{h}_t, \overline{T}_t, \overline{W}_t), \quad t \in \mathcal{H} \setminus \{1\} \tag{8.5}$$

and

$$(\sum_{s\in\mathcal{S}_t} w_l^s q_l^{s,\tau}, \sum_{s\in\mathcal{S}_t} w_l^s h_l^{s,\tau}, \sum_{s\in\mathcal{S}_t} w_l^s T_l^{s,\tau}, \sum_{s\in\mathcal{S}_t} w_l^s W_l^{s,\tau}) := (\overline{q}_t^\tau, \overline{h}_t^\tau, \overline{T}_t^\tau, \overline{W}_t^\tau), \quad t \in \mathcal{H}, \tau \in \mathcal{T}_t \tag{8.6}$$

and solving the deterministic problem.

$$MHEV := \min_{x,y} = \sum_{t=1}^{H} (\overline{c}_t x_t + \sum_{t\in\mathcal{T}_t} \overline{q}_t^\tau y_t^\tau) \tag{8.7}$$

S.T

$$Ax_1 = \overline{h}_1 \tag{8.8}$$

$$\overline{T}_t x_{t-1} + \overline{W}_t x_t = \overline{h}_t, \quad t \in \mathcal{H} \setminus \{1\} \tag{8.9}$$

$$\overline{T}_t^1 x_t + \overline{W}_t^1 y_t^1 = \overline{h}_t^1, \quad t \in \mathcal{H} \tag{8.10}$$

$$\overline{T}_t^\tau y_t^{\tau-1} + \overline{W}_t^\tau y_t^\tau = \overline{h}_t^\tau, \quad t \in \mathcal{H}, \tau \in \mathcal{T}_t \setminus \{1\} \tag{8.11}$$

They then go on to define the *Multi-Horizon Expected result of Strategic Decision*, MHEES, which is obtained by solving (3.49) - (3.55) while having the strategic decision variables $\overline{\mathbf{x}}$ fixed at the values obtained from the MHEV. Further, they prove that $MHSP \leq MHEES$.

The *Value of Strategic Decision*, VSD, is defined as:

$$VSD := MHEES - MHSP \geq 0 \tag{8.12}$$

The VSD measures the difference in outcomes between two strategies: one where decisions are made with foresight (anticipating future stages and uncertainties) and one where decisions are made on a stage-by-stage basis without considering future uncertainties. In other words, the VSD quantifies the additional benefits obtained from making strategic decisions that consider the possible outcomes in future stages rather than making decisions based purely on the information available at the current stage. This can be seen as a measure of the "value" of strategic, forward-looking decision-making in the presence of uncertainty.

Then Maggioni et al. (2020a) define the *Value of Strategic Decision at strategic stage t*, VSD_t, as:

$$VSD_t := MHEES_t - MHSP \geq 0, \quad t \in \mathcal{H} \tag{8.13}$$

Where MHEES_t, *Mulit-Horizon Expected result of Strategic Decision*, is obtained by solving (3.49) - (3.55) fixing the strategic decisions $\overline{\mathbf{x}}$ at the optimal values obtained from the MHEV up to stage t.

The VSD_t allows for the examination of the value of strategic decisions not just in the entire planning horizon but also at each individual stage of the decision-making process.

Further they prove that $MHSP \leq MHEES_1 \leq MHEES_2 \leq ... \leq MHEES_{H-1}$, which gives $VSD_1 \leq VSC_2 \leq ... \leq VSC_{H-1}$.

Table 8.5 show the results for both MHSP and the VSD, with data represented both in absolute terms and as a percentage of the MHSP for Normal price (n), High Price (h), Low Price (l), High Variance (v), and Very Volatile (vv) instances across stages 1, 2, and 3. The instances in consideration for this analysis are C3E1S2N8, corresponding to the aforementioned electricity cost generation profiles. A striking insight from the results is the significant value of stochastic programming across all stages and instances. Specifically, the VSD ranges from 8-16% of the MHSP for the first stage, 11-19% for the second stage, and displays an even wider range from 12-54% for the third stage.

Table 8.5: Value of stochastic programming for C3E1S2N8Txx instances

Instance	**MHSP (mill. €)**	**VSD_1**		**VSD_2**		**VSD_3**	
		mill €	**% ($\frac{VSD}{MHSP}$)**	**mill €**	**% ($\frac{VSD}{MHSP}$)**	**mill €**	**% ($\frac{VSD}{MHSP}$)**
C3E1S2N8Tn	3537	331	9.4 %	403	11.4 %	437	12.4 %
C3E1S2N8Th	4169	339	8.1 %	703	16.9 %	1794	43.0 %
C3E1S2N8Tl	2276	364	16.0 %	446	19.6 %	512	22.5 %
C3E1S2N8Tv	3740	324	8.7 %	658	17.6 %	1297	34.7 %
C3E1S2N8Tvv	3099	338	10.9 %	428	13.8 %	583	18.8 %

The VSD exhibits a strictly increasing trend across the stages, as anticipated based on existing literature. However, a noteworthy observation is a relatively minor increase for the normal electricity cost scenario, which only escalates from 9.4 to 12.4%. The VSD was presumed to rise steeply with increasing stages due to the balanced scenario tree implementation of our problem, resulting in more strategic decisions being locked in later stages. Upon inspection of the instance, it is observed that the two electricity cost scenarios sampled are quite similar in terms of variability and cost, leading to the expected value of operational input aligning closely with the actual ones.

The largest VSD_1 is observed for C3E1S2N8Tl, with a cost reduction of 16% from modeling it as a stochastic problem. The reason for this is the two electricity scenarios sampled exhibit some large variations in electricity prices between hours, relative to the average cost of electricity cost, which can be seen in Figure 8.3. By using the expected value of the electricity costs these effects are reduced. To a degree, these effects can also be observed in the C3E2S2N8Tvv instance, but to a lower degree, which is an argument for it having the second highest VSD_1.

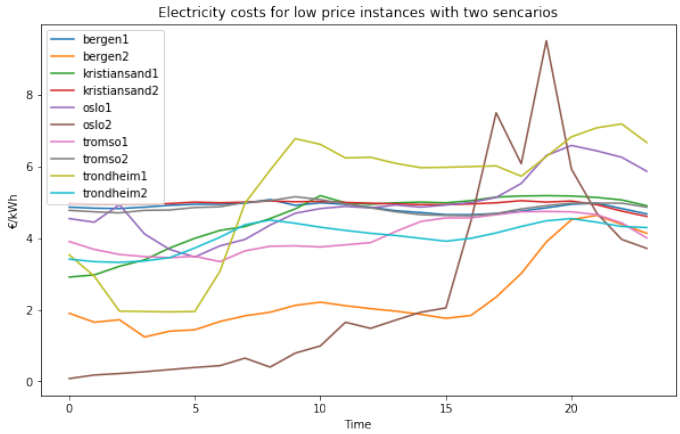

Figure 8.3: Electricity prices for *low price* instances with two electricity scenarios.

The largest values of the VSD_2 and VSD_3 are found in C3E1S2N8Th and C3E1S2N8Tv. These are the instances with the highest average electricity prices and also the largest absolute differences in electricity prices between the maximum and minimum of a day as seen in Figure 8.4. This leads to the optimal solution, MHSP, to install very large capacities to produce as much as possible during the hours with the lowest electricity cost. This is an optimal solution due to the electricity costs being the most important part of the cost of hydrogen. When you use the expected electricity cost the absolute difference between hours gets leveled out, which pushes the VSD solution in a direction where it is not optimal to invest in very much excess capacity. In addition, using the expected demand to decide on investments will lead to under-investments in high-demand scenarios and over-investments in low-demand scenarios. Since investment costs account for the smallest proportion of the total costs when producing hydrogen, overinvestment will affect the total costs less than underinvestment. With underinvestment, one would either have to produce during all hours of the day, which incurs high costs when electricity prices are high, or bear the high cost of not meeting the entire demand

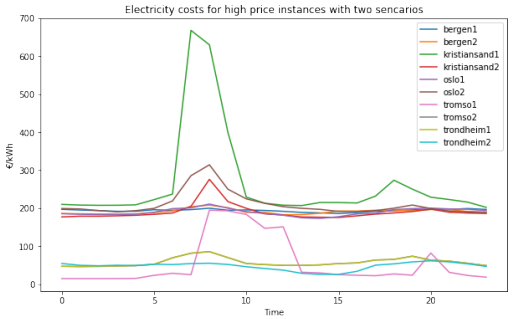

(a) Electricity prices for high price instances with 2 scenarios.

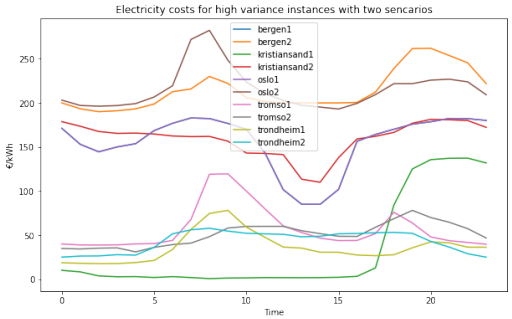

(b) Electricity prices for high variance instances with 2 scenarios.

Figure 8.4: High price and variance electricity cost instances

8.2.2 Value of Production Flexibility

In the following sections, we will evaluate the value of the production flexibility for PEM and Alkaline. This will be done by analyzing the results from C1E1S25N2Tx, C1E2S50N2Tx, and C1E1S100N2Tx for different electricity cost generation strategies *Nor-*

mal price (n), *High price* (h), *Low price* (l), *High Variance* (v), and *Very Volatile price* (vv). This section presents the most interesting data from these instances on an aggregated level for each stage and the average result from all instances with the same electricity cost. More in-depth data can be found in Appendix A.

As we have a three structure of demand scenarios, where you can have different investment decisions for each scenario, we will use that notation summarized in Table 8.6 and depicted in Figure 8.5 to distinguish the investment decisions.

Table 8.6: Node hierarchy used in the following sections

Node	Stage	Parent node	Total Demand (tH_2/day)
1	1	-	4 750
2	2	1	34 002
3	2	1	35 617
4	3	2	119 399
5	3	2	124 706
6	3	3	131 723
7	3	3	140 488

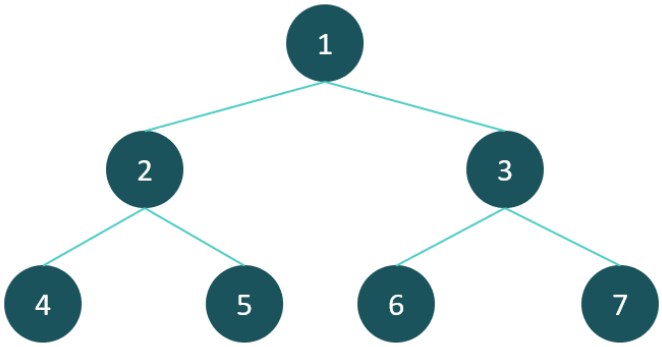

Figure 8.5: Illustration of the node hierarchy used in the following sections

8.2.2.1 Share PEM Installed

This section explores the share of installed capacity of PEM electrolyzers across various electricity price generation profiles, within the hydrogen supply chain in Norway. Five generation strategies were examined: *Normal price*, *High price*, *Low price*, *High variance* in price, and *Very volatile* prices. Figure 8.6 presents the results of each stage, which were aggregated from each demand node within that stage. Moreover, the data corresponding to each electricity price profile was collected from instances E4S25, E2S50, and E1S100.

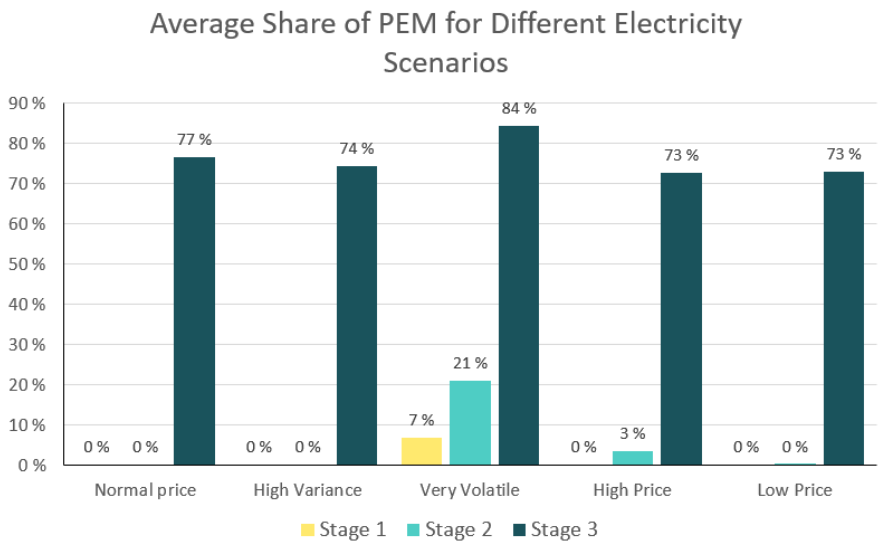

Figure 8.6: Average share of PEM installed in stages 1, 2, and 3 for the different electricity cost schemes for C1E3S25N2, C1E2S50N2, and C1E1S100N2 scenarios.

According to the analysis, in the *Normal, Low price, and High variance* scenarios, the Alkaline technology dominated the first two stages with no PEM installed. The dominant performance of Alkaline over PEM in these stages can be attributed to PEM's lower production efficiency and higher investment costs. Specifically, for the first and second stages, PEM has 10% and 4% higher production costs and 13% and 4% higher investment costs, respectively. These factors overshadow the flexibility offered by PEM, as the volatility of the electricity cost data was insufficient to leverage this advantage.

However, when the scenarios involved High prices and Very volatile prices, PEM gained more traction, albeit to varying degrees:

- In the High price scenario, the share of PEM installed was zero in the first stage and minimal in the second stage.
- While under Very volatile prices, PEM's flexibility became a more desirable attribute. Therefore, the first and second stages saw greater use of this technology than for the other price profiles due to the considerable hourly variations in electricity prices, enabling more effective utilization of PEM's flexibility.

In the third stage, PEM emerged as the dominant technology under all circumstances. In contrast, Alkaline was not installed in any instances due to the technologies reaching an equal level of production efficiency and nearly equivalent investment costs.

8.2.2.2 Cost Split for Different Instances

This subsection discusses the distribution of total costs over its sub-categories production, investment, and transportation, for five different electricity price profiles: *Normal price, High Price, Low Price, High Variance,* and *Very Volatile* prices. The results are visually represented in Figure 8.7, where the data displayed for each stage corresponds to the average cost distribution of all demand nodes within the respective stage. Additionally, the data from each electricity price profile is collated from instances E4S25, E2S50, and E1S100.

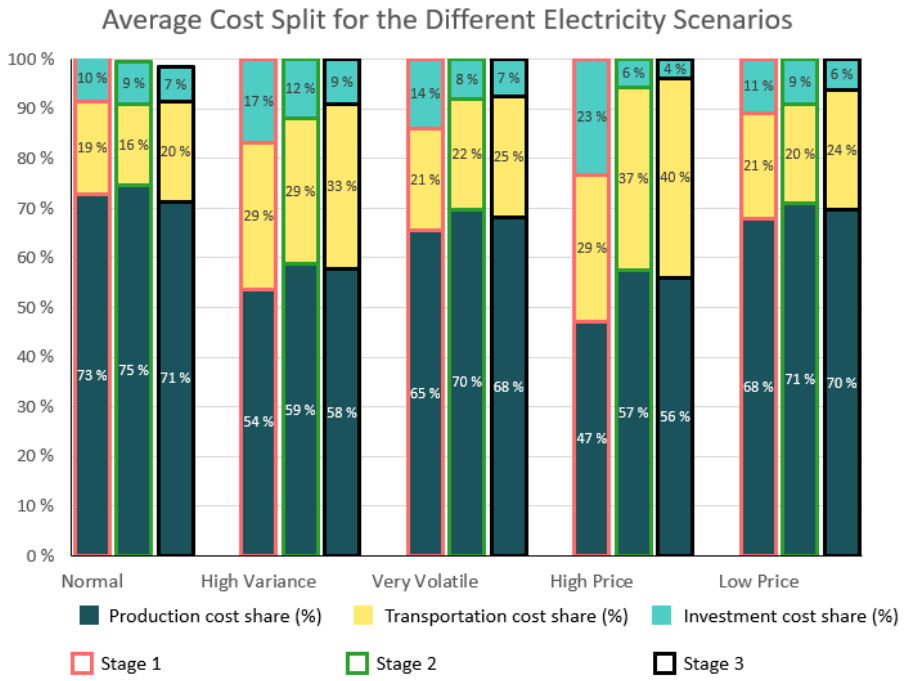

Figure 8.7: Average cost split between production, transportation, and investment costs for the different electricity cost schemes aggregated for each stage for C1E3S25, C1E2S50, and C1E1S100 scenarios.

Across all profiles, the cost distribution appears remarkably similar. However, it's noteworthy that as the stages progress, the average cost of installing capacity (€/(tH2/day)):

$$\overline{inv_h} = \frac{\sum_{\delta=1}^{h} \sum_{l \in \mathcal{N}_h} (\pi_l \sum_{i \in \mathcal{I}} \sum_{p \in \mathcal{P}} \sum_{k \in \mathcal{K}} C_{kp}^{l} y_{ikp}^{l})}{\sum_{h \in [1,\ldots,h]} \sum_{l \in \mathcal{N}_h} (\pi_l \sum_{i \in \mathcal{I}} \sum_{p \in \mathcal{P}} \sum_{k \in \mathcal{K}} y_{ikp}^{l})}, \tag{8.14}$$

decreases more significantly than the average production efficiency (kWh/(kgH2)), directly impacting the production cost, as this is a number that is multiplied by the electricity price.:

$$\overline{prodeff_h} = \frac{\sum_{\delta=1}^{h} \sum_{l \in \mathcal{N}_h} (\pi_l \sum_{i \in \mathcal{I}} \sum_{p \in \mathcal{P}} \sum_{k \in \mathcal{K}} F_{p}^{\delta l} y_{ikp}^{l})}{\sum_{h \in [1,\ldots,h]} \sum_{l \in \mathcal{N}_h} (\pi_l \sum_{i \in \mathcal{I}} \sum_{p \in \mathcal{P}} \sum_{k \in \mathcal{K}} y_{ikp}^{l})} \tag{8.15}$$

This observation is outlined in Table 8.7.

Table 8.7: Change in the average cost of installing hydrogen production capacity and the production efficiency

		Stage		
Electricity Scheme	**Measure**	**1**	**2**	**3**
Normal price	$\Delta\overline{inv}_h$ in (%)	-	18 %	30 %
	$\Delta\overline{prodeff}_h$ in (%))	-	2 %	2 %
High variance	$\Delta\overline{inv}_h$ in (%)	-	15 %	27 %
	$\Delta\overline{prodeff}_h$ in (%))	-	2 %	2 %
Very volatile	$\Delta\overline{inv}_h$ in (%)	-	19 %	30 %
	$\Delta\overline{prodeff}_h$ in (%))	-	1 %	2 %
High price	$\Delta\overline{inv}_h$ in (%)	-	34 %	28 %
	$\Delta\overline{prodeff}_h$ in (%))	-	0 %	3 %
Low price	% $\Delta\overline{inv}_h$ in (%)	-	19 %	31 %
	$\Delta\overline{prodeff}_h$ in (%))	-	2 %	2 %

The reduction in the share of investment costs across all electricity price profiles is primarily due to differences between the two electrolyzers' rates for investment cost decreases and production efficiency increases over time. In the first two stages, Alkaline electrolyzers are installed, with comparatively higher efficiency. From 2023 and towards 2033, however, PEM, a currently less commercially mature production technology, experience a significantly steeper increase in its production efficiency compared to Alkaline. In 2033, PEM has reached the same level of production efficiency as Alkaline. This gives a steeper decline in the expected installation cost per capacity than in production efficiency. Moreover, later stages see greater demand levels, resulting in the installation of higher capacities that experience more economies of scale.

8.2.2.3 Excess Capacity Installed

This subsection examines the excess hydrogen production capacity installed across five different electricity price profiles: *Normal price, High Price, Low Price, High Variance*, and *Very Volatile* prices. From the findings in Section 8.2.2.1, it was shown that Proton Exchange Membrane's (PEM) initially higher investment and operation costs often outweigh the value of its increased production flexibility. PEM was therefore shown to not be the preferred choice of technology until after its costs matched those of Alakaline. Therefore, we investigate alternative strategies for obtaining flexibility when installing production capacity, such as installing excess capacity in order to produce heavily during periods with lower electricity prices. Nevertheless, it's crucial to note the non-linear increase between the available capacity levels to invest in along with the penalty cost for not meeting the demand, as these factors can incentivize installments of excess capacity.

Figure 8.8 presents excess capacity installed over the different electricity price profiles. For each stage, the data presented has been aggregated for all strategic nodes within the respective stage. Additionally, data for each electricity price profile is collected from instances with configurations C1E4S25N2, C1E2S50N2, and C1E1S100N2.

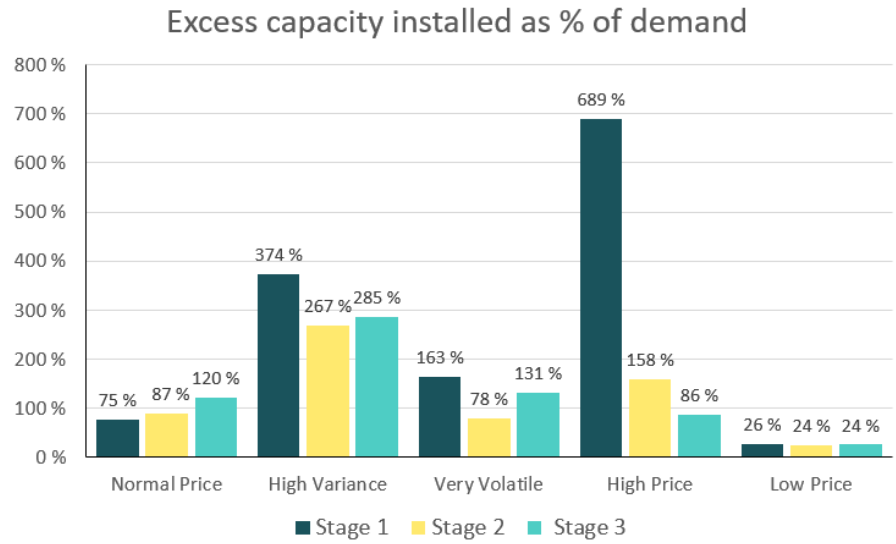

Figure 8.8: Excess capacity installed as a % of total demand in stages 1, 2, and 3 under the different electricity price profiles for instances with configuration C1E3S25N2, C1E2S50N2, and C1E1S100N2.

Except for the *low price* instances, the model tends to install considerably more capacity than necessary to meet demand across all electricity scenario generation strategies, ranging from an excess of 72% to 698%. However, for the *low price* instances, the model appears to install capacity closely matching the total demand. This behavior is attributed to *low price* scenarios having notably low and less volatile electricity prices, making it optimal to produce throughout the day until demand is satisfied. This trend implies that flexibility in terms of installing excess capacity is more valuable than the flexibility offered by PEM compared to Alkaline. This is because investment costs constitute a fraction of total costs, justifying an increase in capacity as long as the excess investment costs are more than offset by the decreased production costs.

In the High Variance, Very Volatile, and High Variance profiles, the highest proportion of excess capacity installments are observed during the first stage. The absence of this trend in the Normal Price and Low Price profiles can likely be attributed to the insufficient economies of scale under these profiles' comparatively lower prices and price volatility. These conditions are insufficient to offset the later stages' production efficiency gains and investment cost reductions.

For the three previously mentioned profiles, the dominance of first-stage excess capacity installments, relative to the capacity needed for demand satisfaction, can be traced back to three determinants. First, the first stage showcases the most substantial economies of scale, signifying a greater potential advantage from excess capacity compared to subsequent stages. Second, the economies of scale are most drastic at the smallest capacity levels and decrease as capacity expands. Given the lower demand during the first stage, many opportunities exist where demand can be met with lower-capacity facilities. However, there is a strong incentive to escalate capacity at these levels, consequently driving a higher incidence of excess capacity installations. Lastly, the first stage precedes two subsequent stages in the model. Thus, when economies of scale apply, it can be more cost-efficient to invest in excess capacity to meet future demand, instead of catering to this demand with later capacity enhancements.

In contrast, the third stage of the model does not have any successive stages. This structural difference means it's not influenced by the third factor - considering later stages when installing excess capacity for cost efficiency. Therefore, less capacity may get installed in this final stage due to the absence of future stages that might necessitate additional capacity.

In light of these findings, there are cases where it may be wise to install an additional level of excess capacity. This strategy allows for more effective planning and utilization of the production site. However, this only holds under certain conditions. First, there should be an anticipation of an increase in demand beyond the installed capacity in subsequent stages, and if the demand is expected to rise in subsequent years, the effect can be more pronounced. Secondly, the economies of scale from installing excess capacity at the stage should be expected to be more significant than the cost reduction effects from potential future increases in production efficiency and decreases in investment costs. Lastly, the electricity prices and their regional differences should be at levels where there are significant economies of scale from having the excess installed capacity. These conditions have been fulfilled since 2021, when electricity prices, volatility, and regional differences have been historically high.

There is a notable anomaly in the first stage of the *High Price* profiles, where an excess capacity of 684% is installed. This anomaly is associated with the beneficial effects of installing large facilities and transporting hydrogen over long distances. In this scenario, you only install capacity in NO3 (Trondheim) and transport it to all customers, as the difference in electricity prices between zones is large. Our input data has economies of scale until capacity level 6, the installed capacity in this instance. Further, as we progress in time, the optimal decision is still only to install capacity in NO3, where you install the maximum available capacity across all demand scenarios in the last stage. This indicates that in this instance, the maximum allowed capacity is lower than what would be the optimal investment, meaning that the excess capacity installed in stages 2 and 3 is lower than what would be optimal given larger maximum allowed installations.

8.2.2.4 Value of Flexibility Given Equal Costs

This section discusses the results from specific instances where the selection of the production technology is locked, making all input factors, barring technology flexibility, constant. Here, investment cost and production efficiencies are kept equal while differences persist in the number of shutdown periods and their lower bounds for capacity utilization during production. These instances are compared to discern the value of production flexibility in isolation. The instances employed include C1E1S100N2Tn, C1E1S100N2Th, C1E1S100N2Tl, C1E1S100N2Tv, and C1E1S100N2Tvv, where each instance is run with the technology lock as described earlier. All instances were solved to a 0.1% optimality gap using the Gurobi optimization software, as the differences in objective value are so low that a 1% optimality gap would not be sufficient to detect differences.

Table 8.8 summarizes the economic outcomes, delineating the cost distribution between investment, production, and transportation. It also specifies the absolute (€) and relative (%) difference in costs between using Proton Exchange Membrane (PEM) and using Alkaline.

Table 8.8: Overview of cost distribution and gains from instances where the choice of production technology is locked to only PEM and only Alkaline

Instance	Stage	Share investment cost		Share production cost		Share transportation cost		Lower Objective value of PEM (value of production flexibility	
		PEM	Alkaline	PEM	Alkaline	PEM	Alkaline	MEUR	%
C1E1S100N2Tn	1	9.2 %	9.2 %	72 %	72 %	19 %	19 %		
	2	8.3 %	9.2 %	72 %	73 %	19 %	18 %	13.3	0.93 %
	3	6.9 %	7.7 %	72 %	72 %	21 %	21 %		
C1E1S100N2Th	1	3.7 %	4.4 %	60 %	61 %	37 %	34 %		
	2	4.1 %	4.1 %	58 %	58 %	38 %	38 %	12.9	0.53 %
	3	3.6 %	3.6 %	52 %	52 %	44 %	44 %		
C1E1S100N2Tl	1	13 %	11 %	66 %	68 %	21 %	21 %		
	2	9.0 %	8.1 %	69 %	69 %	22 %	23 %	3.9	0.39 %
	3	6.8 %	6.5 %	68 %	69 %	25 %	25 %		
C1E1S100N2Tv	1	8.5 %	7.9 %	60 %	61 %	31 %	31 %		
	2	7.1 %	7.3 %	57 %	58 %	35 %	35 %	5.1	0.24 %
	3	7.4 %	7.9 %	54 %	54 %	38 %	38 %		
C1E1S100N2Tvv	1	8.8 %	11.1 %	69 %	69 %	22 %	20 %		
	2	9.3 %	9.4 %	70 %	70 %	20 %	20 %	14.1	0.95 %
	3	8.0 %	8.1 %	68 %	68 %	24 %	24 %		

The objective value reduces maximally by around 0.9% under the *Normal Price* (n) and *Very Volatile* (vv) profiles, contrasting with a minimal reduction of 0.24% under the *High Variance* (v) profiles. These findings suggest modest economic benefits linked to production flexibility. Nonetheless, they corroborate earlier subsections' outcomes, highlighting that these economic benefits do not outweigh PEM's relatively higher investment and production costs in the first two stages.

Moreover, in the equal cost case, the cost distribution between investment, production, and transportation remains similar between PEM and Alkaline. This is related to the specific investment decisions being quite similar between the stages as in cases where costs are not equal. There is no trend where either Alkaline needs to install more capacity to be able to switch off production during high price hours, or PEM installs more capacity to respond fast to volatile electricity prices. The total expected installed capacity for the different instances split by stages can be seen in Table 8.9.

Table 8.9: Expected total installed capacity for instances C1E1S100N2Tn, C1E1S100N2Th, C1E1S100N2Tl, C1E1S100N2Tv and C1E1S100N2Tvv split by stages.

Installed Capacity (MW)	Stage 1		Stage 2		Stage 3	
Instance	PEM	Alkaline	PEM	Alkaline	Pem	Alkaline
C1E1S100N2Tn	15	15	137.5	150	501.25	571.25
C1E1S100N2Th	10	10	110	110	360	360
C1E1S100N2Tl	15	16	100	88.5	331.5	323.5
C1E1S100N2Tv	21	20	166	182.5	926	932.5
C1E1S100N2Tvv	15	20	152.5	170	617.5	602.5

A more thorough investigation of the results shows that the difference in costs resulting in the lower objective value of the instances with PEM technology comes from marginal lower production costs for each stage. These minor differences are hard to spot in Table 8.8, but one can see that the *Share production cost* for PEM is always equal to or lower than that of Alkaline. The absolute value of the production cost is, across all instances and stages, lower for PEM but only marginally so. This shows that PEM allows for a more efficient production plan than Alkaline, but that the electricity price input data is not

volatile enough for it to make a significant impact.

In conclusion, these results show that our instances' economic gain from the modeled production technology flexibility is relatively low. The main reason behind this is the sampled historical electricity price input data from the Norwegian power market does not have properties that give significant value to the modeled production technology flexibility of PEM. The price of electricity in Norway is often quite stable hour to hour within a day, where there either exists a general declining or increasing trend in the data, or there are single hours with spikes in prices (either in terms of low or high prices). Given this kind of price profile and movements observed in our data, both PEM and Alkaline can produce quite similar and optimal production plans. For flexibility to be valued, one needs electricity prices that are more volatile on an hour from hour basis for a substantial share of the time.

8.2.2.5 Cost of Hydrogen

The discussion in this subsection revolves around the average cost of hydrogen production across various electricity price profiles - *Normal price* (n), *High Price* (h), *Low Price* (l), *High Variance* (v), and *Very Volatile* (vv). The instances utilized for the analysis are C1E1S100N2, C1E2S50N2, and C1E4S25N2 for the respective electricity scenario generation strategies. All instances are resolved using Gurobi optimization software until a 1% optimality gap is obtained.

Figure 8.9 summarizes the average expected levelized costs of hydrogen (LCOH), a metric used for indicating the cost of producing a kg of hydrogen under each electricity price and for each stage. This corresponds to the average investment and production costs from hydrogen production but does not include transportation costs explicitly, only implicitly, because transportation costs and restrictions affect where facilities are located. The investment costs consist of the annualized investment costs multiplied by the length a stage represents (5 years). This is done since you can use investments from the first stage to produce hydrogen in later stages. I.e., the second stage includes the share investment cost from stage 1 that can be distributed to the years of stage 2. As evident from the figure, the average cost of hydrogen production demonstrates a downward trend as time progresses across all instances. This observation aligns with expectations, given the increased production efficiency, declining investment costs, and improved economies of scale resulting from establishing larger facilities over time.

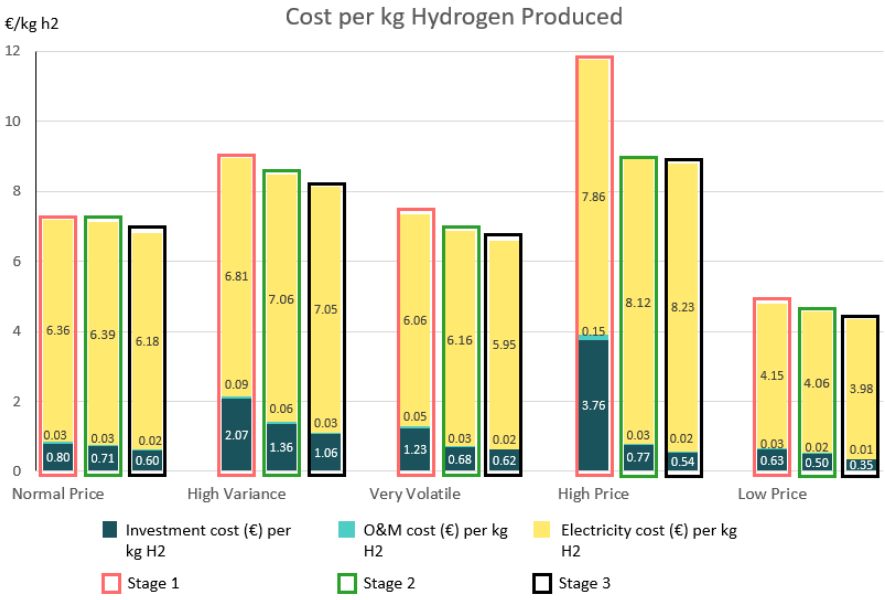

Figure 8.9: Average cost per kg hydrogen produced excluding the transportation costs.

As expected, the highest average cost of hydrogen production is seen in the *High Price* electricity price profile, and correspondingly the lowest is seen in the *Low Price* profile. The distribution between investment and production costs demonstrates a decreasing pattern as we move forward in time, indicating an initial installation of excess capacity to cater to later stages. This trend can be attributed to the decrease in average installation cost per capacity surpassing the rate of increase in average production efficiency, as discussed in Section 8.2.2.3.

The findings also emphasize the dominant role of electricity costs in determining the total hydrogen production cost. In concurrence with the insights shared in Section 2.1.1.3, electricity costs account for most of the levelized cost of hydrogen (LCOH) production across all results. On average, electricity costs contribute to 86% of LCOH. This is aligned with other literature suggesting electricity consists of 70-88% (IEA, 2019, UK Government, 2022, IRENA, 2020b) of the LCOH. We are at the higher end of this range due to us using forecasts of the future technical specifications, which have a considerably lower investment cost, and electricity cost from historical realizations in the Norwegian market, which is higher than the costs used in other studies.

8.2.3 Investments in Hydrogen Production Capacity

The analysis of the configuration of investments in hydrogen production technologies for Norway's supply chain, based on the C3E1S2N8Tn and C3E1S2N8Th instances solved to optimality within 1% with Gurobi, presents several key insights. The reasoning behind choosing these instances is that the Normal electricity price profile represents the value chain given historical prices, while the high electricity profile is representative of the experienced high prices in 2021 and 2022. Figures 8.10, 8.11, and 8.12 delineate the investments' configuration for the first stage, expected second stage solution, and expected third stage solution. It is important to note that the scale of the y-axis changes between each stage as the demand and installed capacity increase with stages. Further, it is important to note that you can only invest in a discrete number of capacities which gives quite large differences between the optimal investments in each location.

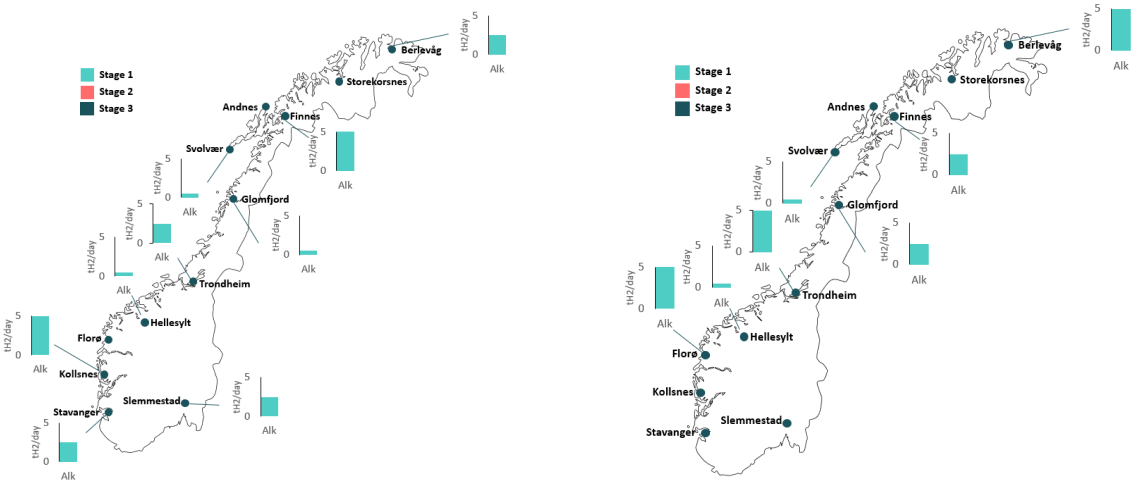

(a) C3E1S2N8Tn **(b)** C3E1S2N8Th

Figure 8.10: First stage investment decisions divided by Alkaline (Alk) and PEM with capacity in tonnes hydrogen per day (tH2/day)

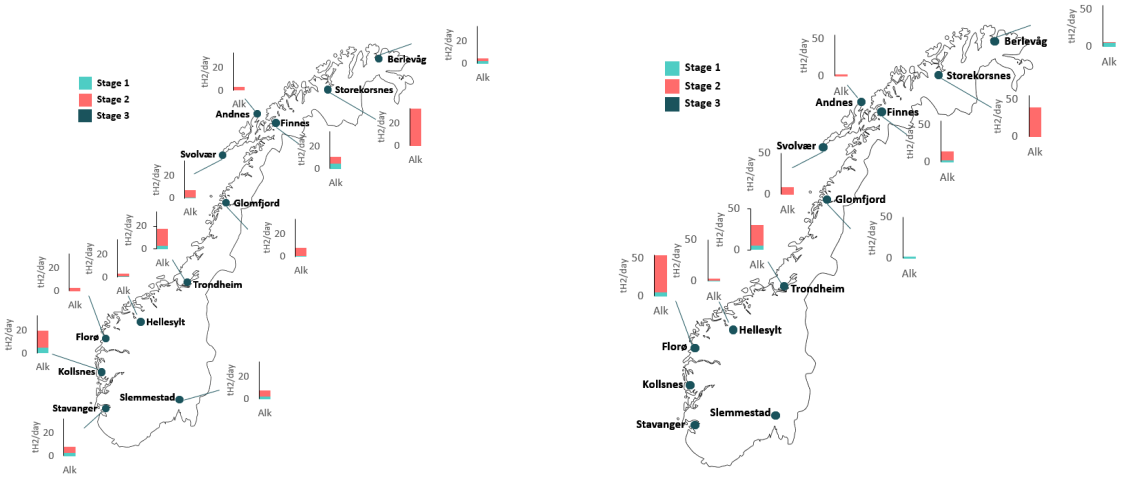

(a) C3E1S2N8Tn **(b)** C3E1S2N8Th

Figure 8.11: First stage and expected second stage investment decisions, divided by Alkaline (Alk) and PEM with capacity in tonnes hydrogen per day (tH2/day)

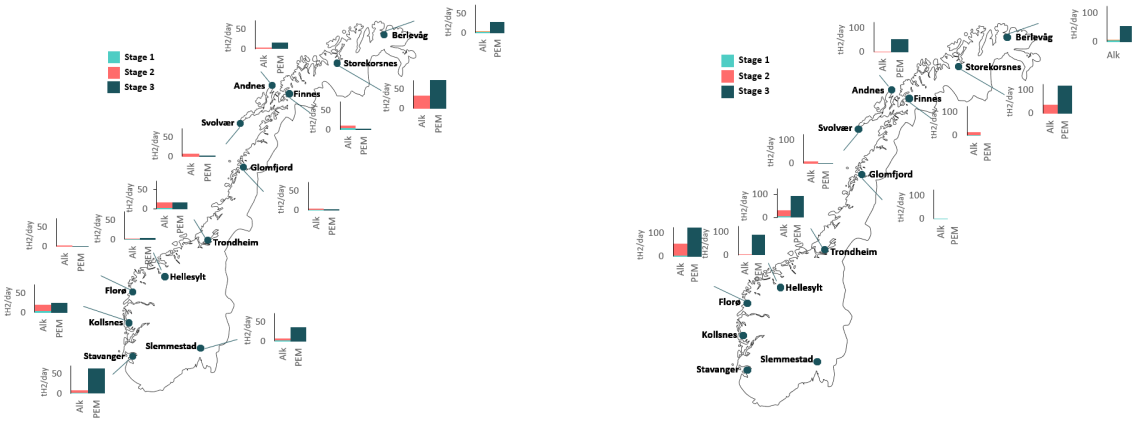

(a) C3E1S2N8Tn **(b)** C3E1S2N8Th

Figure 8.12: First stage, second stage expected and third stage expected investment decisions divided by Alkaline (Alk) and PEM with capacity in tonnes hydrogen per day (tH2/day)

From these figures, it's apparent that the size of the investments increases as we progress in time, with the first stage witnessing the lowest investments and the last stage experiencing the highest. Table 8.10 presents the total installed capacity divided between the technologies, the average demand, and the average investment size.

Table 8.10: Aggregated results for C3E1S2N8Tn that describe the average installed capacity over the stages.

	C1E1S2N8Tn			**C1E1S2N8Th**		
Stage	**1**	**2**	**3**	**1**	**2**	**3**
Average Demand (tonnes H2/ day)	11846	85367	293842	11846	85367	293842
Total Installed Capacity (tonnes H2/day)	21500	121188	397498	10250	80700	348931
Total Excess Capacity	181 %	142 %	135 %	87 %	95 %	119 %
Avg. Investment size (tonnes H2/day)	2.4	8.3	23	1.7	8.8	38
Share of installed capacity PEM	0 %	0 %	100 %	0 %	0 %	100 %
Total share PEM	0 %	0 %	70 %	0 %	0 %	77 %

Moreover, the selection of technology appears to be stage-specific. The first two stages see installations of Alkaline technology exclusively, while the third and final stage only witness PEM installation. This observation aligns with the findings in Section 8.2.2.1, where the instances had more electricity scenarios but a smaller customer-location space.

In the *Normal Price* profile, an interesting pattern emerges concerning the supply chain's configuration. Every candidate facility location receives investments, suggesting that a distributed hydrogen supply chain is favored, with production capacity installed proximal to demand. This preference for decentralized production is further substantiated by the fact that hydrogen is transported at a distance of 161 km on average, significantly below the limit of 1000 km. This suggests that transportation costs are substantial enough to outweigh the economies of scale that could be gained from centralized production. At maxima, hydrogen is transported 725 km. However, this is between Svolvær (in NO4) and Namsos (in NO3), where the model takes advantage of the differences in electricity prices and economies of scale and transports hydrogen from NO4 to NO3.

For the high electricity price profile, we see no capacity installation in the southern elec-

tricity zones (NO1, NO2, and NO5). This is related to the *high price* instance having very large price differences between the southern and northern electricity zones. It, therefore, is optimal to install capacity only in the zones with low electricity prices and transport it south. In the north, there are signs of a distributed supply chain as all locations in NO3 and NO4 receive investments. In addition, it is prominent that the average capacity of the facilities is larger for the *High Price* instance, with a more centralized production setup, as one needs to install large facilities in NO3 to satisfy demand in the south.

The findings of the configuration of the hydrogen production value chain are consistent with the findings of Refsdal and Sindre (2022). They also looked at a hydrogen facility location problem and solved a problem both for 2020 and 2030 technology specification, but with deterministic demand. The results also suggested a distributed value chain, with Alkaline being the dominant technology in 2020 and PEM the dominant technology for 2030 specifications.

8.2.4 Flow of Hydrogen Between Bidding Zones

The Norwegian electricity market is divided into five bidding zone as explained in Section 2.5. These bidding zones have different prices, where the trend is that the northernmost bidding zones (NO3 and NO4) have considerably lower prices than the southernmost (NO1, NO2, and NO5). This observation can be seen in Figure 8.13 showing the average monthly electricity price over the whole period we sample data from where the largest price differences have occurred in the last years. Table 8.11 show the specific average electricity price over the scenarios in C3E2S2N8Tn for the different electricity bidding zones.

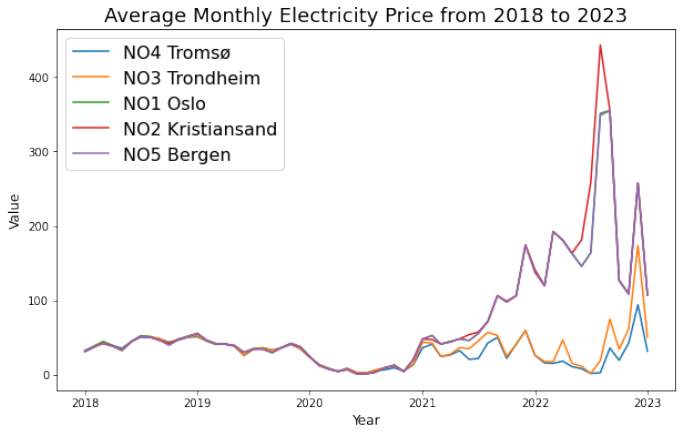

Figure 8.13: Average monthly electricity price for NO1, NO2, NO3, NO4 and NO5 from 2018 to 2023.

Table 8.11: Average electricity price for the bidding zones in C3E1S2N8Tn

Bidding zone	**Average Electricity Price (€/MWh) in C1E1S2N8Tn**	**Average Electricity Price (€/MWh) in C1E1S2N8Th**
Oslo (NO1)	38.21	199.92
Kristiansand (NO2)	38.88	226.84
Trondheim (N03)	28.02	59.058
Tromso (NO4)	21.76	57.28
Bergen (NO5)	38.43	192.58

Figures 8.14, 8.15, and 8.16 illustrate the import/export dynamics between the five Norwegian bidding zones: NO1 Oslo, NO2 Kristiansand, NO3 Trondheim, NO4 Tromsø, and NO5 Bergen.

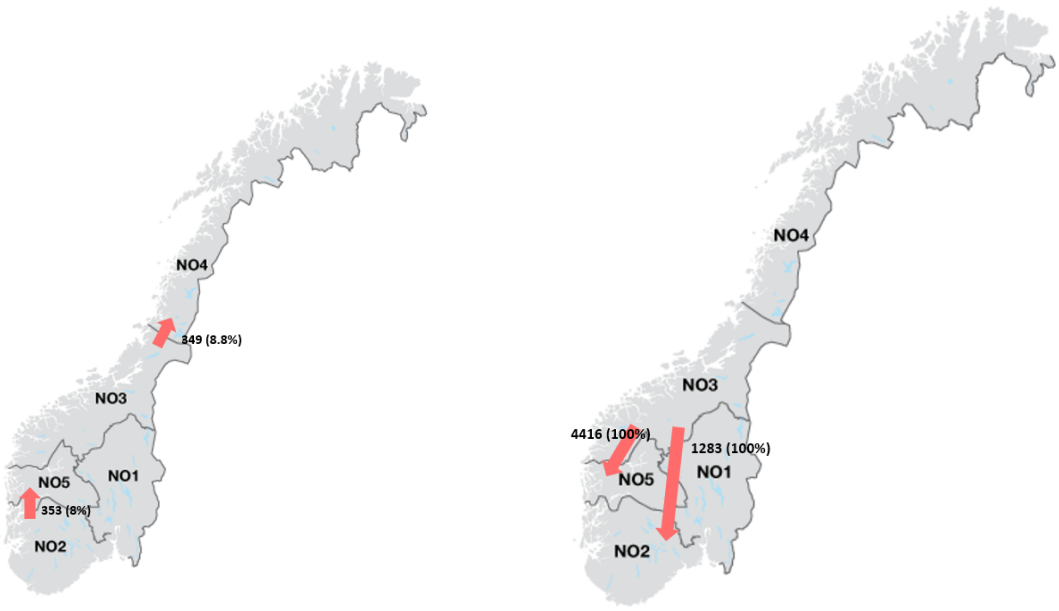

(a) C3E1S2N8Tn **(b)** C3E1S2N8Th

Figure 8.14: Hydrogen flow between bidding zoned in the first stage.

For the Normal electricity price profile, in the first stage, exportation between NO2 and NO5, with approximately 8% of the demand in NO5 being supplied by a facility in NO2. Given that electricity prices in these zones are typically similar, this observation initially appears unexpected. However, on deeper analysis, it becomes clear that this situation results from the equal distance of a major customer in NO5 to the nearest possible facilities in both NO2 and NO5. Given the greater demand for NO2 during the first stage, it appears the model leverages economies of scale to build a larger facility in NO2. As the demand in NO5 increases in subsequent stages, the flow between these two zones decreases, thereby allowing the facilities in NO5 also to take advantage of economies of scale.

Further, there is export from NO3 to NO4, which also is transportation from a bidding zone with a higher electricity price. Investigation of the data also reveals a customer close to the border of NO3 in NO4, which have similar distances to the closest facility in NO3 and the closest facility in NO4. As there is more demand in NO3 than NO4, the model takes advantage of the economies of scale, builds a larger facility in NO3, and supplies the customer in NO4 from NO3.

For the High electricity price profile, there is export from NO3 to NO2 and NO5. Where all demand in NO2 and NO5 are satisfied by facilities in NO3. This is related to the very large difference in electricity price, which is approximately 4x as expensive in NO2 and NO5 as in NO3. There is no export between NO3 and NO1 as there is no demand for NO1 in the first stage.

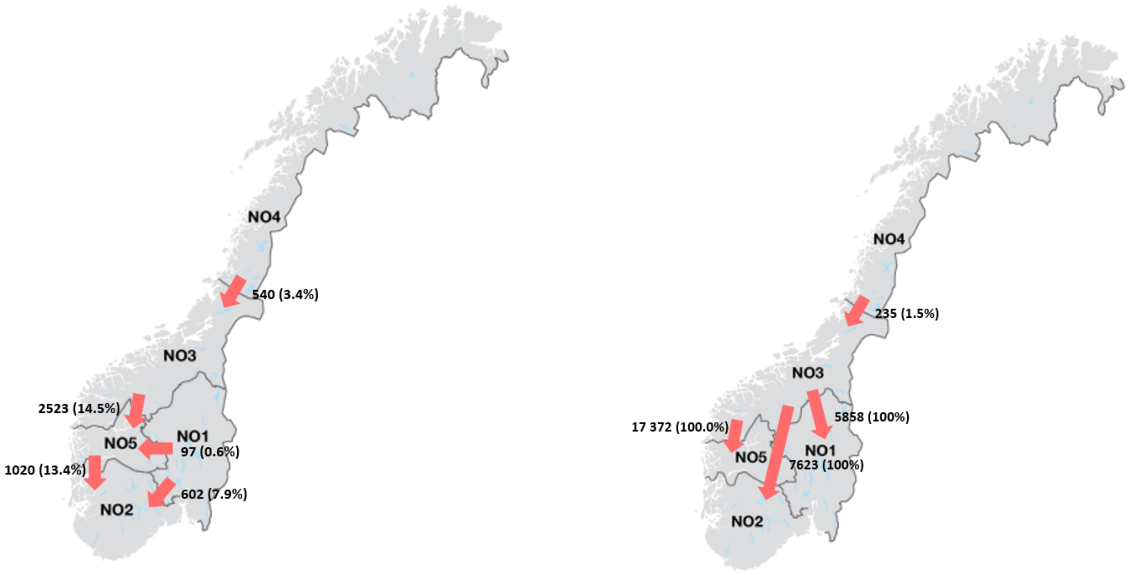

(a) C3E1S2N8Tn **(b)** C3E1S2N8Th

Figure 8.15: Expected hydrogen flow between bidding zoned in the second stage.

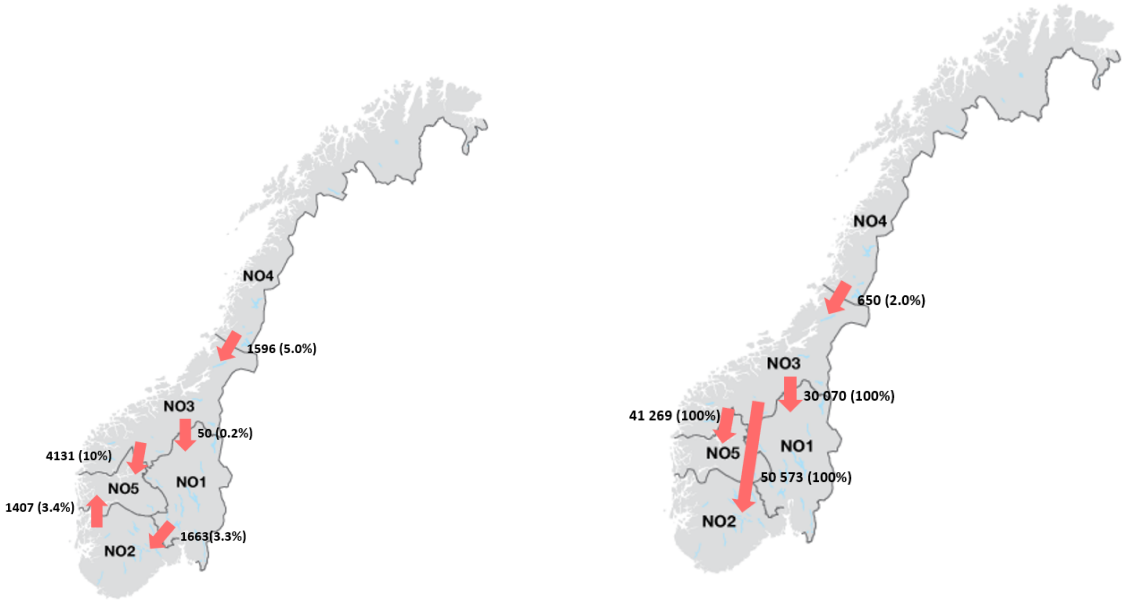

(a) C3E1S2N8Tn **(b)** C3E1S2N8Th

Figure 8.16: Expected hydrogen flow between bidding zoned in the second stage.

For the Normal electricity price instance, in the later stages, there emerges a trend of hydrogen flowing from northern to southern bidding zones. Most notably, there is a significant hydrogen flow from NO3 to NO5, accounting for more than 10% of the total demand in both the second and third stages. But there is also a substantial hydrogen flow from NO4 to NO3 and N01 to NO2. This north-to-south hydrogen transport pattern is an interesting aspect of the supply chain configuration and signifies the interplay between electricity price differences and transportation costs across different regions. Across all stages, the average distance hydrogen is transported is 161 km, which is way lower than

the maximum allowed distance of 1000 km. However, it is essential to note that all bidding zones receive investments as seen in Section 8.2.3. This suggests that the transportation costs often outweigh the lower electricity prices between bidding zones. Therefore, it could be interesting to see how many extra kilometers the model will transport hydrogen between bidding zones to fulfill demand. To do this, we define the following numbers:

For the High electricity price instance, the same trend as in the first stage is prominent, where facilities in NO3 fulfill all demand in the south in NO1, NO2, and NO5. In addition, there is some export between NO4 and NO3, which might be related to the slightly lower price in NO4, and the installed capacity in NO3 is not enough to satisfy all demand in NO1, NO2, and NO5, as well as its own demand.

- *Extra Distance between i and j in stage h node l* (ED_{ijhl}) is the difference between the distance transported hydrogen between a customer (j) and facility (i) in different bidding zones, and the distance between closest facility in the bidding zone of the customer j and customer j.
- *Average Extra Distance in stage h* (AD_h) is the average of the ED_{ijhl} for a stage h over all i and j. This is adjusted for the total volume of hydrogen transported between bidding zones.
- *Max Extra Distance in stage h node l* (MED_{hl}) is the maximum of the difference between the distance hydrogen is transported between a customer and facility in different bidding zones, and the distance between the closest facility in the bidding zone of the customer j and customer j.
- *Max Extra Distance in stage h* (MED_h) is the maxima of MED_{hl} for a stage h.
- *Average Max Extra Distance in stage h* (AED_h) is the average of the MED_{hl} for a stage. This is adjusted for the total volume transported between bidding zones in total. This is adjusted for the total hydrogen transported between hydrogen in that stage.

Table 8.12 summarizes the values for MED_h, AED_h and AD_h.

Table 8.12: Max and average extra distances transported hydrogen

	C1E1S2N8Tn			**C1E1S2N8Th**		
	Stage 1	**Stage 2**	**Stage 3**	**Stage 1**	**Stage 2**	**Stage 3**
MED_h	4 km	536 km	312 km	756 km	464 km	480 km
AED_h	4 km	24 km	4 km	230 km	282 km	328 km
AD_h	-40 km	-81 km	-100 km	230 km	215 km	269 km

For the Normal electricity price instance, the maximum extra distance hydrogen is transported is 546 km between Svolvær (south N04) and Namsos (north in NO3), and occurs in the second stage. In the third stage, this decrease decreased to 312 km, while in the first stage, the model does not transport hydrogen any further than necessary. When one looks at the AD_h, it shows that, on average, when there is transportation between bidding zones, the distance is lower between the chosen facility, i for customer j, than the distance is to the closest facility to j in j's bidding zone. This means that a key driver of export between bidding zones is lower transportation distances. Still, a prerequisite for this is that the electricity price is lower in the bidding zone where there is production.

For the High electricity price instance, the hydrogen demand in NO2 and NO5 is satisfied by facilities in NO3. This leads to high values for MED_h, AED_h, and AD_h. This finding underlines that huge differences in electricity prices can lead to an optimal investment scheme where you transport hydrogen long distances.

Chapter 9

Future Research

This Chapter focuses on possible future research based on the results and findings in this thesis. Firstly possible improvements of the Lagrangian relaxation are presented in Section 9.1. In Section 9.2, we discuss how the electricity input data might affect our results and changing these might alter the results. After, a discussion on how one can improve the representation of the technology flexibility is carried out in Section 9.3. Finally, other frameworks for solving this problem are presented in Section 9.4.

9.1 Lagrangian Relaxation

As seen in Section 8.1.3, our Lagrangian relaxation has a longer solution time than solving the model with Gruobi and provides larger gaps. The only metric where our Lagrange relaxation outperforms Gurobi is that it can solve larger problem instances. This section will describe future research on improving the Lagrange relaxation for this problem.

9.1.1 Solving the Lagrangian Subproblem

Given sufficient time, our Lagrangian relaxation finds a good lower bound. But the running time is higher than that for solving the model with the commercial solver Gurobi. This means that the main problem of the Lagrangian relaxation is the running time being too high. Our analysis in Section 8.1.4 shows that solving the Lagrangian Subproblem consumes the most time. Therefore, one can gain the most in terms of reducing the total running time by improving the solution time of the Lagrangian Subproblem.

In this thesis, we tried to do this by formulating the problem as a shortest-path problem. Still, our preliminary research suggested that our implementation of this did not perform well. This might be related to the curse of dimensionality (Bellman, 1952). One could improve the performance of this way of solving the subproblem by finding ways of cutting off parts of the solution space.

It is worth noting that alternative methods might further accelerate the solution time for the Lagrange subproblem. However, the exploration and adaptation of such methods lie outside the scope of this thesis. We acknowledge the potential for future advancements in this area, yet we do not propose any concrete recommendations.

9.1.2 Improving the Upper Bound

In Section 8.1.3, it is evident that the upper bound heuristic is the main reason for our Lagrange relaxation providing sub-optimal gaps. This could be related to the fact that our upper bound heuristic aims to install sufficient demand to satisfy demand while balancing not installing too much. This seemed like a good strategy as our Lagrange relaxation could give solutions that installed very little or very much capacity. However, we see in Section 8.2.2 that optimal solutions often install much excess capacity and utilize this

flexibility to produce nothing during high-price electricity periods of a day and much during low-price electricity periods. How much excess capacity is installed depends on the electricity scenarios.

In essence, our upper bound heuristic consist of two procedures that both affect how much capacity is installed:

1. *Increase capacity* in order to satisfy demand
2. *Decrease capacity* in order to ensure not too much installed capacity

For improving the 1) *Increase capacity*, one can add something that gives the heuristic an incentive to install more capacity than the minimum in order to satisfy demand. This could be done by increasing the capacity, solving the production and customer allocation problem, and checking if the objective value improves. Or by using information from the Lagrangian multipliers to give incentives for installing excess capacity.

To improve the heuristic one could remove 2) *Decrease capacity*, as we know, excess installed capacity has a substantial economic value. One could also alter how much excess capacity needs to be installed before one reduces the capacity. The current implementation checks whether the excess capacity is larger than the difference in capacity between the current capacity and the capacity at one capacity level lower. By checking with, for instance, two or three lower capacity levels, one would give the heuristic a bias for installing excess capacity.

9.1.3 Relaxing the Non-anticipativity Constraints

We decided to relax the demand constraint linking facilities to customers, as this has been done much in facility location literature. However, it is also possible to relax the non-anticipativity constraints (5.4) linking the stages together. Investigation into how relaxing this constraint will affect the model might be interesting.

9.2 Better Representation of Volatility in Electricity Prices

Our analysis shows that for the electricity price input data used in this thesis only in instances with very volatile electricity prices, our modeled flexibility of PEM is valued enough to compensate for the higher investment and production costs. The main reason behind this is that the Norwegian grid has historically had very stable electricity prices daily. This means that the electricity data we sample scenarios from are not volatile enough, except for the constructed very volatile price instances, for flexibility to be important when investing.

The flexibility differences between PEM and Alkaline are larger on lower time scales. We use 1 hour as the time resolution, but one can buy electricity on a 15-minute time scale in inter-day trading in Norway (Olje- og energidepartementet, 2022). Lowering the time resolution could therefore affect the model in the direction of giving a higher value to flexibility.

The future electricity grid in Norway will be more affected by renewable energy from volatile sources such as wind. As well as the increased impact on the electricity markets in Europe with more electricity cables connecting the Norwegian market to the markets in Europe. This will affect the prices in the Norwegian electricity market, which might

become more volatile. As the design of the hydrogen value chain is not dependent on historical electricity prices but rather on future prices, altering how we construct electricity scenarios could affect the results.

Finally, we have assumed that when producing hydrogen in Norway, one connects the production to the Norwegian electricity grid. This assumption might not hold as many hydrogen plants may rely on connecting to dedicated renewable energy, such as wind and solar, which are more volatile than the electricity grid. Using electricity cost data from such sources might alter the results. However, it is important to note that this might alter the problem at hand: Where one might need to add the decision to invest in the sufficient capacity of renewable energy generation to the problem. This will add a restriction on how much electricity you have for hydrogen production related to the production from the wind or solar park or/and an optimization on whether you should use the electricity to produce hydrogen or sell it to the grid.

9.3 Better Modeling of Technology Flexibility

As seen in Section 8.2.2, the lower production and investment cost of Alkaline technology outweighs the higher production flexibility offered by PEM until the investment and production costs are similar. This might be related to our simplified modeling of flexibility:

1. Restricting technologies to be turned off at least S periods after being turned off
2. Restricting the allowable range of the installed capacity one can produce hydrogen at.

In reality, switching on and off production strains the technologies differently, in addition to different costs related to heating and pressurizing the technology when turning it on. Further, Alkaline has modes it can be operated in, such as standby mode, which has an associated cost but a shorter start-up time than completely turning it off.

In addition, a balancing market for electricity in Norway ensures the consumption and production of electricity are balanced (Olje- og energidepartementet, 2022). Here one can get paid to make electricity consumption available within short time frame such as seconds or minutes, to balance the market. The faster the response time, the higher the premium is for making this capacity disposable. A prerequisite here is to have energy sources with a fast response time, which might be the case for PEM but not Alkaline. Adding the possibility to dedicate a certain amount of the installed capacity to participate in this market could increase the value of flexibility.

It is worth noting that making the modeling of the flexibility more complex will make an already hard problem to solve harder. Therefore, it could be an idea to split the decisions of i) first solve where to invest in production capacity and which customers each facility should serve, and then ii) solve what technology and capacity to invest in when designing the hydrogen supply chain in Norway.

9.4 Alternative Solution Methods

This section discusses possible solution methods that could be applied to reduce the solution time of our model.

9.4.1 Nested Benders Decomposition

Nested Benders Decomposition is a widely recognized technique for solving multi-stage problems. Rooted in mathematical programming, it provides an efficient framework for large-scale, complex problems where decisions are taken in stages. The strength of Nested Benders lies in its ability to decompose the original problem into a series of interconnected sub-problems. This way, each stage of decision-making can be considered independently, allowing for more manageable computational complexity and enhancing the practicality of solutions. This technique has found extensive application across numerous domains, including energy system modeling (MacRae et al., 2016) and supply chain optimization (Khatami et al., 2015), where multi-stage decision-making under uncertainty is a common challenge. Investigation of this technique applied to our model could be interesting.

9.4.2 Stochastic Dual Dynamic Programming

Lara et al. (2020) presents a Multistage Stochastic Mixed-integer Programming model, focusing on optimizing power generation expansion over several years. Key factors integrated into this model include detailed operational constraints, intermittency of renewable generation, power flow dynamics between regions, energy storage options, and a multiscale representation of strategic and operational uncertainty. This model resembles our own, particularly with its multistage multi-horizon problem with integer recourse characteristics. Therefore, exploring this method could provide insightful strategies for future research.

To cope with the substantial computational challenge, which escalates exponentially with each stage in the scenario tree, the researchers utilized the Stochastic Dual Dynamic Integer Programming (SDDiP) algorithm. Notably, this algorithm, albeit computationally intensive, was expedited effectively via parallel processing. An intriguing aspect of this study was the simultaneous application of both Benders and Lagrange cuts on the non-anticipativity constraints. This approach may be worth investigating in the context of our model.

9.4.3 Scenario Clustering

The operational stage of the model introduced in Chapter 5 is inspired by the work of Refsdal and Sindre (2022). They also evaluate the value of flexibility when designing the hydrogen value chain in Norway, but only under uncertain electricity prices and in a two-stage setting. In their report, they encounter run-time problems when using large input data to represent the real world accurately. To overcome this, they utilize a scenario clustering framework form Hewitt et al. (2022) developed for two-stage stochastic problems. This framework has not yet been developed for multi-stage stochastic problems, not to mention the multi-stage multi-horizon problem presented in this thesis. However, looking into how to adapt this framework to multi-stage, multi-horizon problems could be interesting. As this is not straightforward, one should start with the multi-stage setting. Adapting this framework to a multi-stage setting can make it possible to solve larger and more realistic decision spaces.

Chapter 10

Concluding Remarks

This thesis investigates the value of the flexibility offered by various hydrogen production technologies, and it's impact on production plant investment decisions in Norway. A stochastic multi-stage multi-horizon facility location problem was introduced to assess the value of flexibility for the optimal location of hydrogen production facilities in Norway. The two technologies, PEM and Alkaline, have different flexibility in terms of the number of periods needed to be closed after an initial shutdown and the load ranges where it is possible to produce hydrogen. The facilities are intended to meet the transportation sector's demand from 2023 to 2038. The analysis encompasses instances with three to 12 production facilities, 13 to 30 demand locations, nine capacities, two technologies, two to 100 electricity price scenarios, five electricity price characteristic schemes, and demand data from 2023 to 2033.

The developed model aims to minimize expected costs associated with investment, production, and transportation in hydrogen production. Lagrangian relaxation was implemented to improve solution times and problem-size management. However, due to the curse of dimensionality and slow Gurobi subproblem resolution, the Lagrangian relaxation showed subpar runtime performance and optimality gap for instances within our set limit of 172,800 seconds (48 hours). Additionally, our upper bound heuristic was found to undervalue the installation of excess capacity for subsequent stages, leading to insufficient capacities. Excess capacity has proven valuable because it provides flexibility by not requiring continuous production throughout the day. Our heuristic aimed to install sufficient capacity to meet demand without favoring excessive installations. This underscores the necessity of heuristic refinement.

Our results suggest a preference for Alkaline technology in Norway's hydrogen supply chain for 2023 and 2028 due to its lower costs. Nonetheless, PEM emerges as the preferable choice by 2033 as it narrows the cost gap. The total cost breakdown of our model aligns with previous studies: production costs account for 60-70%, investment costs for 5-10%, and transportation costs for 20-30% of total costs.

A distributed supply chain configuration with an average hydrogen transport distance of 161 km proved optimal, echoing findings of Refsdal and Sindre (2022) and Stádlerová and Schütz (2021). Furthermore, hydrogen flow tends to move from northern to southern Norwegian electricity bidding zones, influenced by lower electricity prices and transportation cost considerations. A slight trend was observed towards building larger facilities early to meet later demand stages, mainly for low-production capacities.

The value of modeling this problem as a stochastic multi-horizon model is highlighted by the high Value of Strategic Decision (VSD), given the presence of both operational (electricity prices) and strategic (demand) uncertainties.

This thesis provides significant insights into the crucial considerations for the location of hydrogen production plants under conditions of uncertainty, and it also advances the field of facility location problems with a first-ever multi-horizon formulation, to the authors' knowledge. While our Lagrangian relaxation technique did demonstrate certain limita-

tions, it nonetheless furnished essential insights that can fuel further research in this field. The study's findings underline key trends in hydrogen production technology and facility location, namely that for all problem instances, one saw the installations of excess capacity to increase proportionately to higher electricity prices. This indicates that flexibility from excess capacity is more valuable than technological flexibility. As we navigate towards a future where hydrogen assumes a crucial role in energy production, these findings will prove instrumental in guiding the optimization of the hydrogen supply chain.

Bibliography

Abdollahipour, A., & Sayyaadi, H. (2022). Optimal design of a hybrid power generation system based on integrating pem fuel cell and pem electrolyzer as a moderator for micro-renewable energy systems. *Energy*, *260*, 124944. https://doi.org/https://doi.org/10.1016/j.energy.2022.124944

Aglen, T. M., & Hofstad, A. (2022). *L-shaped decomposition for the two-stage stochastic facility location problem with capacity adjustments* (Master's thesis). NTNU. Norway. https://ntnuopen.ntnu.no/ntnu-xmlui/handle/11250/3024656

Almansoori, A., & Shah, N. (2006). Design and operation of a future hydrogen supply chain: Snapshot model. *Chemical Engineering Research and Design*, *84*(6), 423–438. https://doi.org/https://doi.org/10.1205/cherd.05193

Almansoori, A., & Shah, N. (2009). Design and operation of a future hydrogen supply chain: Multi-period model. *International Journal of Hydrogen Energy*, *34*(19), 7883–7897. https://doi.org/https://doi.org/10.1016/j.ijhydene.2009.07.109

Andrenacci, S., Yejung, C., Raka, Y., Talic, B., Colmenares-Rausseo, L., & SINTEF. (2022). Electrolysers towards mawp 2023 targets and beyond. *HAELOUS*. https://doi.org/10.5281/zenodo.7144913

Arbeidslivet.no. (n.d.). *Fakta: Hviler og pauser for yrkessjåfører*. Retrieved 6th February 2023, from https://www.arbeidslivet.no/Arbeid1/Arbeidsmiljo-og-HMS/Fakta-Hviler-og-pauser-for-yrkessjaforer/

Bellman, R. (1952). On the theory of dynamic programming. *Proceedings of the National Academy of Sciences*, *38*(8), 716–719. https://doi.org/10.1073/pnas.38.8.716

Birge, J. R., & Louveaux, F. (2011). *Introduction to stochastic programming* (2nd ed.). Spinger New York. https://doi.org/https://doi.org/10.1007/978-1-4614-0237-4

Broadleaf. (2021). *The colour of hydrogen*. Retrieved 15th February 2023, from https://broadleaf.com.au/resource-material/the-colour-of-hydrogen/

Corengia, M., & Torres, A. I. (2022). Coupling time varying power sources to production of green-hydrogen: A superstructure based approach for technology selection and optimal design. *Chemical Engineering Research and Design*, *183*, 235–249. https://doi.org/https://doi.org/10.1016/j.cherd.2022.05.007

Correia, I., & Captivo, E. (2003). A lagrangean heuristic for a modular capacitated location problem. *Annals of Operations Research*, *122*(1), 141–161. https://doi.org/https://doi.org/10.1023/A:1026146507143

Correia, I., & Saldanha-da-Gama, F. (2019). *Facility location under uncertainty*. Spinger New York. https://doi.org/10.1007/978-3-030-32177-2_8

Damman, S., Sandberg, E., Rosenberg, E., Pisiciella, P., & Johansen, U. (2020). *Large-scale hydrogen production in norway - possible transition pathways towards 2050* (No. 2020-00179). SINTEF Digital. https://ife.brage.unit.no/ife-xmlui/handle/11250/2650236

Danebergs, J., & Aarsskog, F. G. (2020a). Estimation of energy demand in the norwegian high-speed passenger ferry sector towards 2030. *IFE/E-2020/003*. https://ife.brage.unit.no/ife-xmlui/handle/11250/2653026

Danebergs, J., & Aarsskog, F. G. (2020b). Future compresssed hydrogen infrastructure for the domestic maritime sector. *IFE/E-2020/006*. https://ife.brage.unit.no/ife-xmlui/handle/11250/2719412

Dantzig, G. B. (1955). "linear programming under uncertainty." *Manage. Sci. 1, 197–206*, *1*(3-4), 197–206. https://doi.org/https://doi.org/10.1287/mnsc.1.3-4.197

DNV. (2019). *Synteserapport om produksjon og bruk av hydrogen i norge*. https://www.regjeringen.no/contentassets/0762c0682ad04e6abd66a9555e7468df/hydrogen-i-norge---synteserapport.pdf

DNV. (2022). *Hydrogen forecast to 2050*. https://www.dnv.com/focus-areas/hydrogen/forecast-to-2050.html

Enerdata. (2022). *Share of renewables in electricity production*. Retrieved 15th February 2023, from https://yearbook.enerdata.net/renewables/renewable-in-electricity-production-share.html

Enova. (2022a). *Enova støtter hydrogenprosjekter i maritim sektor med 1,12 milliarder kroner*. Retrieved 22nd May 2023, from https://kommunikasjon.ntb.no/pressemelding/enova-stotter-hydrogenprosjekter-i-maritim-sektor-med-112-milliarder-kroner?publisherId=17848299&releaseId=17941867

Enova. (2022b). Enova støtter hydrogenprosjekter i maritim sektor med 1,12 milliarder kroner. Retrieved 1st May 2023, from https://presse.enova.no/pressreleases/enova-stoetter-hydrogenprosjekter-i-maritim-sektor-med-112-milliarder-kroner-3190840

Escudero, L. F., Garín, A., Merino, M., & Pérez, G. (2007). The value of the stochastic solution in multistage problems. *TOP*, *15*, 48–64. https://doi.org/https://doi.org/10.1007/s11750-007-0005-4

Gardarsdottir, S. (2021). *Assumptions matter when assessing blue & green hydrogen*. Retrieved 21st January 2023, from https://blog.sintef.com/sintefenergy/assumptions-matter-when-assessing-blue-green-hydrogen/

Govindan, K., Fattahi, M., & Keyvanshokooh, E. (2017). Supply chain network design under uncertainty: A comprehensive review and future research directions. *European Journal of Operational Research*, *263*, 108–141. https://doi.org/10.1016/j.ejor.2017.04.009

Hewitt, M., Ortmann, J., & Rei, W. (2022). Decision-based scenario clustering for decision-making under uncertainty. *Annals of Operations Research*, (315), 747–771. https://doi.org/10.1007/s10479-020-03843-x

Holmberg, K. (1994). Solving the staircase cost facility location problem with decomposition and piecewise linearization. *European Journal of Operational Research*, *75*(1), 41–61. https://doi.org/https://doi.org/10.1016/0377-2217(94)90184-8

Holmberg, K., Rönnqvist, M., & Yuan, D. (1999). An exact algorithm for the capacitated facility location problems with single sourcing. *European Journal of Operational Research*, *113*(3), 544–559. https://doi.org/https://doi.org/10.1016/S0377-2217(98)00008-3

Howarth, R. W., & Jacobson, M. Z. (2021). How green is blue hydrogen? *Energy Science & Engineering*, *9*(10), 1676–1687. https://doi.org/https://doi.org/10.1002/ese3.956

IEA. (2019). The future of hydrogen, seizing today's opportunities. Retrieved 15th February 2023, from https://www.iea.org/reports/the-future-of-hydrogen

IRENA. (2020a). Green hydrogen - a guide to policy making. *International Renewable Energy Agency*. https://www.irena.org/publications/2020/Nov/Green-hydrogen

IRENA. (2020b). Green hydrogen cost reduction - scaling up electrolysers to meet the 1.5°c climate goal. *International Renewable Energy Agency*. https://www.irena.org/-/media/Files/IRENA/Agency/Publication/2020/Dec/IRENA_Green_hydrogen_cost_2020.pdf

Ishimoto, Y., Voldsund, M., Nekså, P., Roussanaly, S., Berstad, D., & Gardarsdottir, S. O. (2020). Large-scale production and transport of hydrogen from norway to europe and japan: Value chain analysis and comparison of liquid hydrogen and ammonia as energy carriers. *International Journal of Hydrogen Energy*, *45*(58), 32865–32883. https://doi.org/https://doi.org/10.1016/j.ijhydene.2020.09.017

ITM-Power. (2022). *Products: World-class turn-key electrolysers from 600 kw to 100 mw.* Retrieved 15th February 2023, from https://itm-power.com/products

Jakobsen, D., & Åtland, V. (2016). *Concepts for large scale hydrogen production* (Master's thesis). NTNU. Norway. https://ntnuopen.ntnu.no/ntnu-xmlui/handle/11250/2402554

Jena, S. D., Cordeau, J.-F., & Gendron, B. (2016). Solving a dynamic facility location problem with partial closing and reopening. *Computers and Operations Research*, *67*, 143–154. https://doi.org/https://doi.org/10.1016/j.cor.2015.10.011

Jena, S. D., Cordeau, J.-F., & Gendron, B. (2017). Lagrangian heuristics for large-scale dynamic facility location with generalized modular capacities. *INFORMS Journal on Computing*, *29*, 388–404. https://doi.org/https://doi.org/10.1287/ijoc.2016.0738

Kaut, M., Midthun, K. T., Werner, A. S., Tomasgard, A., Hellemo, L., & Fodstad, M. (2014). Multi-horizon stochastic programming [Special Issue: Computational Techniques in Management Science]. *Computational Management Science*, *11*(1–2), 179–193. https://doi.org/10.1007/s10287-013-0182-6

Khatami, M., Mahootchi, M., & Farahani, R. Z. (2015). Benders' decomposition for concurrent redesign of forward and closed-loop supply chain network with demand and return uncertainties. *Transportation Research Part E: Logistics and Transportation Review*, *79*, 1–21. https://doi.org/https://doi.org/10.1016/j.tre.2015.03.003

Lai, C.-M., Chiu, C.-C., Liu, W.-C., & Yeh, W.-C. (2019). A novel nondominated sorting simplified swarm optimization for multi-stage capacitated facility location problems with multiple quantitative and qualitative objectives. *Applied Soft Computing Journal*, *84*. https://doi.org/10.1016/j.asoc.2019.105684

Lara, C. L., Siirola, J. D., & Grossmann, I. E. (2020). Electric power infrastructure planning under uncertainty: Stochastic dual dynamic integer programming (sddip) and parallelization scheme. *Optim Eng*, *21*, 1243–1281. https://doi.org/https://doi.org/10.1007/s11081-019-09471-0

Leo, E., & Engell, S. (2018). Integrated day-ahead energy procurement and production scheduling. *IEEE Transactions on Power Systems*, *66*, 950–963. https://doi.org/10.1515/auto-2018-001610.1515/auto-2018-0016

Li, L., Manier, H., & Manier, M.-A. (2019). Hydrogen supply chain network design: An optimization-oriented review. *Renewable and Sustainable Energy Reviews*, *103*, 342–360. https://doi.org/https://doi.org/10.1016/j.rser.2018.12.060

Linde plc. (2021). *Linde to supply world's first hydrogen-powered ferry.* Retrieved 22nd May 2023, from https://www.linde.com/news-media/press-releases/2021/linde-to-supply-world-s-first-hydrogen-powered-ferry

MacRae, C., Ernst, A., & Ozlen, M. (2016). A benders decomposition approach to transmission expansion planning considering energy storage. *Energy*, *112*, 795–803. https://doi.org/https://doi.org/10.1016/j.energy.2016.06.080

Madsen, S. A. (2019). Tep4520 1 industriell prosessteknikk, fordypningprosjekt: Hydrogen export technology from extreme areas. *Fordynpingsporsjekt at NTNU*.

Maggioni, F., Allevi, E., & Tomasgard, A. (2020a). Bounds in multi-horizon stochastic programs. *Annals of Operations Research*, *292*, 605–625. https://doi.org/https://doi.org/10.1007/s10479-019-03244-9

Maggioni, F., Allevi, E., & Tomasgard, A. (2020b). Multi-horizon stochastic programming. *Computational Management Science*, *292*, 605–625. https://doi.org/10.1007/s10479-019-03244-9

Marsten, R. E., Hogan, W. W., & Blankenship, J. W. (1975). The boxstep method for large-scale optimization. *Operations Research*, *23*(3), 389–405.

Mathis, S., & Koscianski, J. (2002). *Microeconomic theory: An integrated approach.* Prentice Hall.

Matute, G., Yusta, J. M., Beyza, J., & Correas, L. (2021). Multi-state techno-economic model for optimal dispatch of grid connected hydrogen electrolysis systems operating under dynamic conditions. *International Journal of Hydrogen Energy*, *46*(2), 1449–1460. https://doi.org/https://doi.org/10.1016/j.ijhydene.2020.10.019

Melo, T., Nickel, S., & Saldanha-da-Gama, F. (2009). Facility location and supply chain management – a review. *European Journal of Operational Research*, *196*(2), 401–412. https://doi.org/https://doi.org/10.1016/j.ejor.2008.05.007

Menon Economics. (2022). *Verdien av den norske hydrogennæringen: Status og fremtidsutsikter*. https://www.menon.no/verdien-av-den-norske-hydrogennaeringen-status-og-fremtidsutsikter/

Miljødierktoratet. (2022). *Klimagassutslipp fra transport i norge*. Retrieved 24th March 2023, from https://miljostatus.miljodirektoratet.no/tema/klima/norske-utslipp-av-klimagasser/klimagassutslipp-fra-transport/

Miljødirektoratet. (2022). *Klimagassutslipp fra transport i norge*. Retrieved 9th December 2022, from https://miljostatus.miljodirektoratet.no/tema/klima/norske-utslipp-av-klimagasser/klimagassutslipp-fra-transport/

Millet, P., & Grigoriev, S. (2013). Renewable hydrogen technologies. In L. M. Gandía, G. Arzamendi & P. M. Diéguez (Eds.). Elsevier. https://doi.org/https://doi.org/10.1016/B978-0-444-56352-1.00002-7

Moseman, A., & Herzog, H. (2021). *How efficient is carbon capture and storage?* Retrieved 15th February 2023, from https://climate.mit.edu/ask-mit/how-efficient-carbon-capture-and-storage

Myklebust, J., Holth, C. B., Tøftum, L. E. S., & Tomasgard, A. (2010). Optimizing investments for hydrogen infrastructure in the transport sector. in: Techno-economic modelling of value chains based on natural gas:with consideration of co2 emissions. https://ntnuopen.ntnu.no/ntnu-xmlui/handle/11250/265786?show=full

Nel. (2021). Nel hydrogen electrolyzers: The worlds most efficient and reliable electrolyzers [Collected bBrigey contacting NEL offices].

Nickel, S., & Saldanha-da-Gama, F. (2019). *Multi-period facility location*. Spinger New York. https://doi.org/10.1007/978-3-030-32177-2_11

Nord Pool. (2022a). *Day-ahead prices*. Retrieved 24th February 2023, from https://www.nordpoolgroup.com/en/Market-data1/Dayahead/Area-Prices/NO/Monthly/?view=chart

Nord Pool. (2022b). *Day-ahead prices*. Retrieved 24th October 2022, from https://www.nordpoolgroup.com/en/Market-data1/Dayahead/Area-Prices/NO/Monthly/?view=chart

Nord Pool. (2023). Nordic ftp server [data retrieved from ftp://ftp.nordpoolgroup.com/Elspot/Elspot_prices/Norway/].

Ocean Hyway Cluster. (2020a). *2030 hydrogen demand for the coastal route bergen-kirkenes c.3 rev. 0* [Workpackage C: Mapping future hydrogen demand.].

Ocean Hyway Cluster. (2020b). 2030 hydrogen demand in the norwegian domestic maritime sector [Workpackage C: Mapping future hydrogen demand.].

Ocean Hyway Cluster. (2020c). Interactive map - potential maritime hydrogen in norway [Workpackage C: Mapping future hydrogen demand].

Ocean Hyway Cluster. (2020d). *Mapping of 2030 hydrogen demand in the norwegian domestic car ferry sector*.

Olje- og energidepartementet. (2022). *Kraftmarkedet*. Retrieved 26th May 2023, from https://energifaktanorge.no/norsk-energiforsyning/kraftmarkedet

Pindyck, R. S., & Rubinfeld, D. L. (2018). *Microeconomics* (9th ed.). Pearson.

Python. (2023a). *Multiprocessing — process-based parallelism*. Retrieved 5th May 2023, from https://docs.python.org/3/library/multiprocessing.html

Python. (2023b). Random — generate pseudo-random numbers. Retrieved 18th May 2022, from https://docs.python.org/3/library/random.html

Ravi, R., & Sinha, A. (2004). Hedging uncertainty: Approximation algorithms for stochastic optimization problems. *Lecture Notes in Computer Science*, *3064*. https://doi.org/https://doi.org/10.1007/978-3-540-25960-2_8

Refsdal, I., & Sindre, T. S. (2022). The impact of flexibility on hydrogen production plant location under uncertain electricity prices.

Sabio, N., Gadalla, M., Guillén-Gosálbez, G., & Jiménez, L. (2010). Strategic planning with risk control of hydrogen supply chains for vehicle use under uncertainty in operating costs: A case study of spain. *International Journal of Hydrogen Energy*, *35*(13), 6836–6852. https://doi.org/https://doi.org/10.1016/j.ijhydene.2010.04.010

Saldanha-da-Gama, F. (2022). Facility location in logistics and transportation: An enduring relationship. *Transportation Research Part E*, *166*, 102903. https://doi.org/10.1016/j.tre.2022.102903

Samferdselsdepartementet. (2020). Retrieved 1st May 2023, from https://www.regjeringen.no/no/dokumenter/meld.-st.-20-20202021/id2839503/?ch=1

Samferdselsdepartementet. (2022). Nasjonal transportplan 2022-2033. Retrieved 4th March 2023, from https://www.regjeringen.no/no/tema/transport-og-kommunikasjon/nasjonal-transportplan/id2475111/

Schütz, P., Stougie, L., & Tomasgard, A. (2008). Stochastic facility location with general long-run costs and convex short-run costs [Part Special Issue: Bio-inspired Methods in Combinatorial Optimization]. *Computers and Operations Research*, *35*(9), 2988–3000. https://doi.org/https://doi.org/10.1016/j.cor.2007.01.006

Schütz, P., Tomasgard, A., & Ahmed, S. (2009). Supply chain design under uncertainty using sample average approximation and dual decomposition. *European Journal of Operational*, *199*(2), 409–419. https://doi.org/https://doi.org/10.1016/j.ejor.2008.11.040

Seljom, P., & Tomasgard, A. (2015). Short-term uncertainty in long-term energy system models — a case study of wind power in denmark. *Energy Economics*, *49*, 157–167. https://doi.org/10.1016/j.eneco.2015.02.004

Shulman, A. (1991). An algorithm for solving dynamic capacitated plant location problems with discrete expansion sizes. *Operations Research*, *39*(3), 423–436. https://doi.org/https://doi.org/10.1287/opre.39.3.423

Simchi-Levi, D., Kaminsky, P., & Simchi-Levi, E. (2004). *Managing the supply chain: Definitive guide*. Tata McGraw-Hill Education.

Sjøfartsdirektoratet. (2023). *Norled og nasa på flytende hydrogen*. Retrieved 8th June 2023, from https://www.sdir.no/aktuelt/nyheter/utslippsfri-og-historisk-ferjetur/

Snyder, L. V. (2006). Facility location under uncertainty: A review. *IEEE Transactions on Power Systems*, *38*, 547–564. https://doi.org/10.1080/07408170500216480

Sridharan, R. (1995). The capacitated plant location problem. *European Journal of Operational Research*, *87*(2), 203–213. https://doi.org/https://doi.org/10.1016/0377-2217(95)00042-O

SSB. (2023). Retrieved 23rd May 2023, from https://www.ssb.no/transport-og-reiseliv/landtransport/statistikk/bilparken/artikler/fire-av-fem-nye-biler-i-2022-var-elbiler#:~:text=I%5C%202022%5C%20ble%5C%20det%5C%20f%5C%C3%5C%B8rstegangsregistrert,prosent%5C%20av%5C%20alle%5C%20personbiler%5C%20helelektriske.

Stádlerová, S., Jena, S. D., & Schütz, P. (2023). Using lagrangian relaxation to locate hydrogen production facilities under uncertain demand: A case study from norway. *Computational Management Science*. https://doi.org/10.1007/s10287-023-00445-3

Stádlerová, S., & Schütz, P. (2021). Designing the hydrogen supply chain for maritime transportation in norway. *Computational Logistics*, *130*(04), 36–50. https://ntnuopen.ntnu.no/ntnu-xmlui/handle/11250/2827487

Statens vegvesen. (2023). *Mf hydra seiler utslippsfritt på flytende hydrogen*. Retrieved 22nd May 2023, from https://www.vegvesen.no/om-oss/presse/aktuelt/2023/03/mf-hydra-seiler-utslippsfritt-pa-flytende-hydrogen/

Statistisk Sentralbyrå. (2021). *12579: Road traffic volumes (2021)*. Retrieved 26th February 2022, from https://www.ssb.no/en/statbank/table/12579/

Statkraft. (2022). *Vannkraft*. Retrieved 24th February 2023, from https://www.statkraft.no/var-virksomhet/vannkraft/

Statnett. (2022). *Derfor har vi prisområder*. Retrieved 28th January 2023, from https://www.statnett.no/om-statnett/bli-bedre-kjent-med-statnett/om-strompriser/fakta-om-prisomrader/

The Norwegian Government. (2022a). *Hydrogen*. Retrieved 11th June 2023, from https://www.regjeringen.no/no/tema/naringsliv/gront-industriloft/hydrogen/id2920298/

The Norwegian Government. (2022b). *Nytt norsk klimamål på minst 55 prosent*. Retrieved 6th December 2022, from https://www.regjeringen.no/no/aktuelt/nytt-norsk-klimamal-pa-minst-55-prosent/id2944876/#:~:text=Norge%5C%20vil%5C%20kutte%5C%20utslipp%5C%20med,i%5C%20v%5C%C3%5C%A5r%5C%20innmelding%5C%20til%5C%20FN.

The World of Hydrogen. (2022). *What is hydrogen*. Retrieved 28th February 2023, from https://www.theworldofhydrogen.com/gasunie/what-is-hydrogen/

Thyssenkrupp. (n.d.). *Water electrolysis: Power to gas*. Retrieved 15th February 2023, from https://www.thyssenkrupp.com/en/company/innovation/technologies-for-the-energy-transition/water-electrolysis.html

UK Government. (2022). *Research and analysis: Hydrogen production costs 2021*. Retrieved 29th January 2023, from https://www.gov.uk/government/publications/hydrogen-production-costs-2021

US. Department of energy. (2022). *Hydrogen storage*. Retrieved 5th February 2023, from https://www.energy.gov/eere/fuelcells/hydrogen-storage

v.d. Broek, J., Schütz, P., Stougie, L., & Tomasgard, A. (2006). Location of slaughterhouses under economies of scale. *European Journal of Operational Research*, *175*(2), 740–750.

Yu, X., Shen, S., & Ahmed, S. (2021). On the value of multistage stochastic facility location with risk aversion. https://doi.org/10.48550/arXiv.2105.11005

Appendix

A Data From Instances to Assesses Value of Flexibility

Table 1: Electricity Scenario Measurements normal electricity prices

Instance	Measure	1	2	3	4	5	6	7
C1E1S100N2Tn	Production cost (%)	73%	73%	75%	69%	70%	70%	71%
	Transportation cost (%)	18%	16%	16%	19%	20%	19%	20%
	Investment cost (%)	12%	9%	9%	7%	7%	5%	7%
	% PEM installed	0%	0%	0%	74%	74%	77%	77%
	Avg Eur/kg H2	6.92	6.71	6.77	6.44	6.50	6.21	6.40
	Avg cost per installed capacity (€/MW)	233000	202176	201765	140050	147494	88669	145085
	Avg production efficiency (kWh/kgH2)	50	49.17	49.15	48.30	48.30	48.27	48.27
	Excess capacity (%)	111%	78%	82%	95%	87%	114%	101%
C1E2S50N2Tn	Production cost (%)	72%	75%	75%	73%	72%	71%	72%
	Transportation cost (%)	19%	16%	16%	21%	21%	20%	21%
	Investment cost (%)	9%	8%	8%	6%	7%	8%	7%
	% PEM installed	0%	0%	0%	73%	78%	80%	80%
	Avg Eur/kg H2	7.31	7.27	7.31	6.97	6.96	7.02	6.95
	Avg cost per installed capacity (€/MW)	245000	203244	201956	138701	136900	151975	142157
	Avg production efficiency (kWh/kgH2)	50.00	49.13	49.12	48.29	48.24	48.22	48.22
	Excess capacity (%)	58%	76%	75%	97%	125%	139%	126%
C1E4S25N2Tn	Production cost (%)	73%	73%	77%	71%	72%	72%	73%
	Transportation cost (%)	18%	16%	16%	20%	21%	20%	20%
	Investment cost (%)	9%	11%	7%	9%	7%	8%	7%
	% PEM installed	0%	0%	0%	76%	69%	81%	79%
	Excess capacity (%)	58%	144%	68%	189%	117%	139%	106%
	Avg Eur/kg H2	7.35	7.46	7.23	7.16	7.02	7.04	6.95
	Avg cost per installed capacity (€/MW)	245000	195095	183827	144145	148761	141927	143818
	Avg production efficiency (kWh/kgH2)	50.00	49.09	49.13	48.26	48.33	48.21	48.23

Table 2: Electricity Scenario Measurements

Instance	Measure	1	2	3	4	5	6	7
C1E1S100N2Th	Production cost (%)	44%	57%	56%	53%	53%	53%	54%
	Transportation cost (%)	29%	39%	39%	44%	44%	44%	43%
	Investment cost (%)	27%	5%	5%	3%	3%	3%	3%
	% PEM installed	0%	0%	20%	71%	71%	73%	73%
	Excess capacity (%)	953%	47%	75%	47%	40%	42%	33%
	Avg Eur/kg H2	11.83	8.18	8.28	7.86	7.86	7.87	7.88
	Avg cost per installed capacity (€/MW)	215000	215000	211650	152500	152500	155550	155550
	Avg production efficiency (kWh/kgH2)	50.00	50.00	50.30	48.57	48.57	48.77	48.77
C1E1S100N2Tn	Production cost (%)	46%	60%	60%	59%	59%	59%	60%
	Transportation cost (%)	28%	36%	36%	37%	37%	37%	36%
	Investment cost (%)	26%	4%	4%	4%	4%	4%	4%
	% PEM installed	0%	0%	0%	80%	80%	80%	80%
	Excess capacity (%)	953%	47%	40%	114%	104%	94%	82%
	Avg Eur/kg H2	12.57	9.26	9.27	9.48	9.47	9.48	9.49
	Avg cost per installed capacity (€/MW)	215000	215000	215000	144657	144657	144657	144657
	Avg production efficiency (kWh/kgH2)	50.00	50.00	50.00	48.39	48.39	48.39	48.39
C1E1S100N2Tn	Production cost (%)	52%	59%	54%	56%	56%	55%	56%
	Transportation cost (%)	31%	36%	36%	40%	39%	40%	39%
	Investment cost (%)	17%	5%	10%	4%	4%	5%	5%
	% PEM installed	0%	0%	0%	74%	77%	56%	56%
	Excess capacity (%)	163%	168%	572%	99%	115%	137%	122%
	Avg Eur/kg H2	10.91	9.03	9.47	8.97	9.10	8.96	8.94
	Avg cost per installed capacity (€/MW)	510000	195100	191000	145289	143294	155440	155440
	Avg production efficiency (kWh/kgH2)	50.00	49.20	49.09	48.32	48.28	48.48	48.48

Table 3: Electricity Scenario Measurements loe electricity prices

Instance	Measure	1	2	3	4	5	6	7
C1E1S100N2Tn	Production cost (%)	67%	70%	70%	69%	69%	69%	69%
	Transportation cost (%)	21%	22%	20%	25%	25%	24%	24%
	Investment cost (%)	13%	8%	10%	6%	6%	7%	7%
	% PEM installed	0%	0%	0%	76%	76%	74%	74%
	Excess capacity (%)	58%	-4%	26%	15%	10%	33%	25%
	Avg Eur/kg H2	4.81	4.43	4.51	4.21	4.22	4.28	4.26
	Avg cost per installed capacity (€/MW)	245000	241223	217853	143812	156425	152876	152876
	Avg production efficiency (kWh/kgH2)	50.00	49.23	49.17	48.29	48.29	48.30	48.30
C1E2S50N2Tl	Production cost (%)	69%	72%	72%	71%	70%	70%	70%
	Transportation cost (%)	22%	19%	19%	24%	24%	23%	23%
	Investment cost (%)	9%	9%	8%	5%	6%	7%	6%
	% PEM installed	0%	0%	0%	78%	70%	74%	74%
	Excess capacity (%)	5%	32%	26%	68%	20%	33%	25%
	Avg Eur/kg H2	4.83	4.72	4.66	4.39	4.47	4.49	4.47
	Avg cost per installed capacity (€/MW)	269000	206908	191964	83311	153198	150062	150062
	Avg production efficiency (kWh/kgH2)	50.00	49.11	49.11	48.25	48.33	48.29	48.29
C1E1S100N2Tn	Production cost (%)	68%	71%	71%	69%	69%	70%	70%
	Transportation cost (%)	21%	20%	20%	25%	24%	24%	24%
	Investment cost (%)	10%	9%	10%	6%	6%	6%	6%
	% PEM installed	0%	1%	0%	67%	71%	69%	71%
	Excess capacity (%)	16%	28%	35%	10%	19%	16%	18%
	Avg Eur/kg H2	4.77	4.58	4.60	4.33	4.34	4.34	4.33
	Avg cost per installed capacity (€/MW)	272273	207299	206063	156503	152769	153985	152268
	Avg production efficiency (kWh/kgH2)	50.00	49.16	49.11	48.38	48.34	48.35	48.32

Table 4: Electricity Scenario Measurements

Instance	Measure	1	2	3	4	5	6	7
C1E1S100N2Tv	Production cost (%)	46%	55%	55%	54%	55%	54%	55%
	Transportation cost (%)	37%	33%	34%	37%	38%	37%	36%
	Investment cost (%)	17%	12%	11%	9%	7%	9%	8%
	% PEM installed	0%	0%	0%	73%	75%	75%	75%
	Excess capacity (%)	426%	268%	251%	281%	301%	280%	256%
	Avg Eur/kg H2	8.56	8.11	8.07	7.82	7.62	7.84	7.82
	Avg cost per installed capacity (€/MW)	224000	194200	194200	145824	112300	144175	144175
	Avg production efficiency (kWh/kgH2)	50.00	49.20	49.20	48.33	48.30	48.30	48.30
C1E2S50N2Tv	Production cost (%)	59%	62%	62%	60%	60%	60%	61%
	Transportation cost (%)	27%	27%	27%	31%	31%	31%	30%
	Investment cost (%)	14%	11%	11%	9%	9%	9%	8%
	% PEM installed	0%	0%	0%	74%	76%	76%	76%
	Excess capacity (%)	268%	246%	230%	275%	295%	274%	251%
	Avg Eur/kg H2	8.83	8.56	8.53	8.28	8.31	8.29	8.26
	Avg cost per installed capacity (€/MW)	229786	193160	193160	144740	143165	143165	143165
	Avg production efficiency (kWh/kgH2)	50.00	49.15	49.15	48.30	48.27	48.27	48.27
C1E4S25N2Tv	Production cost (%)	56%	59%	60%	58%	58%	58%	60%
	Transportation cost (%)	25%	27%	28%	32%	32%	33%	32%
	Investment cost (%)	19%	14%	11%	11%	10%	9%	8%
	% PEM installed	0%	0%	0%	71%	71%	75%	75%
	Excess capacity (%)	426%	356%	251%	344%	325%	280%	256%
	Avg Eur/kg H2	9.51	9.01	8.60	8.42	8.41	8.31	8.29
	Avg cost per installed capacity (€/MW)	228500	193742	195100	146873	146873	144400	144400
	Avg production efficiency (kWh/kgH2)	50.00	49.16	49.20	48.34	48.34	48.30	48.30

Table 5: Electricity Scenario Measurements

Instance	Measure	1	2	3	4	5	6	7
C1E1S100N2Tvv	Production cost (%)	66%	69%	68%	69%	69%	71%	68%
	Transportation cost (%)	20%	23%	23%	23%	23%	23%	24%
	Investment cost (%)	15%	8%	8%	8%	7%	6%	7%
	% PEM installed	20%	14%	24%	84%	82%	84%	84%
	Excess capacity (%)	163%	62%	75%	147%	112%	130%	115%
	Avg Eur/kg H2	7.19	6.54	6.60	6.46	6.44	6.34	6.31
	Avg cost per installed capacity (€/MW)	250100	209455	207690	142780	144509	110349	144068
	Avg production efficiency (kWh/kgH2)	51	49.68	49.9	48.31	48.35	48.39	48.39
C1E2S50N2Tvv	Production cost (%)	65%	70%	74%	67%	68%	68%	69%
	Transportation cost (%)	22%	22%	20%	25%	24%	25%	24%
	Investment cost (%)	13%	8%	7%	8%	8%	7%	7%
	% PEM installed	0%	0%	20%	83%	84%	83%	83%
	Excess capacity (%)	163%	84%	75%	143%	145%	130%	115%
	Avg Eur/kg H2	7.36	6.97	7.13	6.73	6.87	6.77	6.75
	Avg cost per installed capacity (€/MW)	240200	204320	168430	143372	142622	143659	143659
	Avg production efficiency (kWh/kgH2)	50.00	49.20	49.70	48.25	48.24	48.35	48.35
C1E1S100N2Tn	Production cost (%)	66%	70%	69%	65%	68%	68%	67%
	Transportation cost (%)	21%	22%	23%	26%	26%	25%	26%
	Investment cost (%)	13%	9%	8%	8%	7%	7%	7%
	% PEM installed	0%	7%	60%	80%	81%	91%	92%
	Excess capacity (%)	163%	99%	75%	158%	159%	107%	115%
	Avg Eur/kg H2	7.48	6.94	6.99	6.60	6.58	6.67	6.57
	Avg cost per installed capacity (€/MW)	240200	194296	205000	144350	111938	145275	143512
	Avg production efficiency (kWh/kgH2)	50.00	49.37	50.70	48.30	48.29	48.62	48.56

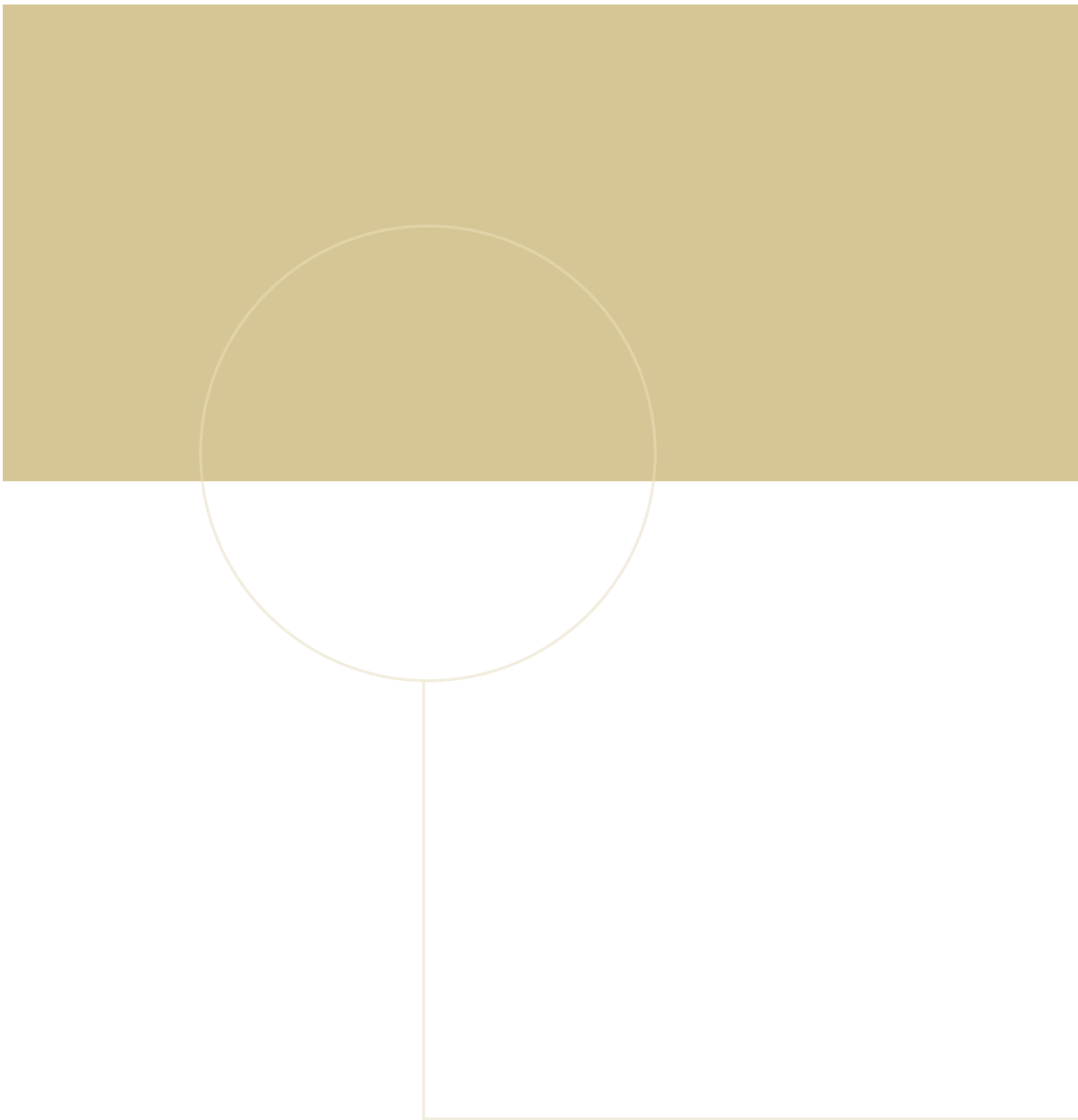

NTNU

Norwegian University of
Science and Technology